COMPARISON OF VISUAL ACUITY MEASUREMENTS IN C57BL6/J MICE
USING TWO DIFFERENT BEHAVIORAL ASSESMENT TASKS

A THESIS SUBMITTED TO
THE GRADUATE SCHOOL OF INFORMATICS
OF
THE MIDDLE EAST TECHNICAL UNIVERSITY

BY

İREM NALÇA

IN PARTIAL FULFILLMENT OF THE REQUIREMENTS FOR THE DEGREE OF
MASTER OF SCIENCE
IN
THE DEPARTMENT OF HEALTH INFORMATICS

JUNE 2014

Approval of the Thesis

COMPARISON OF VISUAL ACUITY MEASUREMENTS IN C57BL6/J MICE USING TWO DIFFERENT BEHAVIORAL ASSESMENT TASKS

Submitted by **İREM NALÇA** in partial fulfillment of the requirements for the degree of **Master of Science in Medical Informatics, Middle East Technical University** by,

Prof. Dr. Nazife Baykal
Director, **Informatics Institute**　　　　　　　　　　———————————

Assist. Prof. Dr. Yeşim Aydın Son
Head of Department, **Health Informatics**　　　———————————

Assoc. Prof. Dr. Ewa Doğru
Supervisor, **Biology Dept., METU**　　　　　　　———————————

Examining Committee Members:

Assoc. Prof. Dr. Tülin Yanık
Biology Dept., METU　　　　　　　　　　　　　———————————

Assoc. Prof. Dr. Ewa Doğru
Biology Dept., METU　　　　　　　　　　　　　———————————

Assist. Prof. Dr. Cengiz Acartürk
Cognitive Science Dept., METU　　　　　　　　　———————————

Assist. Prof. Dr. Yeşim Aydın Son
Health Informatics Dept., METU　　　　　　　　———————————

Assist. Prof. Dr. Levent Şenyüz
Psychology Dept., Hacettepe University　　　　　———————————

Date: 13.06.2014

I hereby declare that all information in this document has been obtained and presented in accordance with academic rules and ethical conduct. I also declare that, as required by these rules and conduct, I have fully cited and referenced all material and results that are not original to this work.

Name, Last name : İrem Nalça

Signature   : _____

ABSTRACT

COMPARISON OF VISUAL ACUITY MEASUREMENTS IN C57BL6/J MICE USING TWO DIFFERENT BEHAVIORAL ASSESMENT TASKS

Nalça, İrem
M.Sc., Department of Health Informatics
Supervisor: Assoc. Prof. Dr. Ewa Jakubowska-Doğru

June 2014, 84 pages

Investigation of physiology, pharmacology, and genetics of vision in animal models requires development of experimental procedures allowing for a reliable behavioral assessment of visual skills. In the present study, two different behavioral assessment tasks to measure visual acuity in C57BL6/J mice were applied and compared. Both tasks were performed in a trapezoidal-shaped pool, with two computer-controlled monitors placed side-by-side at one end of the pool, and with an invisible platform located under the monitor presenting vertical grating of different spatial frequencies. The purpose of the first task was to revisit Prusky's method of assessing visual acuity with an arbitrary discrimination criterion of 70% correct responses (Prusky *et al*., 2000). The second task investigated a potential improvement of visual acuity by repeated visual discrimination training to an arbitrary performance criterion of 75% correct responses. The visual acuity threshold for our strain of C57BL6/J mice as assessed by Prusky's method was at 0.43 cpd. In the second task, all animals performed above the arbitrary discrimination level on all tested spatial frequencies up to 0.86 cpd. Our results show that repeated visual discrimination training procures a substantial enhancement in the visual acuity of adult mice suggesting that visual cortex retains its capability for activity-dependent neuroplasticity throughout the adulthood. The data analysis confirmed that the percent of correct choices and the escape latency are reliable indices for the behavioral assessment of visual functions with methods similar to ours. To understand how repeated visual discrimination training procures visual acuity enhancement, the accompanied morphological and physiological changes in the visual cortex should be investigated.

ÖZ

C57BL6/J FARELERDE GÖRME KESKİNLİĞİ ÖLÇÜMLERİNİN İKİ FARKLI DAVRANIŞSAL DEĞERLENDİRME TESTİ KULLANILARAK KARŞILAŞTIRILMASI

Nalça, İrem
Yüksek Lisans, Sağlık Bilişimi Bölümü
Tez Yöneticisi: Doç. Dr. Ewa Jakubowska-Doğru

Haziran 2014, 84 sayfa

Hayvan modellerinde görmenin fizyolojisinin, farmakolojisinin ve genetiğinin araştırılması, görsel becerilerin davranışsal değerlendirilmesine olanak sağlayan güvenilir deneysel prosedürlerin geliştirilmesini gerektirmektedir. Bu çalışmada, C57BL6/J farelerde görme keskinliğini ölçmek için iki farklı davranışsal değerlendirme testi uygulanmış ve karşılaştırılmıştır. Her iki test de, bir ucuna yan yana iki bilgisayar kontrollü monitörün ve farklı uzamsal frekanslardaki dikey siyah-beyaz çizgileri gösteren monitörün altına görünmez bir platformun yerleştirildiği, ikizkenar yamuk şeklindeki havuzda gerçekleştirilmiştir. İlk testin amacı, Prusky'nin görme keskinliğini değerlendiren metodunu, ayırt etme kriteri %70 doğru seçim varsayılarak, yeniden incelemektir (Prusky *et al*., 2000). İkinci test, görme keskinliğinin, performans kriteri olarak belirlenen %75 doğru seçim seviyesine kadar tekrarlanan görsel ayırt etme eğitimi ile olası gelişimini araştırmaktadır. C57BL6/J fareler için görme keskinliği eşik değeri Prusky'nin metodu ile 0.43 cpd bulunmuştur. İkinci testte ise, tüm hayvanlar 0.86 cpd'ye kadar test edilmiş olan tüm frekanslarda, varsayılan ayırt etme seviyesinin üzerinde performans göstermişlerdir. Sonuçlarımız tekrarlanan görsel ayırt etme eğitiminin, erişkin farenin görme keskinliğinde önemli ölçüde gelişim sağladığını ve görsel korteksin, aktivite bağımlı nöroplastisite yeteneğini erişkinlik boyunca koruduğunu göstermektedir. Veri analizi, doğru seçimlerin yüzdesinin ve platformu bulma süresinin görsel fonksiyonların benzer davranışsal metotlarla değerlendirilmesinde güvenilir göstergeler olduğunu doğrulamıştır. Tekrarlanan görsel

ayırt etme eğitiminin görme keskinliğini nasıl arttırdığını anlamak için, görsel kortekste eşlik eden morfolojik ve fizyolojik değişiklikler araştırılmalıdır.

Anahtar Kelimeler: fare, görme keskinliği testi, görsel su testi, tekrarlanan görsel ayırt etme eğitimi

ACKNOWLEDGEMENTS

TABLE OF CONTENTS

LIST OF TABLES

LIST OF FIGURES

LIST OF ABBREVIATIONS

ANOVA	Analysis of Variance
BBB	Blood-Brain Barrier
BRT	Boosted Regression Trees
°C	Degree Celsius
cd	candela
cGMP	Cyclic guanosine monophosphate
cm	centimeter
cpd	cycles per degree
CQP	Conic Quadratic Programming
deg	degree
EE	Enriched Environment
EFP	Evoked Field Potentials
ERG	Electroretinogram
Ft	Feet
GAM	Generalized Additive Models
GCV	Generalized Cross Validation
h	hour
Hz	Hertz
IPL	Inner Plexiform Layer
LCD	Liquid-Crystal Display
LSD	Least Significant Difference
LSE	Least Squares Estimation
LTP	Long Term Potentiation
MARS	Multivariate Adaptive Regression Splines
MLR	Multiple Linear Regression
m	meter
mm	millimeter
ms	millisecond
nm	nanometer
NMDA	N-methyl-D-aspartate receptor
OPL	Outer Plexiform Layer
PE	Pigment Epithelium
PERG	Pattern Electroretinogram
PLS	Partial Least Squares
PND	Posterior Nodal Distance

PRSS	Penalized Residual Sum of Squares
RGC	Retinal Ganglion Cell
sec	second
SEM	Standard Error of Means
SPSS	Statistical Package for the Social Sciences
TiO$_2$	Titanium dioxide
TMARS	Two-step Multivariate Adaptive Regression Splines
UV	Ultraviolet
VEP	Visual Evoked Potential
vGAT	vesicular GABA transporter
VGluT-1	Vesicular glutamate transporter 1
VGluT-2	Vesicular glutamate transporter 2
W	Watt

CHAPTER 1

INTRODUCTION

1.1. Aim of the Study

Visual acuity is a measure of spatial resolution of the visual system. In other words, it is a measure of the ability of detecting fine details of visual stimuli. Many behavioral tasks such as Morris water maze, Barnes maze, radial arm maze investigating spatial learning and memory in rodents rely on visual cues and animals' performance on these tasks are highly affected by their visual abilities. Therefore, it is important to evaluate animals' visual functions correctly before performing these behavioral tasks. Also in studies involving manipulations of spatial learning and memory or with transgenic or knock out animals, to ensure that the visual processing is not impaired would strengthen the value of the studies. For accurate estimation of visual acuity, all the factors including the task procedure and parameters such as brightness, luminance and contrast of the visual stimuli must be considered. The aim of the present study was to revisit Prusky's method of assessing visual acuity in C57BL6/J mice and to investigate a potential improvement in visual acuity by repeated visual discrimination training. For this purpose, using natural tendency in mice and rats to escape from water, two different behavioral assessment tasks to measure visual acuity in C57BL6/J mice are applied and compared.

1.2. Anatomy of the Mammalian Eye

The eye consists of three main layers; the external layer formed by the sclera and cornea (Kolb, 2012), the choroid and the retina (Figure 1.1). Sclera which is the outermost layer determines the structural stability and shape of the eye. Sclera is opaque while cornea is transparent and allows light rays to enter the eye. Cornea is the first refractive surface with a refractive index of approximately 1.376. Cornea is protected and lubricated by epithelial layer called conjunctiva (Garhart & Lakshminarayanan, 2012).
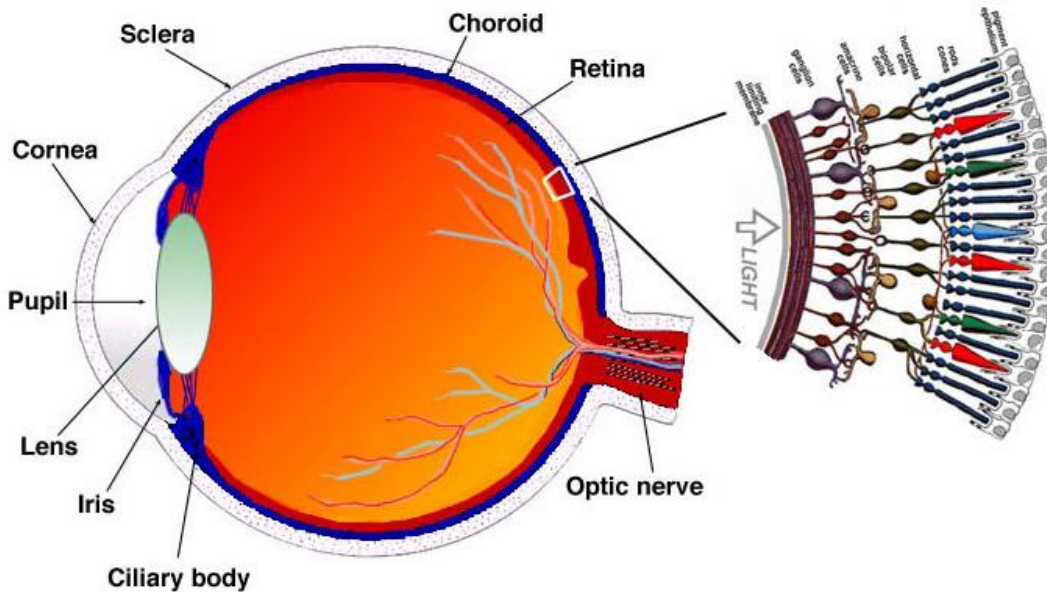
Figure 1.1: Schematic section of the human eye. (Figure taken from http://webvision.med.utah.edu/book/part-i-foundations/simple-anatomy-of-the-retina/)

The choroid layer found beneath sclera contains blood vessels and supplies oxygen and nutrients to the retina. In the front portion of the eye, choroid layer forms the ciliary body containing ciliary muscles that together with suspensory ligament adapt the shape of the lens. In the very front of the eye, there is a colored disc called iris. The iris is the portion where the pigmentation of the choroid layer can be seen since it is not covered by the sclera. It contains sphincter (circular) and dilator (radial) muscles and works as a diaphragm to regulate the size of the pupil, thus controlling the amount of light entering the eye. Behind the iris, there is a transparent, elastic but solid, ellipsoid structure called the crystalline lens. The lens is suspended in place and connected to the ciliary body by the suspensory ligaments (zonular fibers). Lens changes its shape to focus the light on the retina. To bring a near object to focus, the ciliary muscles contract, suspensory ligaments relax and the lens thickens increasing its refractive power. This process is called accommodation. To change focus to a distant object, ciliary muscles relax, tension of the suspensory ligaments increase and the lens flattens thus resulting in a decreased refractive power. The refractive index of the lens changes between 1.406 and 1.386 (Garhart & Lakshminarayanan, 2012).

Mammals usually accommodate by changing the lens curvature but some species use other ways. For example, fish move the lens only forward or backward just as a camera

lens moves to focus. Some mollusks contract or expand the whole eye and alter the distance between the lens and the retina. Birds of prey which focus on rapidly moving objects over long distances accommodate by altering the curvature of the cornea (Hecht, 2002).

The anterior chamber which is the space between the cornea and the iris is filled with aqueous humor which nourishes the anterior portion of the eye. It is an optically clear, watery liquid that is secreted into the chamber by the ciliary body and has a refractive index of approximately 1.336 for sodium D line. The posterior chamber which is the space between the lens and the retina is filled with vitreous humor which supports the eye ball. It is a transparent, jellylike substance and has a refractive index of approximately 1.336, same as the aqueous humor. Unlike aqueous humor, the vitreous humor does not get replaced (Hecht, 2002; Garhart & Lakshminarayanan, 2012).

The human retina is a multi-layered network of nerve cells consisting of approximately 200 million photoreceptors, both rods and cones. Visible light is absorbed and transformed into nerve impulses by these photoreceptors and sent to the brain by the optic nerve. Rods are sensitive to dim light (responsible for so called scotopic vision in darkness), but unable to discriminate color or generate well defined images. In contrast cones function in bright light, generate detailed and colored vision (responsible for so called photopic vision during the day), but they are not functional at low light levels (Hecht, 2002). Macula is the central area of the retina and contains twice as many cones as rods, thus enabling detection of color and fine detail. In the central region of the macula, there is fovea which consists of only cone photoreceptors. Towards the periphery of the retina, the cone density declines while the rod density increases (Garhart & Lakshminarayanan, 2012).

Retinas of all vertebrates consist of three layers of cell bodies and two layers of synapses (Figure 1.2). In the outer nuclear layer, cell bodies of rods and cones are found. The inner nuclear layer contains cell bodies of the bipolar cells, as well as horizontal and amacrine inhibitory interneurons. In the ganglion cell layer, cell bodies of ganglion cells and displaced amacrine interneurons are positioned (Kolb, 2011).
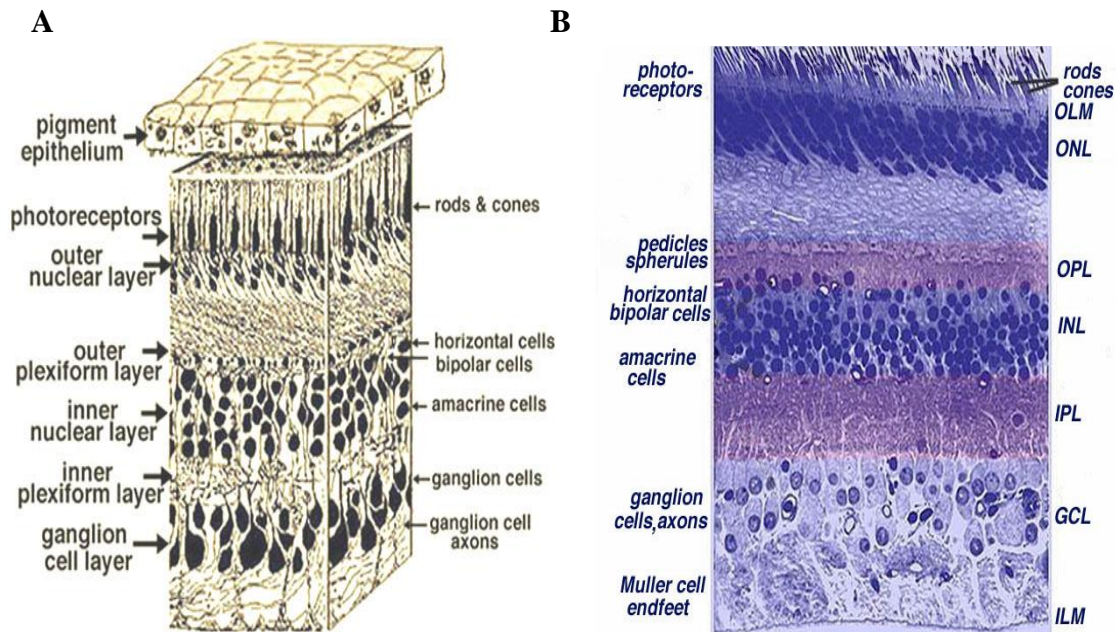
Figure 1.2: A) 3-D demonstration of a portion of human retina. B) Light micrograph of a vertical section of central human retina. (Figures taken from http://webvision.med.utah.edu/book/part-i-foundations/simple-anatomy-of-the-retina/)

Between these three cell layers, there are two neuropils where synaptic contacts take place. The first area of neuropil is the outer plexiform layer (OPL). OPL is the layer where connections between rod and cones, and vertically working bipolar cells and horizontally oriented horizontal cells take place (Kolb, 2011). The second neuropil of the retina is the inner plexiform layer (IPL) which contains the synapses between bipolar, amacrine and ganglion cells. IPL is thicker in simpler organisms like frogs, pigeons and squirrels than higher organisms like primates. The thickness of IPL is a sign of a retina performing more peripheral and specialized image processing (Garhart & Lakshminarayanan, 2012).

Pigment epitheliums (PEs) are darkly pigmented cells and they absorb the light which is not absorbed by the photoreceptors. This process reduces scattering. Diurnal species which are active during bright day light have dark PEs while nocturnal species which are active in dim light have a tapetum. The tapetum is placed behind the retina and acts like a mirror. It reflects uncaptured photons back to the photoreceptors. This creates a second chance for the photoreceptors to capture the photons and increases the sensitivity of these animals to light. The wavelength of light reflected by the tapetum is close to the absorbance peak of rhodopsin which is the photopigment contained by the rods (Garhart & Lakshminarayanan, 2012).

In human eye, there are three types of cones enabling trichromatic vision. The first type responds to light of long wavelengths in the yellow region (564-580 nm) and is named L cones or red cones, the second type responds to medium wavelengths in the green region (534-545 nm) and is named M cones or green cones, the third type responds to short wavelengths in the violet region (420-440 nm) and is named S cones or blue cones. On the other hand, the rods are sensitive to low light levels at around 420 nm (Figure 1.3) (Garhart & Lakshminarayanan, 2012).
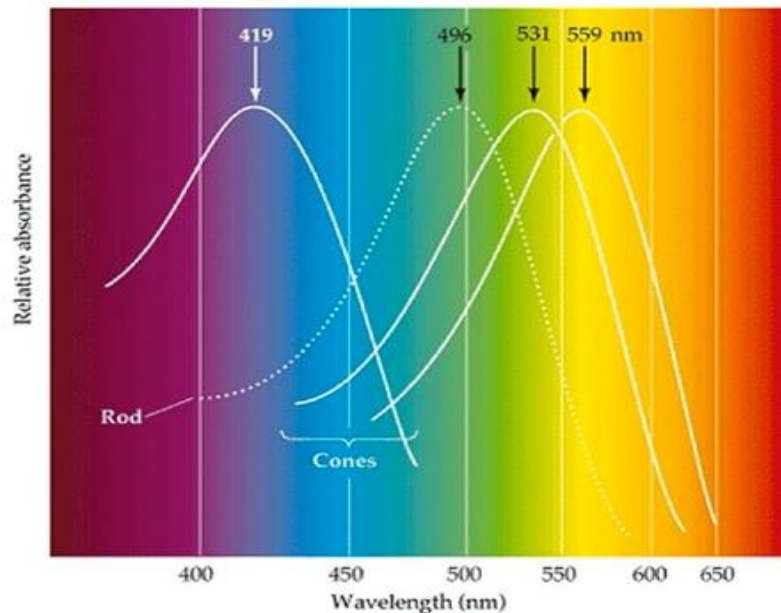
Figure 1.3: Absorbance spectra of rod and cone photoreceptors. (Figure taken from http://openwetware.org/wiki/BIO254:Phototransduction)

Absorption of photons by the photoreceptors causes bleaching of photopigments, iodopsin in cones and rhodopsin in rods, and activation of G-protein called transducin which in turn activates cGMP phosphodiesterase. cGMP phosphodiesterase breaks down cGMP (Cyclic guanosine monophosphate), an intracellular second messenger which opens cGMP-gated sodium channels. Decrease in cGMP concentration leads to closure of sodium channels, decrease in the depolarizing sodium current and thus hyperpolarization of the receptor cells (Fu & Yau, 2007). These signals are processed in the retina and sent to the higher levels of the visual system by the optic nerve which contains ganglion cell axons (Garhart & Lakshminarayanan, 2012).

When a photoreceptor absorbs light, it sends a synaptic response to bipolar cells which transfer the signal to the retinal ganglion cells. Because the number of fibers in the optic nerve (approximately 1.2 million) is much lower than the number of photoreceptors (more than 120 million), it implies a lot of neural convergence from receptors to bipolar cells and from bipolar cells to ganglion cells. The reciprocal inhibition between retinal cells known as lateral inhibition is responsible for reading contrast between the elements of visual field and for edge detection. However, in the fovea located in the middle of the retina where cone receptors are prevailing, there is almost 1:1 connection between cone, bipolar and ganglion cells so fovea generates the most detailed and accurate image as a result of a great spatial resolution. In contrast to this, in the periphery of the retina, rod cells are multiply connected to nerve fibers (Hecht, 2002), so spatial resolution declines considerably (Garhart & Lakshminarayanan, 2012).

1.2.1. Comparison of Human and Rodent (Mouse or Rat) Eyes

Rodent eye has very similar structure with human and other mammalian eyes (Figure 1.4).
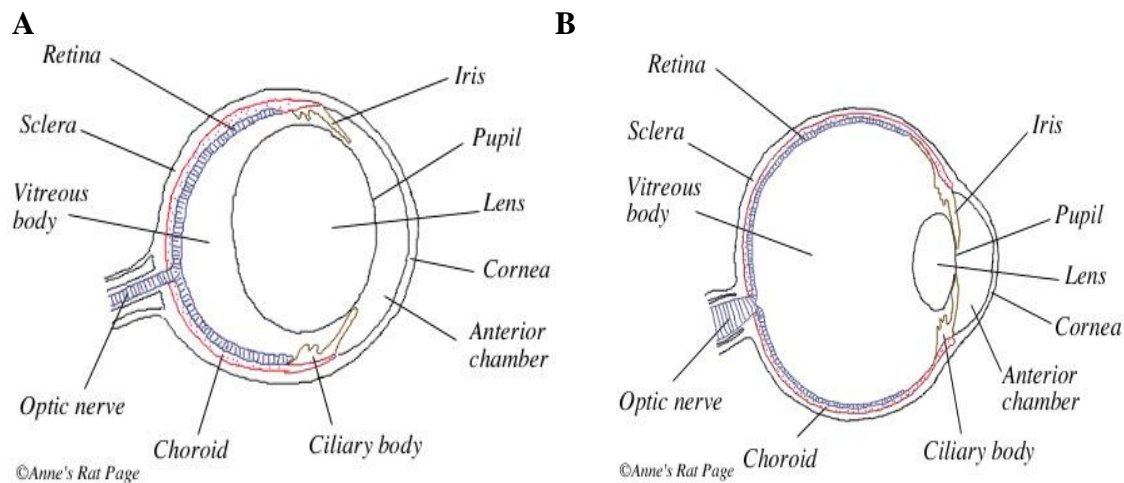
Figure 1.4: Anatomical drawing of A) Rat eye, and B) Human eye. (Figure taken from http://www.ratbehavior.org/Eyes.htm)

In both humans and rats, light passes through the cornea and then through the pupil. Like human pupil, a rat's pupil size changes according to light intensity. Observations on experiments revealed that a rat's pupil diameter ranges between 0.2 mm and 1.2 mm (Block, 1969). The duration of contraction is as fast as that of human's. A contraction from 2 mm to 0.5 mm occurs in 500 ms (Lashley, 1932).

Then, the light passes through the lens which acts as a filter selectively blocking certain wavelengths. The light wavelengths passing through the lens differ between species. For instance, rat lens allows the light visible for human and additionally almost 50% of the ultraviolet light (Gorgels and van Norren, 1992). The transmittance of the human lens ranges roughly between 390 nm and 780 nm, however people whose lenses are surgically removed gain sensitivity to ultraviolet light (Hetch, 2002). Gorgels and van Norren (1992) isolated the rat lens and measured its spectral transmittance. They measured the transmittance of the rat lens as follows; 93-95% at 700 nm, 70-80% at 400 nm, 50-60% at 360 nm, 4-18% at 320 nm and <2% at 310-300 nm indicating that the rat lens is significantly transparent to ultraviolet light.

Human lens changes its shape by contraction or relaxation of the ciliary muscle, thus refracting the incoming light to different degrees depending on the distance of the visual objects. It ensures accommodation and formation of net images on the retina. On the contrary, rat lens seems unable to change its shape. Although suspensory ligament of the rat lens is relatively larger compared to that in human, ciliary muscles of the rats are observed to be variable. Lashley (1932) found no trace of ciliary muscle in the majority of rat eyes he examined. In few rat eyes only small but clearly differentiated ciliary muscle were detected. At its maximum thickness, he observed 6 to 8 layers of smooth muscle fibers, a few of which terminate in the ciliary process. Woolf (1956) stated that rodents including the rat, mouse, rabbit, and hamster, had no cells with granular cytoplasm in their ciliary region, so he did not qualify these cells as smooth muscle fibers. Similar view had been earlier presented by Detwiler (1949) who also studied the rat's and additionally chinchilla's eye accommodation abilities. Artal *et al*. (1998) reported no change in the refractive power of the rat lens with atropine. The latter observation is in line with previous reports but does not prove inability of the lens to change its shape because the rats were anesthetized so ciliary muscles could have already been fully relaxed.

When the light reaches the retina, it is absorbed by the photoreceptors. Humans have two types of photoreceptors; rods which function in dim light and cones which function in bright light. Cones consist of three types in human; red, green and blue which are responsible for color vision. Rat retina contains rods and cones as well but it is rod-dominated since the rat is a strongly nocturnal animal and it involves only two types of cones; green (middle wavelength sensitive cones or M-cones) and blue (short wavelength sensitive cones or S-cones), so rats have dichromatic vision and cannot see reds. In addition, the rats' blue cones are sensitive to shorter wavelengths than humans' blue cones, thus making the retina more sensitive to ultraviolet light (Jacobs *et al*., 1991;

Jacobs *et al*., 2001). Behavioral experiments have shown that rats can distinguish greens, blues-ultraviolets; however their perception of color must be much weaker than ours since rats have fewer cones than we do. About 88% of a pigmented rat's cones are the middle green type, and 12% are the long blue-UV cones. Photoreceptor counts in albino rats revealed that only 1% of all photoreceptors are cones and approximately 7% of the cones contain UV-sensitive photopigment. In recent years experiments on the role of UV light brought forward an idea that the UV cones in some rodents might be a mediator on their circadian rhythm (Jacobs *et al*., 2001). Electroretinogram (ERG) and behavioral studies revealed a peak response at approximately 510 nm for the M-cone pigment of rat (*Rattus norvegicus*) (Neitz and Jacobs, 1986). Likewise, spectrophotometric measurements of reconstituted M-cone pigment of rabbit (*Oryctolagus cuniculus*) and rat (*Rattus norvegicus*) revealed maximal absorption at wavelength of 509 nm (Radlwimmer and Yokoyama, 1998). Deegan II and Jacobs (1993) stated that ERG measurements of the response of rat retina to UV light yielded a peak at 359 nm. Likewise, spectral measurement of reconstituted UV pigment revealed a maximal absorption value at 358 nm for the rat and at 359 nm for the mouse (Yokoyama *et al*., 1998). From the latter results it is seen that cone pigments of the mouse are similar to those of the rat, however, there are some differences. One of the differences between the cones of the rat and the mouse is their overall ratio. As earlier mentioned, the overall cone ratio of the rat is 1%, whereas the mouse has relatively more cones with the overall ratio of 3%. Also, in contrary to rats, mice UV cones outnumber M cones. Second difference is the spatial distribution of the two cone types. A topographic separation of M and UV cones was observed in the mouse but not in the rat retina. The dorsal retina of the mouse contains both types of cones in a ratio of 1:10 while the ventral retina contains only UV cones. This indicates that the two cone types are populated in opposite retinal halves of the mouse retina, whereas the spatial distribution of the two cone types is more homogeneous in the rat. Among other experimental animals, the rabbit has also been proved to have a heterogeneous distribution of cones over retina, however the area lacking M cones was found to be different (Szél *et al*., 2000). The third difference is related to the fact that some cones in the mouse co-express M and UV pigments whereas no such pigment co-expression is observed in rat cones (Jacobs *et al*., 2001). Also, Ekesten *et al*. (2000) stated an additional difference in the interaction of single retinal ganglion cells and cone inputs of mice compared to primates. They reported that in some regions of the mouse retina, there is no interaction between short and middle wavelength sensitive cones. This may blunt their color vision even more. Since short wavelength sensitive cones receive no excitatory or inhibitory input from the middle wavelength sensitive cones, they respond to ultraviolet light as white light. Generally, brightness seems to be more important to small rodents than color. It is much easier to train them in the brightness discrimination than color discrimination task (Jacobs *et al.* 2001).

Besides different ratios of cones and rods in small rodents and humans, in the rat retina, the receptive fields of the rat ganglion cells are larger than those in the human fovea and each neural cell responds to larger number of photoreceptors compared to that in the human retina, leading to an increase in sensitivity to light at low intensities but

producing a decline in visual acuity (Brown, 1965). The low acuity is also affected by the low capability of the rat lens to change its shape and thus accommodate to produce net retinal images of the visual objects present at different distances from the animal. There is also a great disagreement over the refractive index of the rat lens. Lashley (1932) claimed that the rat is severely myopic while Johnson (1900), Walls (1942) and Rochon-Duvigneaud (1947) stated that the rat exhibits a marked hypermetropia (Block, 1969). On the other hand, Hughes (1977) stated a refractive index close to that of an emmetropic eye when the pupil is small and a refractive index indicating ametropia when the pupil is large. With poor optics of the eye and very coarse neural grain of the retina (high convergence of photoreceptors on the retinal neurons) (Artal *et al*., 1998), rat visual acuity is more than 20 times worse than that of humans.

As a consequence of the rat's small eyes and low visual acuity, rats have a great depth of focus (depth of vision) (Green *et al*., 1980). When the eye is focused for a certain distance, the observer will have a blurred vision of nearer or farther objects (Campbell, 1957). However, the retina is not infinitely sensitive to optical blur; hence the eye's depth of focus is finite. That is to say visual stimuli from a certain distance in front of the eye to optical infinity are in equivalent focus for an unaccommodated emmetropic observer, but objects closer than this range are seen blurred (Green *et al*., 1980). In other words, depth of focus determines the range over which all visual stimuli within this range are at the same focal distance. Green *et al*. (1980) developed formulas for calculating depth of focus and showed that depth of focus is inversely proportional to the size and visual acuity of the eye. Accordingly, small eyes with low visual acuity have large depth of focus as in the case of rats. In humans, the depth of focus of the unaccommodated eye is from 2.3 meters to infinity (Green *et al*., 1980) whereas in rats, the depth of focus is from 7 centimeters to infinity (Powers & Green, 1978).

1.3. Spatial Vision and Visual Acuity

When a camera gets closer to an object, the image in the photograph appears larger. On the contrary, objects far from the camera appear smaller in the photograph. This is also valid for the retinal image. The size of an image on the retina is not determined by the object's size. The important aspect which specifies the size of the retinal image is the ratio of the object's size to its distance from the eye. The optical (physical) angle between the most distal points of the viewed object is the visual angle (θ) which can be calculated from the following equation: $\tan \theta = S / D$, where S is the linear size of the object and D is its linear distance from retina. The retinal size of the object (R) is given by the equation; $R / n = \tan \theta$, where n is the eye's nodal distance (in human eye around 16 mm). Accordingly, three objects of different sizes at different distances creates the same size of image on the retina, because they all correspond to the same angle in space (Figure 1.5) (Hodos, 2012).
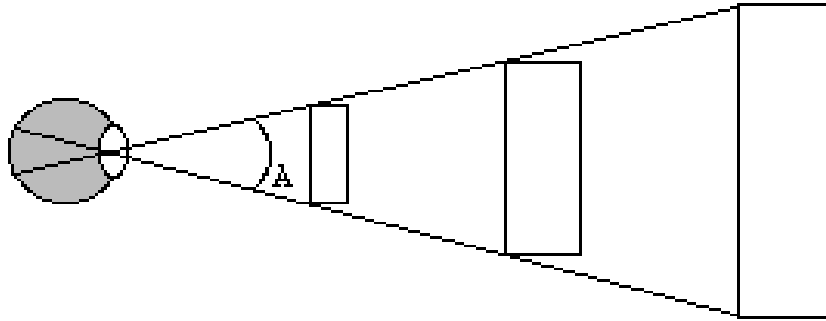
Figure 1.5: Law of the visual angle: Objects corresponding to the same angle in visual space creates the same size of image on the retina. (Figure taken from http://www.teuton.org/~dtj/essays/moon_illusion.html)

This is also known as the law of visual angle. By knowing the visual angle of a visual stimulus, the size of the retinal image can be obtained without knowing the absolute size or distance of the stimulus. Visual angle is expresses in terms of radians, degrees or minutes (Hodos, 2012).

Visual acuity, that is the ability to detect the small details of objects in the visual field, is one of the most important features of spatial vision. Visual acuity of a certain species represents the finest detail that species is able to distinguish in a pattern of high contrast. Visual acuity and discrimination plays a crucial role in animals' adaptation to their environment and their survival. For example, a bird can detect small animals to feed on while roosting on a tree, foraging on the ground or in flight by means of visual acuity. A well developed and sensitive vision also has an advantage over defense of territory, mate selection and navigation (De Valois & De Valois, 1990; Hodos, 2012; Hodos, 1993).

Visual acuity depends partly on the retinal anatomy and partly on the optics of the eye, whereas it also depends on the characteristics of the objects in visual space. In the retina, the density of photoreceptors and the number of photoreceptors converging on a single ganglion cell influence visual acuity. On the other hand, object characteristics involve luminance of the object, its contrast with the background, mobility etc. If the luminance of the object and its contrast with the background is high, visual acuity is higher (Hodos, 2012).

1.4. Factors Affecting Visual Acuity

1.4.1. Luminance of the Visual Stimuli and Environment

When we try to read a book under dim light we have difficulty in reading and after a while our eyes get tired. However, if we take a book with the same font size under bright light, we can read without any difficulty. This is an example which demonstrates that human visual acuity is dependent not only on the anatomy of the retina and optics but also on the luminance of the object. Amount of light which is reflected or emitted from the visual stimuli influences the amount of light that falls on the retina of the eye. The amount of light on the retina is termed retinal illuminance and stated in troland unit. One troland is equal to the quantity of light that falls on the retina when viewing a surface with a luminance of 1 cd/m^2 through a pupil with an area of 1mm^2. The definition particularly refers to human retina since the axial length of the eye influences the retinal illuminance. In eyes of the species with longer axial length, the image of the visual stimulus on the retina will be larger, but the illumination per unit area of the retina will be less. So, if an animal's eyes have longer axial length than human eye, the amount of trolands will reduce. On the contrary, if an animal's eyes have shorter axial length than human eye, the amount of trolands will increase. Adjustment for non-human eyes uses posterior nodal distance (PND). PND is the length between posterior nodal point of the eye and photoreceptor layer of the retina. Ratio for correction is human PND^2 / animal PND^2. Also many nocturnal animals including owls and members of Caprimulgidae family like nightjars, nighthawks, whippoorwills have a tapetum lucid which is placed behind the retina that reflects the light that has fallen on the retina back to the photoreceptors. This reflected light must also be considered while defining retinal illuminance (Hodos, 2012).

In addition to the luminance of the object (light reflected or emitted from the object) overall illuminance of the environment also influences visual acuity. At higher levels of illuminance, only cone receptors are functional (Photopic vision), whereas at lower levels of illuminance, only rod receptors are functional (Scotopic vision). At intermediate levels of illuminance both rods and cones are functional (Mesopic range). Martin (1982) compared his own results and also those from the literature on human, owls and pigeons collected under varying illuminances. He stated that under a wide range of illumination variation, humans have better visual acuity than owls and pigeons. Under photopic conditions, pigeons have better visual acuity than owls until the illuminance falls into mesopic range. In the scotopic range, humans have better visual acuity than owls only until the lowest levels of illuminance. In the lowest levels of the scotopic range visual acuity of human drops below owl visual acuity (Hodos, 2012).

1.4.1.1. The Explanation of the Variation of Visual Acuity with Illumination (Theory Put Forward by Hecht)

Visual acuity depends on the resolving power of the retina and Hecht (1927) assumed that the resolving power is determined by the quantity of light sensitive elements per unit area of the retina (Wilcox, 1932).

In case of low visual acuity, retinal elements have large distances in between. On the contrary, in case of high visual acuity, distances between retinal elements are small. If one intends to interpret the variation in visual acuity with the amount of illumination in this point of view, he or she would assume that the quantities of retinal elements per unit area of the retina are changeable. However, this is not the case because the quantity of rods and cones in the retina are fixed. Therefore, it is more sensible to suppose that the variation in visual acuity is due to variation of these retinal elements' functionality in different illumination cases. Hecht supposed that the sensitivity of photoreceptors, both rods and cones, differed individually and they varied in their absolute thresholds of response to illumination (Hecht, 1927; Hecht 1928; Wilcox, 1932).

In lowest illuminations, vision is intervened by rods. The number of functioning rods is small and this condition results in a resolving surface on the retina with the receiving points (retinal receptors) distributed distantly, so the visual acuity is low. However, as the illumination increases, more rods become functional as they reach their threshold. The distance between receiving elements becomes smaller and visual acuity increases. Once the illumination begins ascending, cones begin to function while rods are still in the play. However, since the increase rate of functioning cones with respect to the increase in illumination is nearly ten times greater than the rate of the rods, at a certain time point the quantity of functioning cones per unit area in the fovea will be greater than the quantity of rods per an equal area in the periphery. Hence, the cones will determine the visual acuity. Visual acuity increases until the point where all the cones are functioning and then remains constant (Hecht, 1927; Hecht, 1928).

1.4.2. Contrast Sensitivity

If we print a text both on a bright, white paper and on a gray paper and compare their readability, we would realize that it is much easier to read the text on a bright, white paper even if the two texts have the same font size. This example is a demonstration of how contrast influences the resolution of fine spatial images (Hodos, 2012).

Difference in the luminance between the whitest and blackest parts of an image is named achromatic contrast. If an image contains only whites and blacks, the contrast is high. However if an image contains no white and no black but only shades of gray, then the contrast is low (Hodos, 2012).

To report the amount of contrast in a grating, differential intensity threshold (Kalloniatis & Luu, 2007) which is defined in the equation of $\%C = (L_{max} - L_{min} / L_{max} + L_{min}) \times 100$, is used. In the equation, $\%C$ represents the percentage contrast, L_{min} represents the luminance of the dark bars, and L_{max} represents the luminance of the light bars (Hodos, 2012).

1.4.3. Pupil Size

The size of the pupil also affects resolution, thus visual acuity. A large pupil allows more light to fall on the retina than a small pupil. However, the size of the pupil has effect on two parameters that in turn affect visual resolution: diffraction and optical (spherical) aberration. Diffraction is spreading of light waves after passing through the pupil. The extent of spreading depends on the relative size of the wavelength of light to the size of the pupil. Spherical aberration occurs due to the increased refraction of light rays which pass through a lens nearer to its edge in comparison with those that pass nearer to the center. Thus, all incoming light rays end up focusing at different points or in other words do not converge at the same point after passing through the lens. A large pupil reduces diffraction but optical aberrations affect the resolution while a small pupil reduces optical aberrations but diffraction limits the resolution. Optimal pupil size is between 3 mm and 5 mm, compensating the diffraction and aberration limits (Kalloniatis & Luu, 2007).

When we enter a dark room from a bright environment, the eyes first adapt by contracting the radial muscles in the iris, thus enlarging pupils to allow more light into the eye. Over a period of about 30 minutes, other chemical adaptations take place to make rods sensitive to light at about a 10.000th of the level required for the cones to respond. After then we are able to see much better in the dark (Gibbs, 1996).

1.4.4. Refractive Errors

Refractive errors affect visual acuity by causing defocus on the retina and thus blur fine detail and decrease contrast sensitivity. Refractive errors cause visual acuity disorders such as myopia (nearsightedness), hyperopia (farsightedness), astigmatism, keratoconus (Kalloniatis & Luu, 2007).

In a myopic eye, the eyeball is too long, thus the image is focused in fronted of the retina. In a hyperoptic eye, the eyeball is too short, thus the image is focused behind the retina (Kalloniatis & Luu, 2007).

Astigmatism is a condition such that when lines along one axis are in focus, lines along the perpendicular axis are out of focus. It occurs as a result of a cylindrical component in the cornea or lens of the eye (Daw, 1995).

Keratoconus is a progressive disorder in which corneal stroma becomes thinner and cornea takes a conical shape. The non-inflammatory thinning of the cornea causes irregular astigmatism, myopia and protrusion. Keratoconus may lead to mild to severe impairment and blurriness of vision (Rabinowitz, 1998).

In an emmetropic eye, regardless of the distance of a visual object from the eye, the image of a visual stimulus is focused sharply on the retina, thus resulting in perfect visual acuity (Kalloniatis & Luu, 2007). In human, eye accommodation takes place when looking at close objects at 6m or less, primarily by changing the lens curvature. The second element of accommodation is pupil constriction reducing spherical aberration which increases when light source approaches the eyes. The third component of accommodation process is the eye convergence reflex. It is related with binocular vision in human and ensures that optical images in both eyes are formed on corresponding areas within the central retina.
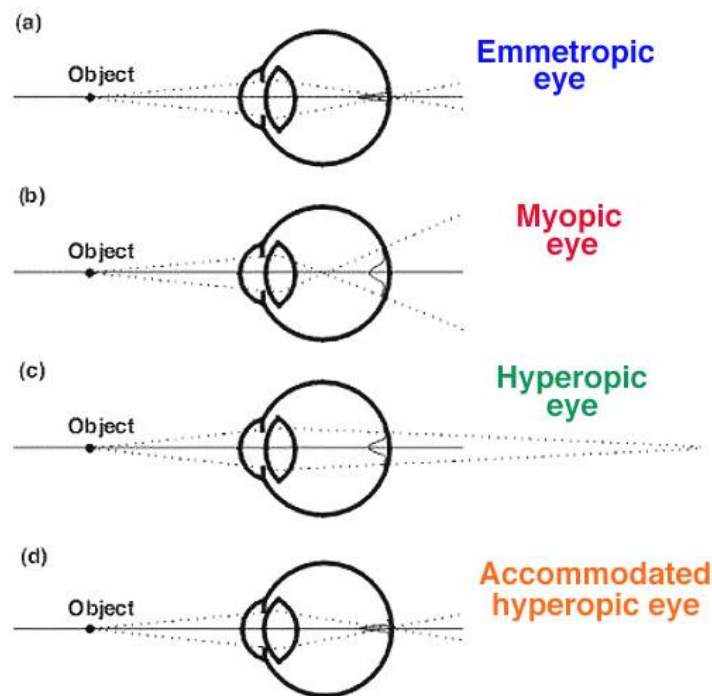
Figure 1.6: Refractive errors which cause visual acuity disorders. (Figure taken from http://webvision.med.utah.edu/book/part-viii-gabac-receptors/visual-acuity/)

1.4.5. Age

Another factor affecting visual acuity is age. Human visual acuity is known to show a peak in young adulthood and a slow decline with each decade afterwards (Hodos, 2012). Decline in the visual acuity with aging occurs due to changes in the optical media of the eye or the central visual system or due to degenerative changes in the retina. Changes which take place in the eye are affected by intensity, duration and spectral composition of light exposure history (Hodos, 1993).

Hodos *et al*. (1991a) tested 17 pigeons that ranged in age from 2 to 17, with high-contrast, square-wave gratings and observed a systematic decline in visual acuity with age. Also, Porciatti *et al.* (1991) recorded electroretinograpic changes in 2-year-old and 10-year-old pigeons and their results were in agreement with age-related losses in visual acuity. A similar decline with aging is reported also for quail (Hodos *et al*., 1991b). Decline in visual acuity with aging has been correlated with photoreceptor and retinal ganglion cell losses. Besides photoreceptor losses, pigeons also have a disease called senile mitosis which leads to a progressive reduction of the maximum pupil diameter with age. Senile mitosis is also seen in humans (Hodos 1993).

Kurkjian and Hodos (1992) stated little alteration in the intensity difference thresholds and no age-related alteration in the visual search (a sensitive indicator of visual aging) of pigeons over the same age span in which visual acuity drops off. These results are important since they indicate that the acuity losses in pigeons are specific to spatial vision and are not related to general age-dependent alterations which could affect cognitive functions such as memory or attention (Hodos, 1993).

1.5. Visual Acuities of Different Species

There are numerous studies on visual acuities of different species including vertebrates and invertebrates. Visual acuity can be estimated by different methods: anatomical, behavioral and electrophysiological methods.

In fish photopic visual acuity is estimated in two ways: anatomically and behaviorally. Anatomical estimates (histological acuity) can be quantified by measuring the density of cone receptor cells in the retina. Behavioral estimates can be quantified by measuring reactive distance which is the distance at which fish responds to a prey (Miller *et al.*, 1993). Gagnon *et al*. (2013) measured visual acuity of 24 pelagic fish species, 5 cephalopods and a gastropod and revealed that the hatchetfish *Argyropelecus aculeatus*, *Sternoptyx diaphana* and the barrel-eye *Opisthoproctus soleatus* are capable of focusing high spatial frequencies whereas for *Avocettina infans*, *Benthosema suborbitale*, *Gonostoma elongatum*, and Scopelosaurus *hoedti* acute vision is important as well.

Birukow (1937) measured the optomotor response of the common frog (*Rana temporaria*) and assessed an acuity of 4.3 cpd which was an unexpectedly high value relative to the estimations derived from retinal cell mosaics (Aho, 1997). However, Aho (1996) also tested the visual acuity of frog (*Rana pipiens*) for gratings, with a two-choice prey-dummy setup, under bright white light and under different brightness levels of green light (500 nm) and measured the highest visual acuity of 2.8 cpd under maximum level of green light. Aho's method yielded a visual acuity value which is more coherent with the retinal grain of frogs. In addition, the visual acuity was measured 0.7 cpd when the brightness was reduced by six orders of magnitude (Aho, 1996).

Birds constitute the most visual dependent class among vertebrates (Hodos, 1993). In nocturnal birds, for instance owls (Fite,1973; Martin & Gordon, 1974; Porciatti *et al*., 1989) and quail (Hodos *et al*., 1991a) visual acuity differs between 6 and 8 cpd. Pigeons have a visual acuity between 12-18 cpd (Ghim & Hodos, 2006; Hahmann & Güntürkün, 1993; Hodos *et al*., 1976; Porciatti *et al*., 1991; Rounsley & McFadden, 2005). Corvidae family which includes crows, rooks, jays, jackdaws, magpies and others have visual acuities varying between 15-33 cpd (Dabrowska, 1975; Fite & Rosenfield-Wessels, 1975). Falcons can distinguish 40-73 cpd (Gaffney & Hodos, 2003; Hirsh, 1982; Reymond, 1987), and eagles are able to detect 120-143 cpd (Reymond, 1985; Shlaer, 1972). In the real world, a spatial resolution of 43 cpd of a falcon corresponds to detecting an insect of 0.23 cm long from a distance of 12 m. Similarly a spatial resolution of 130 cpd of an eagle corresponds to detecting the same insect from 35 m (Hodos, 2012).

Mammals have large variation in visual acuity, ranging from low visual acuity of microchiropteran bats and small rodents (0.4–1.0 cpd) to high visual acuity of diurnal anthropoid primates (30–64 cpd). It is hypothesized that species with higher visual acuities rely on vision more than species with lower visual acuities for their basic needs such as finding food and avoiding predators. Likewise, the lower visual acuity of some species may indicate their reliance on nonvisual senses rather than visual capabilities (Veilleux & Kirk, 2014).

Gianfranceschi *et al*. (1999) summarized from various sources; the retinal ganglion cell (RGC) density, retinal magnification factor, estimated visual acuity and behavioral acuity of some mammalian species (Table 1.1). In species that have one-to-one correspondence between their cones and ganglion cells in the highest density region of the retina, like the primate fovea, the upper limit of visual acuity is determined by the density of the cones, whereas in species in which there is a significant degree of convergence of cones onto ganglion cells, visual acuity can be estimated from the peak density of the retinal ganglion cells (RGC) (Gianfranceschi *et al*., 1999).

Table 1.1: Visual acuity estimated from retinal RGC density and behaviorally determined acuity.

Species	Peak RGC (density/mm^2)	Retinal magnification factor (mm/deg)	Estimated visual acuity (cpd)	Behavioral visual acuity (cpd)
Cat	7000	0.22	9	6
Dog (beagle)	12200	0.18	10.2	6.3
Dolphin	671	0.25	2.5	2.4
Rabbit	2500	0.17	4.3	3.4
Horse	6500	0.47	20.37	22.25
Microchiropteran bat (*Rhinolophus ouxl*)	2000	0.0016	0.35	0.2
Native cat (*Dasyurus hallucatus*)	2600	0.01	2.6	2.5
Wild type mouse	4500	0.015	1	0.6
Bcl2 transgenic mouse	10100	0.015	1.6	0.6
Rat	2000	0.59	1.3	1

Figure 1.7 shows the plot of estimated and behavioral visual acuities of the mammals listed in Table 1.1. For most species the behavioral acuity is very close to the estimated acuity, however for the species whose habits do not depend primarily upon vision, the behavioral visual acuity is lower, as in the case of the rat and the mouse (Gianfranceschi *et al.*, 1999).
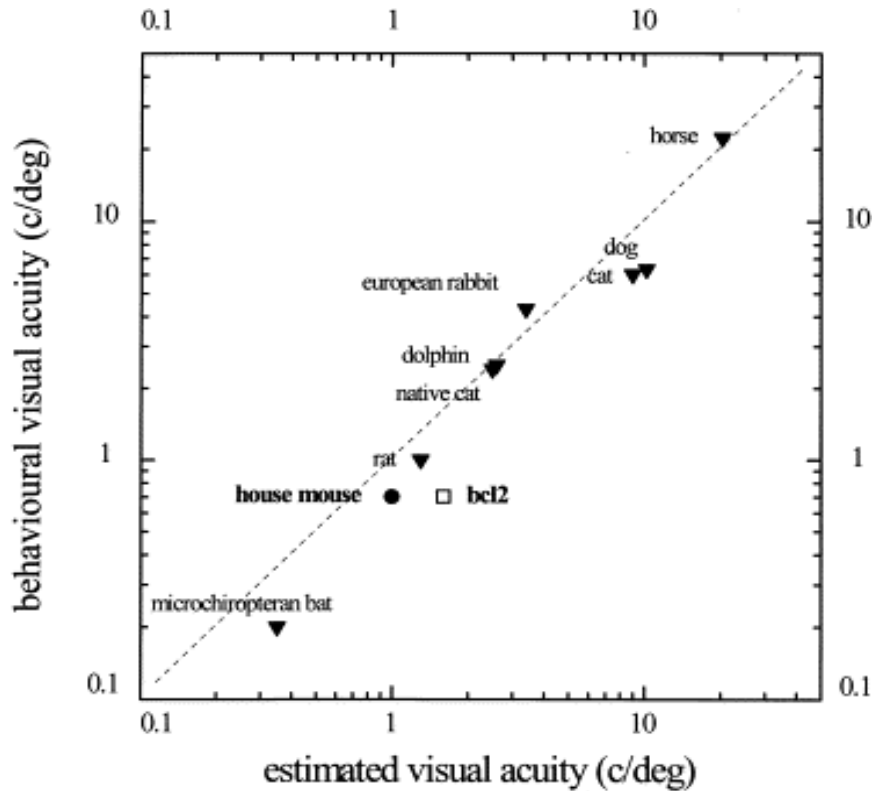
Figure 1.7: Plot of estimated and behavioral visual acuities of mammals. (Figure taken from Gianfranceschi *et al*., 1999)

RGC of *Bcl2* transgenic mouse is twice that of wild type mouse, so estimated visual acuity of *bcl2* mouse is higher than estimated visual acuity of wild type mouse; however behavioral acuities of the two strains are the same. This finding indicates that the presence of more neurons than normal do not conclude with higher behavioral visual acuity. A possible reason for this may be a rewiring of the visual pathway (Gianfranceschi *et al*., 1999). Vast of the studies with rodents reveal a visual acuity of ~1 cpd for rats, ~0,5 cpd for albino rats and ~0.5 cpd for wild type and *bcl2* mice (Prusky *et al*., 2000; Gianfranceschi *et al*., 1999; Sinex *et al*., 1979).

Albino animals have a number of differences in their visual systems and their vision is poorer than that of normally pigmented animals. The main reason of albinos having poor vision is that they have melanin pigment neither in the iris which controls the amount of incoming light nor deeper in the eye where normally light is absorbed. Consequently, light scatters inside the eye and over time causes retinal degeneration. In addition, albinos have abnormal neural connections between the eyes and the brain compared to normally pigmented individuals. Thus, studies on vision are often carried out on pigmented strains (e.g. C57BL/6 strain) rather than albino strains.

In various studies with primates, visual acuity of chimpanzee, rhesus monkey and cebus monkey are found to be very close to human visual acuity which is 30 cpd in healthy individuals (Spence, 1934; Weinstein & Grether 1940). Matsuzawa (1990) stated that a 6.5-year-old female chimpanzee learned to discriminate letters of the alphabet perfectly in a matching-to-sample task with 26 letters as choice alternatives, and a visual acuity test involving letters of various sizes revealed that the chimpanzee's acuity was comparable to that in healthy humans. Cavonius and Robbins (1973) compared the ability of rhesus monkeys (*Macaca mulatta*) to detect the gap in Landolt C test with similar human data and stated that at high luminance levels the acuity of human is slightly better than that of rhesus, but rhesus have better acuity at scotopic luminance levels.

Veilleux and Kirk (2014) investigated the relationship between eye size and visual acuity in a sample of mammals. Their results showed that visual acuity is positively correlated with eye length and ~35% of the variation in visual acuity between mammalian species can be explained by the variation in the eye length. These results suggest that larger eyes enable more detailed sampling of a larger retinal image by the photoreceptors, thus mammals with larger eyes tend to have higher visual acuity than mammals with smaller eyes. However, this rule is not valid for invertebrates; the spatial acuity of Salticids (Jumping spiders) exceed that of known for any other animal with similar eye size (Harland *et al*., 2012). Veilleux and Kirk (2014) also identified several species which have higher visual acuity than the other species in their taxonomic groups, including the giraffe (*Giraffa camelopardalis*; 25.5 cpd), cheetah (*Acinonyx jubatus*; 23 cpd) and western grey kangaroo (*Macropus fuliginosus*; 11.2 cpd).

1.6. Psychophysical Methods Used in Visual Acuity Experiments

Psychophysics, which was procreated by G.T. Fechner in 1860s, is a set of experimental and statistical methods for mathematically quantifying sensory experiences resulting from an external physical stimulus. In a classical psychophysical approach, the weakest stimulus a subject can detect is defined as a threshold. Although the threshold varies for different individuals, it is assumed that at one point in time it is not perceived by any individual (Engen, 1988). Many models have been developed for evaluating sensory capabilities of animals (Luce & Krumhansl, 1988), but the most common used methods with animals are; the method of limits and the method of constant stimuli (Hodos, 2012).

In the method of limits, the subject is presented with a series of stimuli, below and above the threshold, with small differences in intensity and in an ascending or descending order (Engen, 1988). In the descending series, the subject is asked to specify when he or she cannot detect the stimulus further but can detect the adjacent one. In the ascending series, the subject is asked to specify when he or she can first detect the gradually strengthening stimulus (Hodos, 2012).

In the method of constant stimuli, two stimuli are presented to the subject at a time. One of the two stimuli is the standard and is always the same (constant stimulus), while the other stimulus changes in each trial. After the subject learns to discriminate the standard stimulus and the variable stimulus, he or she is presented a series of variable stimuli, each paired with the constant stimulus, and asked to make the judgment of standard and variable in each trial. The percentage of correct judgments is plotted as a psychometric function to assess the smallest noticeable difference between the constant and variable stimulus. Various methods are developed for different species to indicate their choice of stimulus during the experiment. To acquire data from animals, psychophysical methods are integrated with classical methods of animal learning which use rewards or punishments. This provides animals to indicate their choices which give information of whether they have detected a stimulus or have been able to discriminate between the stimuli. In the absolute threshold experiments, the threshold is usually accepted as the midpoint of no discrimination and perfect discrimination, which corresponds to the stimulus intensity that can be detected 50% of the time. On the other hand, if the experiment relies on a relative judgment to detect the finest difference between stimuli that is readily detectable, 50% correct corresponds to chance performance. In these experiments, the threshold is accepted at the midpoint of chance performance and perfect performance, which corresponds to the stimulus with 75% (sometimes 70% or 80%) correct performance (Hodos, 2012).

1.7. Measurements of Spatial Resolution

1.7.1. Snellen Eye Chart

In humans visual acuity is measured by variations of Snellen eye chart which was first presented by the Dutch ophthalmologist Hermann Snellen, in 1862. Snellen chart involves a series of letters with the top row having the largest letter and each subjacent row gradually having smaller letters. In clinical examinations, the patient views the chart at a constant distance and is asked to state the lower row she or he can read. Visual acuity is put into report as the Snellen fraction that is the ratio of the distance at which patient can read the letters to the distance at which a person who has healthy vision without any disorders can read the letters. Standard viewing distance is 20 feet (6 meters) so that a person with normal vision has a Snellen fraction of 20/20 or in metric units 6/6. So, a patient with Snellen acuity of 20/40 is able to read the letters at 20 ft. when a person with normal vision is able to read at 40 ft. It is important to notice that the normal values refer to an untrained subject. When a subject is trained by viewing gratings under optimal illumination in laboratory conditions, he or she can perform a higher visual acuity than the so-called normal values (Hodos, 2012; De Valois & De Valois, 1990).

Figure 1.8: Snellen eye chart (Figure taken from http://www.allaboutvision.com/eye-test/)

1.7.2. Landolt C and Illiterate E Charts

Measuring visual acuity with a standard Snellen chart has some disadvantages. One problem is that some letters are more easily distinguishable while some letters are more difficult to distinguish even if they are in the same size. Distinguishing B and I, is much easier than distinguishing B and R. In the example of B and I, general shapes of the letters are adequately different to distinguish, so a person with a poor visual acuity may still be able to identify the letters by using low spatial frequency components even if she or he cannot discriminate the fine details that are based on high spatial frequencies components. One solution that is being used to overcome this problem is using nearly equal discriminable letters in the chart. Another problem is that when the length of rows in the chart is constant the number of letters per row increases as the size of the letters and their relative spacing decreases. In this situation, a person may have a different visual acuity performance than if the number of letters and their spacing were equal in each row. Bailey and Lovie (1976) introduced a new design of the chart using equal number of letters on each row and between-letter, between-row spacings equal to the letter size (De Valois & De Valois, 1990).
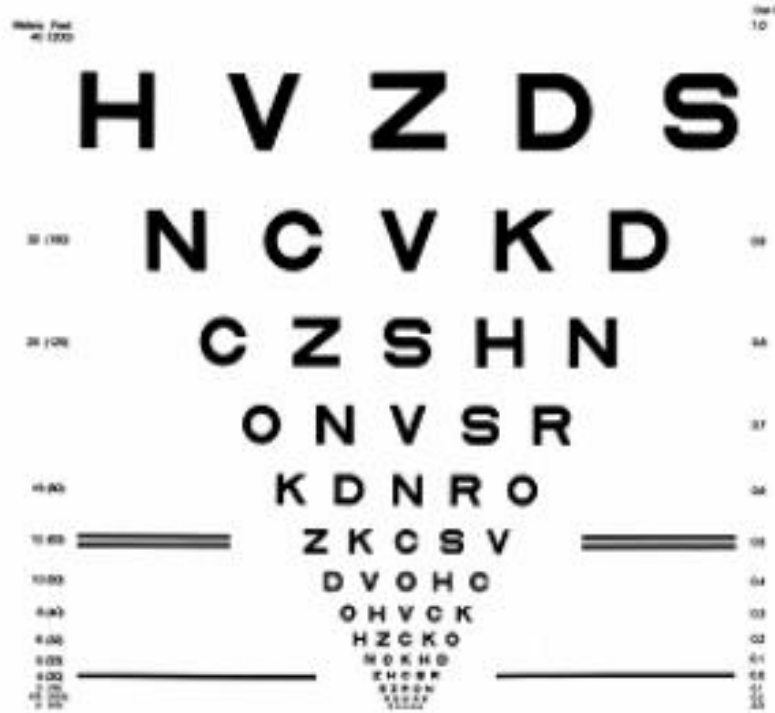
Figure 1.9: Bailey-Lovie chart. (Figure taken from http://www.visionaware.org/info/your-eye-condition/eye-health/low-vision/low-vision-examination/1235)

Snellen chart also has a limitation that only people who can read the alphabet can be examined. This restricts the use of the chart with small children and people who cannot read. To overcome these problems two other variations of the chart are also used. One of them is Landolt C chart which uses circles with one side cut off, like a C letter. A circle can have a gap at any of the four directions; top, bottom, right, left and the subject is asked where the gap is. Another version named illiterate E or tumbling E chart uses a stimulus resembling the capital letter E. Similar to the Landolt C chart, stimulus E can point any of the four directions and the subject is asked to tell the direction. Both two tests overcome the necessity of letter identification (De Valois & De Valois, 1990).

A   **B**
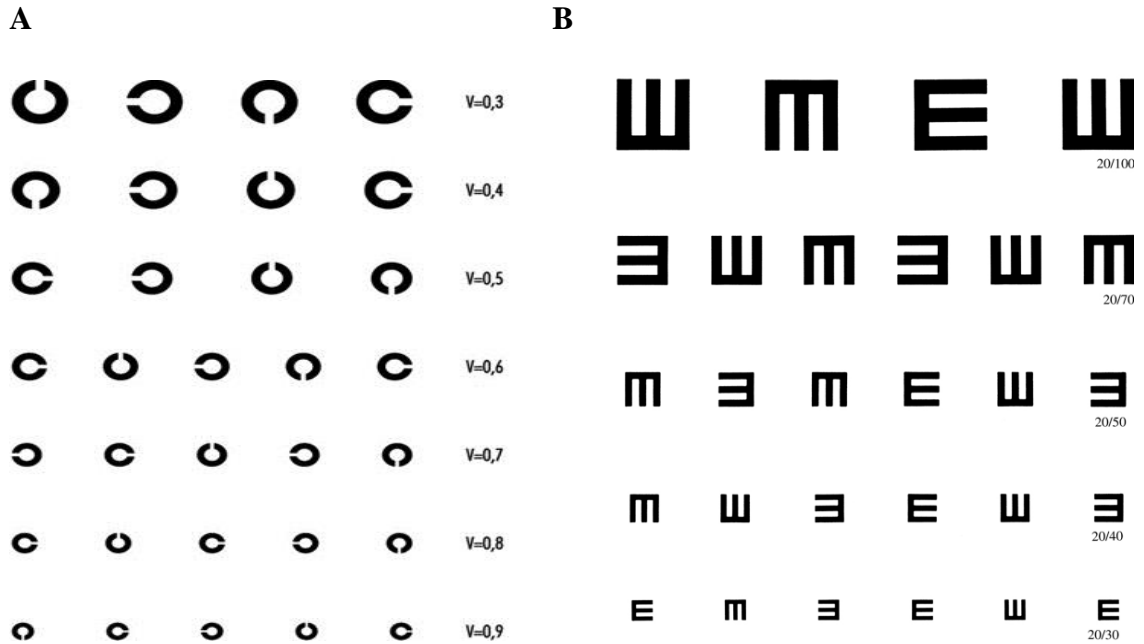
Figure 1.10: A) Landolt C and B) Illiterate E charts. (Figures taken from A) http://www.ilo.org/oshenc/part-i/sensory-systems/item/461-vision-and-work and B) http://www.aao.org/eyecare/treatment/upload/Test-Chart-for-Children.jpg)

Snellen chart is efficiently used in clinical examinations of visual acuity to assess patients' quality of vision for reading, however, which parts of the letters are being used by the patients is not precise. Therefore, in laboratory studies of visual acuity assessment, black and white gratings are used as visual stimuli. Gratings are comprised of black bars alternating with white bars of equal width. To assess visual acuity by gratings, different spatial frequencies are used when presenting black and white bars. As the spatial frequency increases, width of the bars decreases. Percentage correct versus spatial frequency is plotted and according to a criterion of 75% correct (midpoint between random guessing of 50% and perfect performance of 100%), finest grating that can be distinguished is identified. Different units are used to represent visual acuity, but most common used one is the spatial frequency of gratings in cycles/degree of visual angle, in which one cycle corresponds to one bar-space pair. Table 1.1 shows different units of spatial frequency used in visual acuity studies (Hodos, 2012).

Table 1.2: Some units of spatial frequency

Unit	Formula
Visual Angle in Minutes	Stimulus height or width / distance x 57.3 x 60
Visual Angle in Minutes	Snellen chart acuity denominator / 20
Cycles/degree of visual angle	30 / minutes of visual angle
Decimal Acuity	1 / minute of minimal separable visual angle

1.7.3. Square Wave and Sine Wave Gratings

Typical visual acuity experiments make use of gratings which usually consist of uniform dark and light bars. If a tiny photocell is passed over such a grating, the resulting electrical signal will be a square wave. A square wave appears as rectangular peaks and troughs. Width of the rectangles informs of the spatial frequency of the grating and amplitude of the rectangles informs of the intensity of illumination. Although a square wave looks simple, a square wave is a sum of a series of sine waves, so a square wave grating consists of many spatial frequencies (Figure 1.10) (Hodos, 2012).
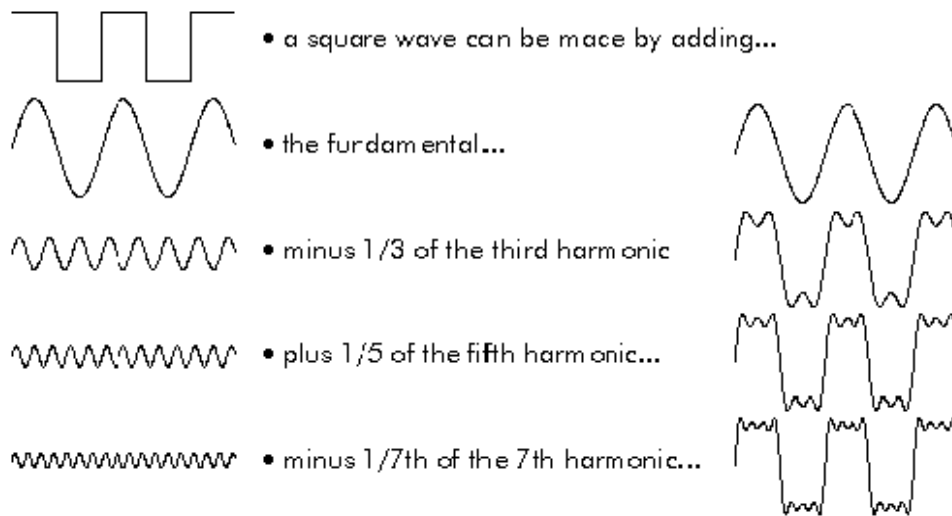
Figure 1.11: The figure shows that a square wave can be constructed by adding together a series of sine waves. (Figure taken from http://www.bores.com/courses/intro/ freq/3_ft.htm)

If we want to study spatial frequency as an independent variable, we would rather use a grating consisting of only one spatial frequency that is a sine wave grating. If a tiny photocell is passed over a sinusoidal grating, the resulting electrical signal will be a sine wave. The frequency of a sine wave represents the number of oscillations per unit distance. For instance, a certain spatial frequency that is an oscillation of luminance or color in space might be 5 cycles per centimeter, but since the dimensions of the visual stimuli are defined in terms of the angle subtended at the eye, the spatial frequency in vision is defined in cycles per degree visual angle (c/deg or cpd) (Hodos, 2012; De Valois & De Valois, 1990). The term cycles per degree corresponds to number of cycles (one black-one white bar pairs) of a grating subtending an angle of 1 degree in the eye (Figure 1.12) (Goldstein, 2010).

A   B
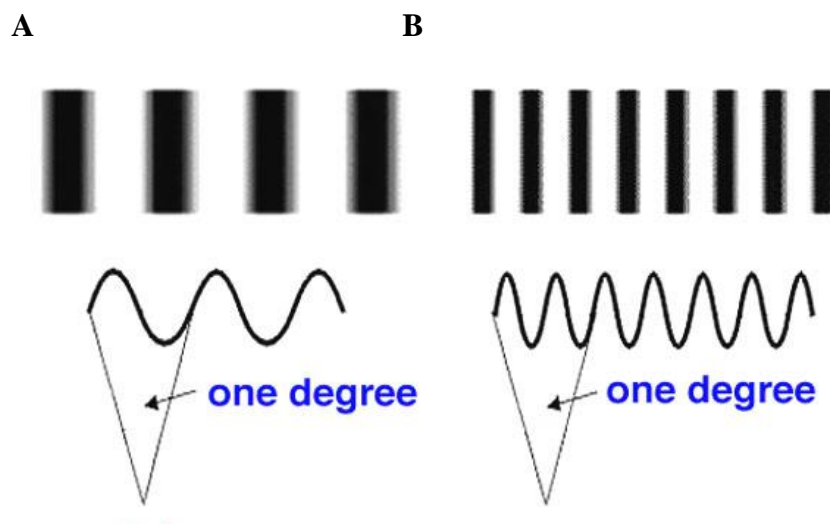
Figure 1.12: A vertical grating with a spatial frequency of A) One cycle per degree, B) Two cycles per degree. (Figure taken from http://webvision.med.utah.edu/book/part-viii-gabac-receptors/visual-acuity/)

The amplitude of a sine wave is the distance from peak to trough of the wave divided by 2 and varies according to the intensity of the grating's luminance. Unlike a square wave grating, a sine wave grating does not consist of uniform dark and light bars. In a sine wave grating, the light bars are darker at their edges and lightest in the center, and conversely dark bars are lighter at their edges and darkest in the center (Figure 1.11). This eliminates the trouble that sharp edges and corners contain many high spatial frequencies as in a square wave grating (Hodos, 2012; De Valois & De Valois, 1990).
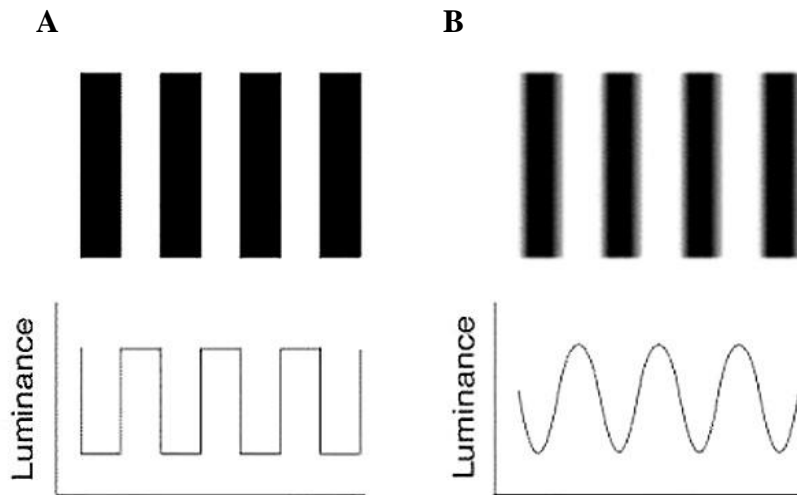
Figure 1.13: A) A square wave grating and B) A sine wave grating. (Picture taken from http://webvision.med.utah.edu/book/part-viii-gabac-receptors/visual-acuity/)

1.7.4. Pattern Electroretinogram (PERG) as an Alternative Psychophysical Tool

Besides behavioral psychophysical measurements, there are approaches to measure visual acuity by applying electrophysiological methods. One of these approaches uses pattern electroretinogram (PERG) to measure responses to visual stimuli of certain patterns. In PERG method, black and white bars of square-wave gratings are presented to an anesthetized subject. Usually spatial frequencies alternating between 7 Hz and 10 Hz are used and gratings are viewed monocularly. An electrode is placed on the cornea or the virtual chamber of the eye and detects the PERG wave generated in the retina at the transition of black and white bars. The PERG wave is amplified, averaged according to the signal-to-noise ratio and filtered to remove the artifacts. A psychometric function is constituted by plotting the PERG amplitude versus the spatial frequency. At square wave gratings of lower spatial frequencies the amplitude of the PERG wave is relatively higher and at square wave gratings of higher spatial frequencies the amplitude of the PERG wave is relatively lower (Hodos, 2012).

Gaffney and Hodos (2003) used PERG method to measure visual acuity of nine American kestrels (*Falco sparverius*). They used square-wave gratings reversed at a 7.5 Hz and averaged 896 reversals at each spatial frequency. Spatial frequencies used were 0.0, 1.22, 1.63, 2.44, 3.25, 3.91, 4.88, 6.51, 9.76 and 19.53 cpd. Figure 1.12 (A) shows PERG waves recorded from a single American kestrel at four spatial frequencies and during noise condition. Each recording shows the average of 896 reversals. The PERG amplitude decreases as the spatial frequency increases (Gaffney & Hodos, 2003).
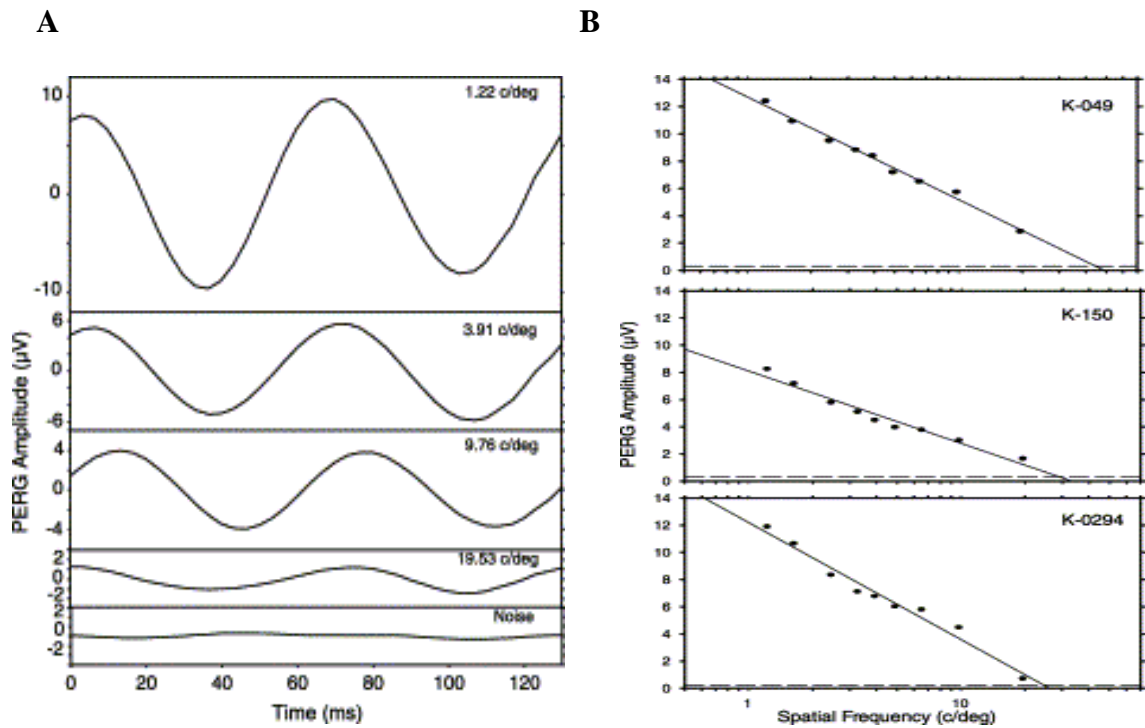
Figure 1.14: A) PERG waves from a single American kestrel at four spatial conditions and noise condition. B) Psychometric functions for three American kestrels; having the highest, lowest and intermediate acuities. (Figures taken from Gaffney & Hodos, 2003)

To assess visual acuity, psychometric functions were constituted by plotting PERG amplitudes versus spatial frequency. Figure 1.12 (B) shows psychometric functions for three American kestrels; having the highest, lowest and intermediate acuities. Dashed line at the bottom indicates the noise level. Visual acuities were defined from the intersection point of regression line and noise line. The acuities ranged between 25 and 45 cpd, mean acuity was 31.4 ± 2.00 SEM cpd and the median acuity was 29 cpd (Gaffney & Hodos, 2003).

Although PERG method is time saving when compared to behavioral methodology, it is important to interpret the data correctly. Hodos *et al*. (2002) who compared the behavioral and PERG methods in assessing contrast sensitivity in pigeons, stated that PERG results are underestimating the visual acuity values obtained with behavioral methods by 37%. In behavioral methodology, data are obtained through binocular viewing which uses the area straight ahead of the bird, an area with a high ganglion cell density. On the other hand, PERG data are obtained through monocular, lateral viewing which also uses another area with a high ganglion cell density. The reason for the difference of the regions being stimulated is the laterally localized eyes of the pigeons.

Birds which have lateral eyes view lateral stimuli with fovea centralis whereas they view frontal stimuli with area dorsalis. Both regions are rich of photoreceptors and ganglion cells but their ganglion cell densities differ by 15%. Fovea centralis which is the region used in PERG method has higher receptor and neuron density. When measuring visual acuity by PERG method, one should take into account to adjust the data by the correction factor (Hodos *et al.*, 2002).

1.8. Visual Acuity Studies with Rodents

In early studies of visual acuity in rodents, discrimination studies constituted a basis (Ash, 1951). Yerkes and Watson (1911) developed a task to measure visual discrimination in rats. In this task, right and left sides of a barrier were marked, each with a different geometrical shape, and if the rat made an incorrect choice an electric shock was given from the floor grid (Corsini, 2002). Lashley (1930) developed a task to measure visual discriminations in rats by a jumping stand in a two-choice paradigm (Prusky *et al*., 2000). The task comprised of a platform on which the rat is placed and two vertical cards each containing a visual stimulus. If the rat jumped towards the right stimulus, a door swang open, the rat landed in a chamber and received a food reward. If the rat jumped towards the wrong stimulus, it bumped against a fixed door and fell into a net below. Waller *et al*. (1960) used a simple water maze to investigate the relationship between water temperature and performance in a black-white discrimination task.

Wiesenfeld and Branchek (1976) trained hooded rats to discriminate horizontal vs. vertical stripes in a maze and tested on stripes subtending 0.5°, 1°, 2° and 4° of visual angle at various distances from the choice point. They found the limit of acuity 1° for most rats at a distance of 20 and 30 cm from the choice point. Sinex *et al*. (1979) estimated the visual acuity of mice 0.5 cpd by an optokinetic investigation. Baker and Emerson (1983) used a two-alternative forced-choice task in a jumping stand and measured the visual acuity of the gerbil, for a horizontal square-wave grating, about 1.5–2.0 cpd. In addition, they indicated that visual acuity for horizontal gratings is reliably better than that for vertical gratings. Seymoure and Juraska (1997) investigated the influence of sex on visual acuity of adult hooded rats by using a forced-choice Y maze and a jumping stand. They found no sex differences in visual acuity thresholds of adult hooded rats and assessed the visual acuity between 1.0 cpd and 1.6 cpd for both sexes. Gianfranceschi *et al*. (1999) used food as a reinforcement in a similar behavioral visual acuity task and assessed the visual acuity of 0.5 cpd for wild type mice and 0.6 cpd for *bcl2* transgenic mice. Porciatti *et al*. (1999) recorded visual evoked potentials (VEPs) from the primary visual cortex and assessed the visual acuity of C57B7L/6J mice 0.6 cpd.

Prusky *et al*. (2000) used a visual water task, which combines the working principles of a Thompson box and a Morris water maze, to assess visual acuity in mice and rats. In the visual water task, a grating was displayed randomly on one of the two monitors at the

wide end of a trapezoidal-shaped tank containing water, animals were trained to swim towards the screen displaying the grating and escape to a platform hidden below it. By using the visual water task, Prusky *et al*. (2000) assessed the visual acuity of C57BU6 mice around 0.5 cpd and the visual acuity of Long-Evans rats around 1.0 cpd. Prusky and Douglas (2003) also used the visual water task to measure visual acuity in each eye of the monocularly and binocularly-deprived mice.

Robinson *et al*. (2001) developed a task enabling to measure visual acuity in the Morris water maze. Two cue cards containing vertical black and white stripes were presented in two adjacent quadrants of the pool. The pool was separated by a barrier with the escape platform located under the cue card with the smaller stripes (1 cm wide). Once animals reached a criterion of 80% correct responses, the cue card with wider stripes (5 cm wide) was randomly changed with different cards having stripes of different widths (1, 2, 3, 4, 5, 10 cm wide). Robinson *et al*. reported that animals learned the discrimination with an acuity of 1.5 cpd.

Based on the procedure of Prusky *et al*., Wong and Brown (2006) measured visual acuity in 14 strains of mice and reported that mice known with normal vision (129S1/SvlmJ, C57BL/6J, DBA/2J) and one albino strain (AKR/J) performed very well while other albino strains (A/J, BALB/cByJ, BALB/cJ) needed longer time to learn the task and reach the arbitrary criterion of visual acuity. They also reported that mice with retinal degeneration (C3H/HeJ, FVB/NJ, MOLF/Ei, SJL/J) and strains with unknown visual skills (CAST/Ei, SM/J, SPRET/Ei) performed only at chance levels.

Wong and Brown (2007) also evaluated age related changes of visual acuity in DBA/2J, C57BL/6J, B6.*mpc1d* and D2.*mpc1b* mice. They reported that at 6 months of age, the strains did not differ in their visual acuity thresholds, but there were significant strain differences in visual acuity threshold when mice were 12 months, 18 months and 24 months of age. As they aged, DBA/2J and D2.*mpc1b* mice had lower visual acuity threshold than C57BL/6J and B6.*mpc1d* mice. Over the four ages tested, the visual acuity threshold of C57BL/6J, DBA/2J and D2.*mp1b* mice decreased with aging and was significantly lower at 12–24 months of age than at 6 months of age. In contrast, the visual acuity threshold of B6.*mpc1d* mice did not differ over the four ages tested.

CHAPTER 2

MATERIALS AND METHODS

2.1. Subjects

7 female C57BL/6 mice were used for visual acuity experiments. Animals were procured from Gazi University as 3 months old and housed in animal facilities at the Middle East Technical University, Department of Biological Sciences Building. The animals were maintained under a 12:12 h light: dark cycle (lights on 7 a.m. and off 7 p.m.) and at around 23°C and 30% humidity. Animals were weighed every day throughout the experiments to ensure their weight maintenance.

2.2. Apparatus

2.2.1. Visual Water Maze

The test box was adopted from previously published study of Prusky and colleagues (2000) (Figure 2.1). It consisted of a trapezoidal-shaped pool surrounded by 55 cm high walls made of 6 mm nontransparent Plexiglas. Dimensions of the pool were 140 cm long and 80 cm wide at one end and 25 cm wide at the other end. Two computer-controlled monitors of 19 inches each were mounted side-by-side at the wider (80 cm) end of the pool. Both the pool and the computer monitors were placed on a solid surface with three triangular braces ($12 \times 12 \times 12$ cm^3) supporting the two long walls of the pool from outside. A midline divider (40 cm high and 41 cm long) extended from the middle of the wider end wall dividing the wall and partially the pool along its long axis into two equal halves. The wider back wall was made of transparent Plexiglas and behind it there were computer monitors on which differential visual patterns were presented to the mice. The length of the midline divider determined the closest distance an animal could get seeing both screens without entering one of the two arms and specified the choice point. The length of the midline divider indicated how punitive the task was, because after an incorrect choice animal had to swim around it to reach to the other arm. A release chute (35 cm long $\times$ 7 cm wide $\times$ 20 cm high) was centered at the narrow end of the pool. Releasing an animal from the release chute removed side biases and guided the animal

to swim towards the midline of the pool. Inner surfaces of the two long walls and the narrow end of the pool, both sides of the midline divider and the front surface of the release chute were flat black to make them opaque and reduce reflections within the pool. A portable transparent escape platform (37 cm long × 13 cm wide × 14 cm high) was placed under one of the computer screens. The pool was filled with lukewarm (22°C) water to a level of 1 cm above the escape platform. White food dye (titanium dioxide (TiO_2)) was used to color water in order to make the platform invisible from the water level. The pool was illuminated by two diffused fluorescent lights, located on the ceiling approximately above the long walls of the pool.
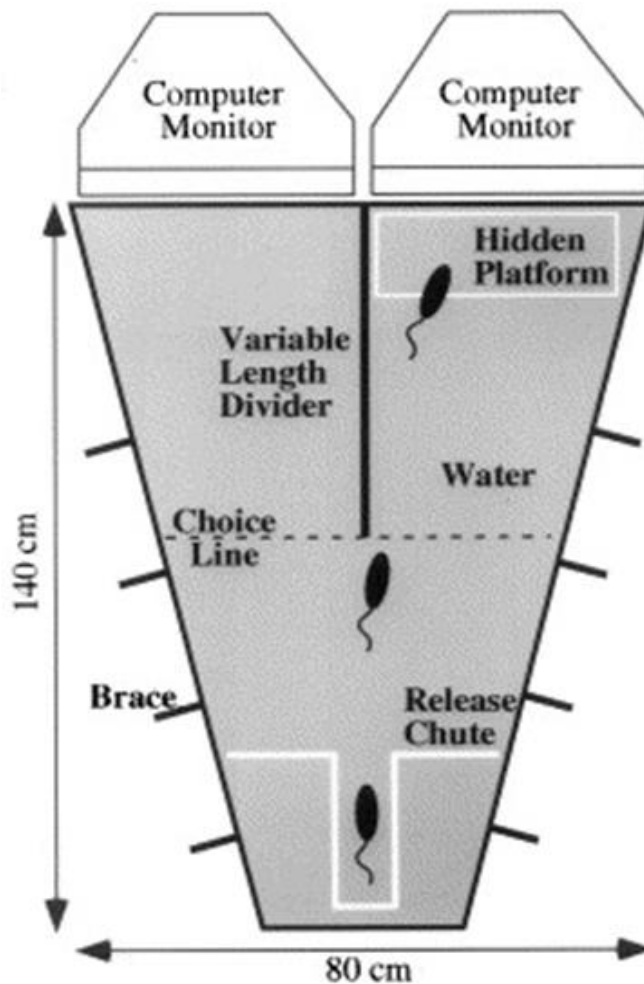
Figure 2.1: The picture of the apparatus used for testing visual functions in small rodents. (Figure taken from Prusky *et al.*, 2000)

2.2.2. Computer Hardware

Two identical 19 inch computer monitors (AOC 919Vz LCD Monitors 19") facing the wide end of the pool, were used to display the visual stimuli. The bottoms of the monitors were adjusted at the water level and the contrast and brightness of the monitors were equalized. Contrast of 50% and brightness of 90% were used.

2.2.3. Computer Software

A custom computer program was used to carry out the experiments. Physical dimensions of the display devices were entered in the program. To display a grating on the screen, gradient enabled box was chosen in the settings and the wanted width of the vertical gratings was entered as millimeters. To display homogeneous gray on the screen, standard enabled box was chosen in the settings. For the statistical analysis of the data SPSS version 22.0 (SPSS 2013) was used.

2.3. Visual Water Task

Although mice are very good instinctive swimmers, they show a natural tendency to escape from water. Working principle of the visual water task brings the principles of a Thompson box (Thompson & Bryant, 1955) and a Morris water maze (Morris *et al.*, 1982) together. During the task, animals were conditioned to associate a vertical grating containing black and white stripes of varying widths with escape from water. Animals first learned to discriminate a low spatial frequency sine-wave grating from homogeneous gray. Then, their discrimination between higher spatial frequency sine-wave gratings and homogeneous gray was measured as an index of their visual acuity. The task consisted of three phases; pre-training, training (visual detection), visual acuity testing.

2.3.1. Pre-Training: Habituation and Shaping

In the pre-training phase, animals were adapted step by step to find the platform concealed below a screen displaying a grating. Low spatial frequency sine-wave grating of 0.17 cycles per degree (cpd) that corresponds to ~4 cm wide black and white vertical bar pairs was displayed on one of the screens and a homogenous gray was displayed on the other screen. The escape platform was placed directly below the screen displaying the grating (Figure 2.2).
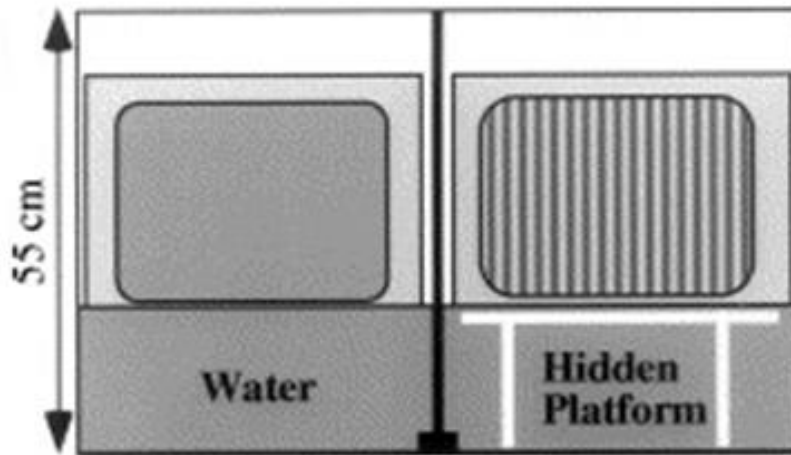
Figure 2.2: A picture illustrating the visual discrimination task that mice were subjected in the course of experiments on visual acuity. (Figure taken from Prusky *et al.*, 2000)

Animals were trained for 8 trials a day. On the first trial, an animal was put into the pool, towards the screen at a short distance from the platform. Subsequent to being put into water, almost every animal swam straight forward, came up against the platform and climbed upon it. They were allowed to stay on the platform for 10 seconds and then were taken to their holding cage. After completing a trial and returning to their holding cage, they warmed up by a lamp with a 60 W bulb placed above the holding cage until the next trial which was started after all animals from the group completed the first trial. So animals could rest and warm up until the next trial. This reduced the chance that animals get hypothermic or get very tired.

On the following trials, same routine was applied but release distance from the platform was step wise increased and the striped image together with the platform beneath it were moved from one side to another. This routine was repeated until all animals could swim to the platform from the opposite end of the pool. If an animal was not able to find the platform in 1 minute, it was gently guided towards the platform. The shaping phase was completed during a single daily training session of 8 trials.

2.3.2. Visual Discrimination Training (Rule Learning)

In the training phase, animals were trained to discriminate between a homogeneous gray and a vertical grating with a low spatial frequency of 0.17 cpd. A low spatial frequency sine-wave grating of 0.17 cpd was presented on one screen and a homogeneous gray was presented on the other screen, same as in the pre-training phase. A single daily training session was composed of 8 trials. The display of the sine-wave grating and

homogeneous gray on the computer screens altered semi-randomly from trial to trial with maximum two consecutive trials with the vertical grating on the same side.

On all trials, animals were released from the release chute at the narrower end of the pool and required to swim until they find the platform. Trials were scored as correct or incorrect according to the first arm the animal entered. That is to say, if the animal first entered by 2/3 of the total distance to the arm where the platform was placed, trial was scored as correct regardless of whether the animal reached the platform or not. If the animal first entered the arm without the platform, the trial was scored as incorrect. Swimming durations (escape latencies) of all animals were recorded by an electronic timer. For the first two days of training, if the animal failed to find the platform after 1 minute, it was guided towards the platform and allowed to stay on the platform for 10 seconds, with the trial recorded as incorrect. The number of correct trials was expressed as percent correct for that day and animals were trained until they reached a high performance criterion level of 75% correct choices during 3 consecutive days of training (18 correct choices out of total 24 trials). Each animal reached the criterion to complete the training on different days. When all animals reached the arbitrary performance criterion, the testing phase began. Prior to the testing phase, all animals were subjected to a single retraining session with the same stimulus parameters as during the training phase.

Sometimes animals developed a spatial bias in their choices. Tree such response patterns can be observed: (1) a side bias, (2) alternations, and (3) a win-stay or lose-shift response. In a side bias, an animal preferably swims to one side, right or left, disregarding the position of the grating stimulus. In alternation response, an animal swam right and left alternately. In a win-stay/ lose-shift response, an animal swims to the side where it had found the platform on the previous trial. Since such behavioral patterns affect the correct measurement of visual acuity, they were eliminated by changing the sequence of right/left grating presentation. For instance, if an animal developed a right side bias, on the following 2-3 trials the grating was presented on the opposite, left side, and on a particular day, the total number of the grating presentations on the left side was twice that on the right side. Sometimes, very rarely, if an animal still displayed a side bias, additional correction trials were given after the session, with the entrance to the preferred arm being closed by a transparent pane of Plexiglas. In this way the animal could view both screens, but the entry to the incorrect arm was prevented. Once the animal swam directly to the correct arm and climbed upon the platform without trying to enter the incorrect arm, correction trials were abandoned.

2.3.3. Visual Acuity Testing

In the testing phase, animals were tested for their visual acuity threshold, where a vertical grating of varying spatial frequencies was displayed on one side of the divider against a homogeneous gray displayed on the other side of the divider. Two different

methods, including the same varying spatial frequencies, were applied to determine the visual acuity threshold of the same group of animals.

2.3.3.1. Method I: Adopted from Prusky *et al.* (2000)

In this method, animals were given 8 trials per day, as in the pre-training and training phases, for 10 testing days. Each daily block of eight trials included vertical gratings of varying spatial frequencies (0.17, 0.32, 0.43, 0.53, 0.55, 0.57, 0.62, and 0.64 cpd) with five frequencies around the expected threshold (Wong & Brown, 2006). The order of presentation of the spatial frequencies over the eight consecutive daily trials was as follows:

Trial 1: 0.17
Trial 2: 0.32
Trial 3: 0.43
Trial 4: 0.53
Trial 5: 0.64
Trial 6: 0.55
Trial 7: 0.62
Trial 8: 0.57

Testing was done every two days and animals were retrained with a spatial frequency of 0.17 cpd on the days in between.

Both on testing and retraining days, the display of the sine-wave grating and homogeneous gray on computer screens altered semi-randomly from trial to trial, with maximum two consecutive trials with the vertical grating on the same side. Trials were scored as correct or incorrect according to the first arm entry. Swimming durations of all animals were recorded by an electronic timer and animals were allowed to stay on the platform for 10 seconds after they had found it. No correction trials were run on test days. If necessary, correction trials were given on retraining days upon the completion of the session.

2.3.3.2. Method II: Alternative Method of Visual Acuity Testing by Repeated Visual Discrimination Training to Criterion

In the second method, small incremental changes were made in the spatial frequency of the vertical grating and an animal was trained with a particular grating frequency until reaching the arbitrary performance criterion level of 75% correct choices during 3 consecutive daily sessions of each involving 8 trials (18 correct choices out of total 24 trials). After an animal reached the criterion, frequency of the grating was increased on the next day and the animal was tested in the same manner until reaching the same

performance criterion level. No retraining was needed in this method, but if an animal adopted a side bias, up to 3 correction trials were given after the daily session.

The display of sine-wave grating and homogeneous gray on computer screens altered semi-randomly between trials, with maximum two consecutive trials with the vertical grating on the same side. As in the previous phases of training, trials were scored as correct or incorrect according to the first arm the animal entered, swimming durations of all animals were recorded by an electronic timer and animals were allowed to stay on the platform for 10 seconds after they had found it.

The order of presentation of the spatial frequencies throughout testing was:

> Test 1: 0.17
> Test 2: 0.32
> Test 3: 0.43
> Test 4: 0.53
> Test 5: 0.55
> Test 6: 0.57
> Test 7: 0.62
> Test 8: 0.64…

If an animal did not reach the desired performance criterion level within 8 consecutive test sessions (8 days) with a particular grating frequency, the animal was discarded from further tests and the frequency below was accepted as the visual acuity threshold.

2.3.3.3. Testing the Visual Discrimination by Training Animals to the Arbitrary Performance Criterion Using from the Beginning the Highest Grating Frequency That the Animals Were Able to Differentiate in the Previous Test

In order to control the effect of repeated visual discrimination training on visual acuity enhancement, a different group of mice (n=6) were trained to discriminate between a homogenous gray and a vertical grating with a low spatial frequency of 0.17 cpd and then were tested to discriminate between a homogenous gray and a vertical grating with a high spatial frequency of 0.86 cpd which was the highest grating frequency that the animals were able to discriminate in the previous test approached with repeated visual acuity training.

Both in training and testing phases, a single daily training session was composed of 8 trials. The vertical grating was presented on one screen and a homogenous gray was presented on the other screen. During training, a spatial frequency of 0.17 cpd was used for displaying vertical gratings as in the previous two methods. After an animal reached the arbitrary performance criterion level of 75% correct choices in discriminating the

vertical grating with a spatial frequency of 0.17 cpd and the homogenous gray during 3 consecutive days of training (18 correct choices out of total 24 trials), it was tested to discriminate between the homogenous gray and a vertical grating with a spatial frequency of 0.86 cpd for 8 days.

Both on training and testing days, the display of the sine-wave grating and homogeneous gray on computer screens altered semi-randomly from trial to trial with maximum two consecutive trials with vertical grating on the same side, trials were scored as correct or incorrect according to the first arm the animal entered, swimming durations of all animals were recorded by an electronic timer and animals were allowed to stay on the platform for 10 seconds after they had found it, as in the first method. Correction trials were given upon the completion of a daily session if an animal had developed a side bias.

CHAPTER 3

RESULTS

3.1. Measuring Visual Acuity in Mice by Applying Classical Prusky's Method

3.1.1. Visual Discrimination Training (Rule Learning)
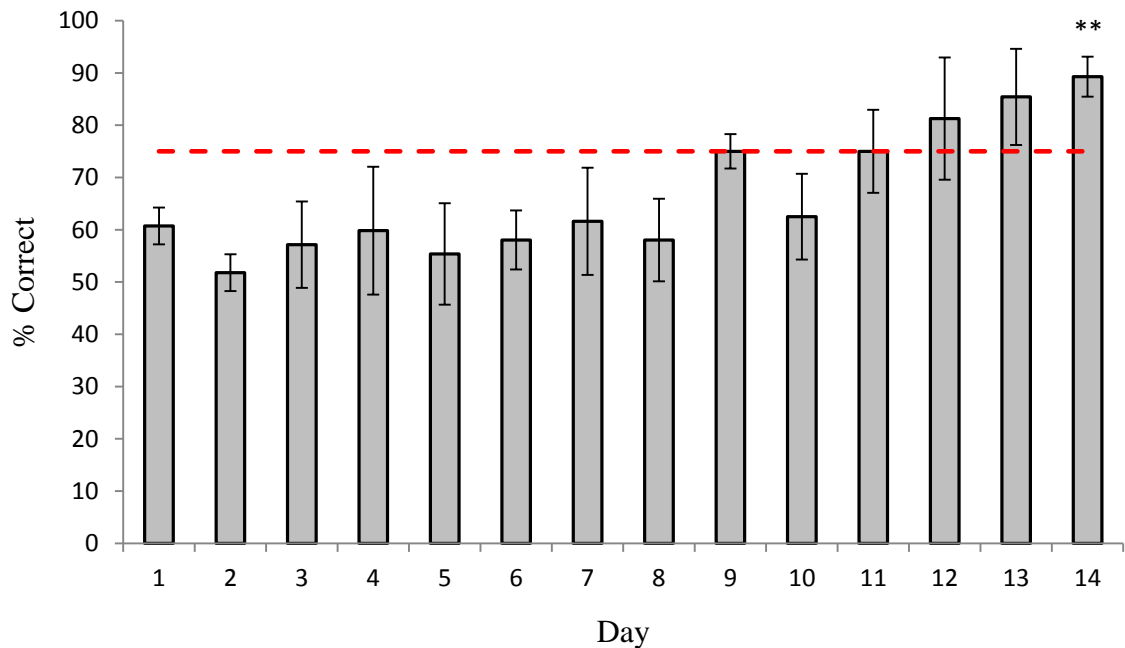
Figure 3.1: Learning graph presenting group mean of the percent (%) of correct choices per session during initial shaping-training phase of method I, during which animals learned to discriminate between homogenous gray representing negative conditioned stimulus (escape platform absent) and black/white vertical grating of 0.17 cpd representing positive conditioned stimulus (escape platform present). The dashed line indicates an arbitrary performance criterion level of 75% correct choices. Bars represent SEM. Asterisk denotes significant difference at $**p \le 0.01$ compared to day 1.

As seen from Figure 3.1, the percentage of correct choices progressively increased throughout the discrimination training. Number of correct responses equal to the required 75% correct performance level was noted on the Day 9. One-way repeated measures ANOVA revealed the effect of day on mean percentage of correct responses significant ($F(11, 66) = 2.42$, $p = 0.01$).
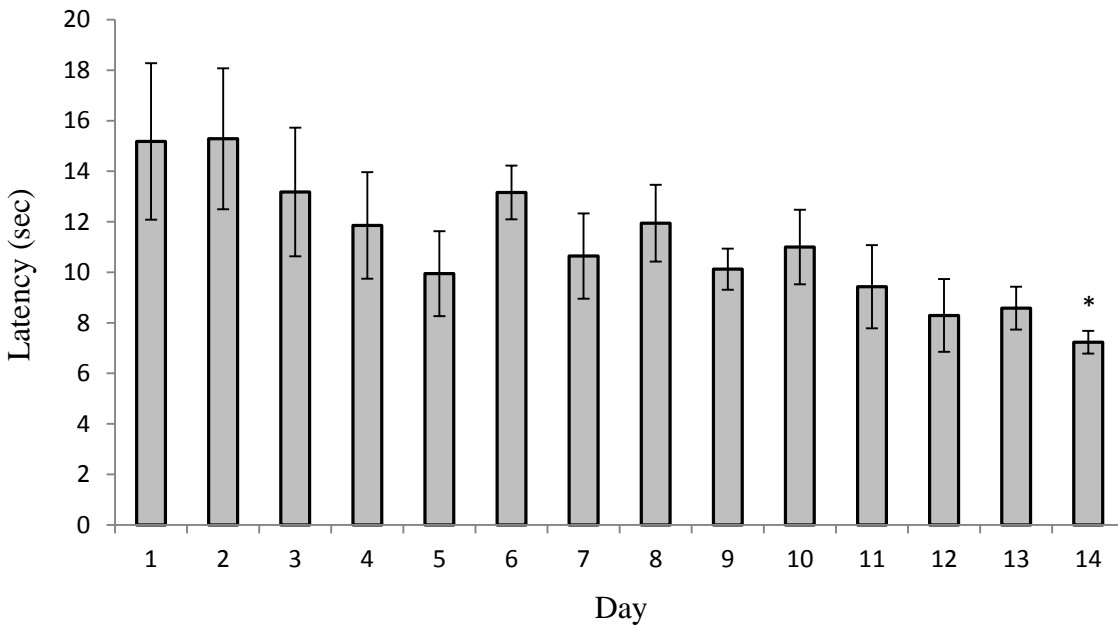
Figure 3.2: Mean escape latency (the swim duration from release chute to hidden platform) (sec) calculated for each day of shaping-training in method I. Bars represent SEM. Asterisk denotes significant difference at *p≤ 0.05 compared to day 6.

Figure 3.2, presents changes in escape latency throughout the shaping-training. As seen from this figure, in the course of training, a successive decrease in escape latency was noted. One-way repeated measures ANOVA applied to these data, revealed the effect of day on escape latency significant ($F(11, 66) = 2.28$, $p = 0.02$). Interestingly, the plateau level around 10 seconds was reached approximately by the time when the performance level of 75% correct choices had been achieved.

3.1.2. Visual Acuity Testing

After animals have reached the high performance level of 75% correct choices over consecutive 24 trials (3 consecutive daily sessions, 8 trials each) during the training phase, the testing of visual acuity began.

Figure 3.3 presents the animals' performance on retraining sessions given in between two test sessions. As seen from this figure, throughout the whole testing period, animals' performance was maintained at the relatively high level of 75% of correct choices. One-way repeated measures ANOVA yielded effect of day insignificant.
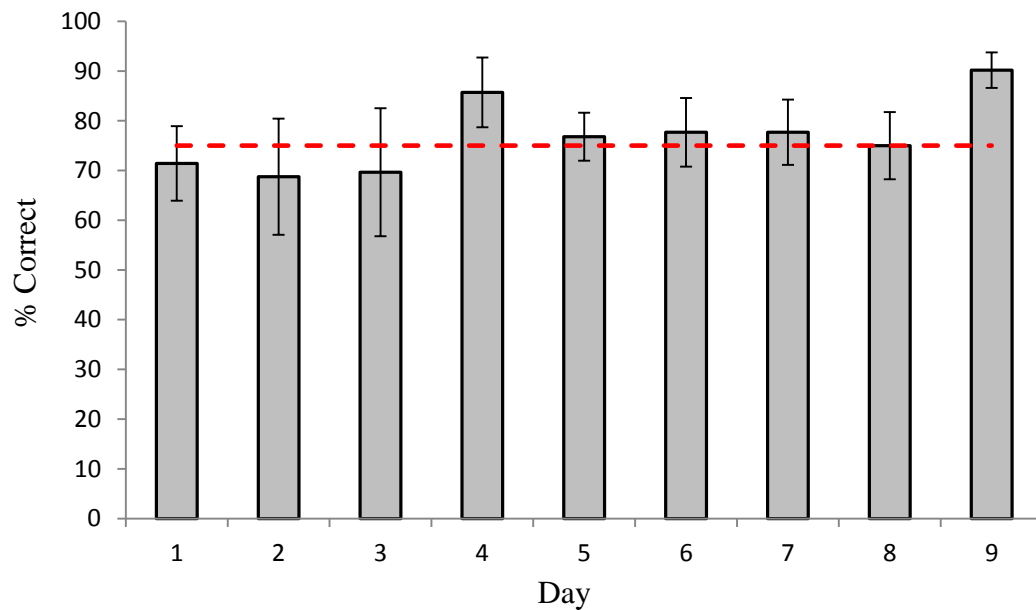
Figure 3.3: Mean percent of correct choices on 9 intermitting retraining days in method I. The dashed line indicates the arbitrary performance criterion level of 75% correct choices. Bars represent SEM.

3.1.2.1. Frequency-Dependent Estimates of Visual Discrimination Based on Individual and Group Data

For each animal, the mean percentage of correct choices has been estimated for the block of ten trials of each spatial frequency independently. For interpreting test results, an arbitrary discrimination level of 70% correct choices is used. The individual data are presented in Figure 3.4 and Table 3.1. Separate graphs of visual acuity measurements in each mouse are presented in Appendix A.
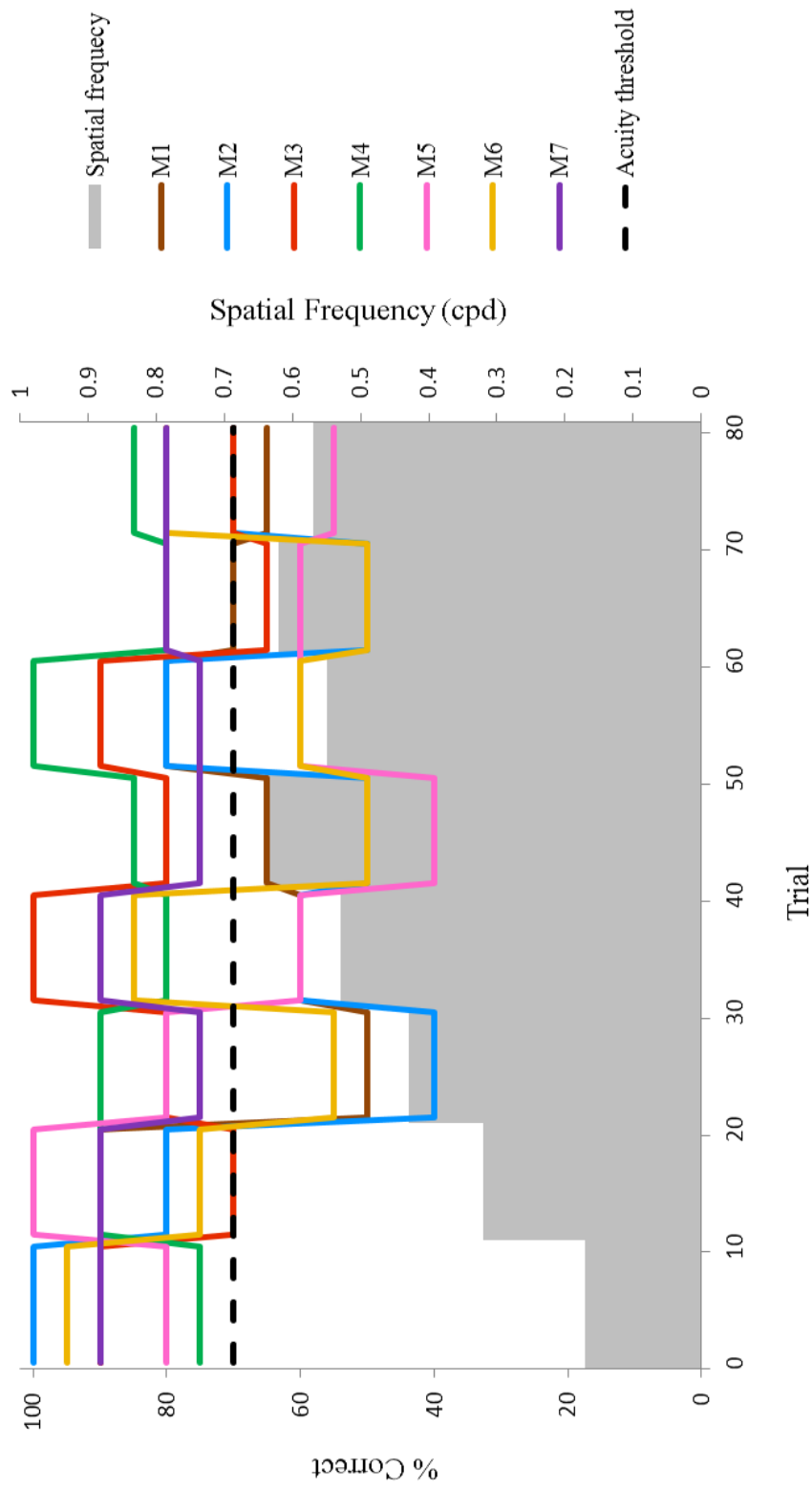
Figure 3.4: Graph presenting the visual acuity measurements in each mouse for each spatial frequency. Gray bars indicate gradually increased spatial frequencies during testing. Colored lines indicate percentage of correct choices of each mouse. Black dashed line indicates the arbitrary discrimination level of 70% correct choices.

Table 3.1: The percentage of correct responses calculated for each grating frequency in each mouse separately.

Mouse number	Grating frequency (cpd)							
	0.17	0.32	0.43	0.53	0.55	0.57	0.62	0.64
M 1	90	90	**50**	60	80	65	70	65
M 2	100	80	**40**	60	80	70	50	50
M 3	90	70	80	100	90	70	**65**	80
M 4	75	90	90	80	100	85	80	85
M 5	80	100	80	**60**	60	55	60	40
M 6	95	75	**55**	85	60	80	50	50
M 7	90	90	75	90	75	80	80	75

In this method of the estimation of a visual acuity threshold representative for the whole group, the grating frequency at which for the first time animal's performance has dropped below the arbitrary level of 70% correct was accepted as the individual acuity threshold (Prusky *et al*., 2000). As seen from Table 1, the individual visual acuity thresholds varied between 0.43 cpd and over 0.64 cpd. A group mean calculated on the basis of individual threshold values is around 0.53 cpd. However, due to the fluctuations in animals' performance on testing trials with the grating frequencies above the estimated threshold, the estimates made are not very reliable. Therefore, we have used another approach based on the group than individual data. Here, the group means of the percentage of correct responses executed at each grating frequency have been calculated (Please see the frequency-of-seeing graph in Figure 3.5).
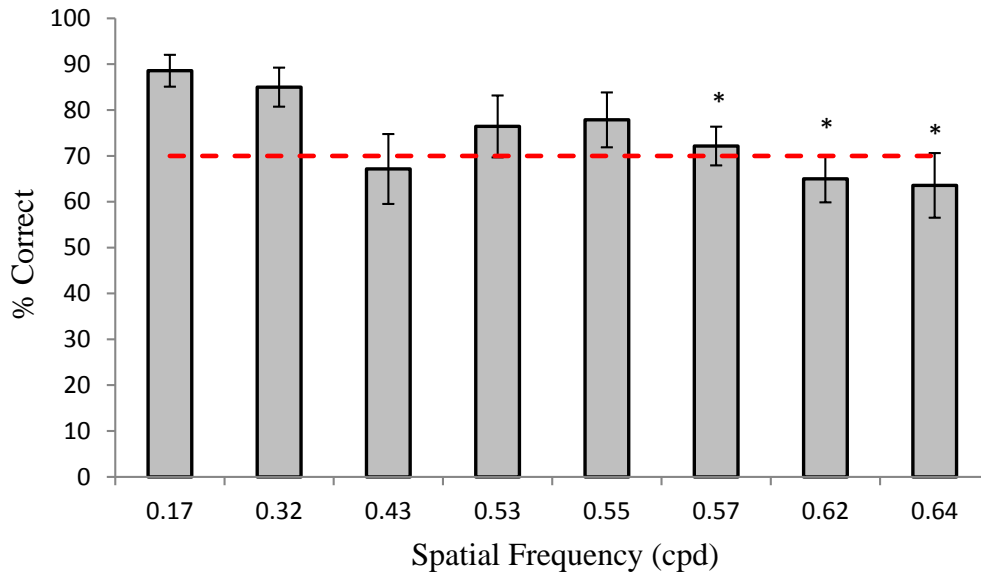
Figure 3.5: Frequency-of-seeing graph presenting group means of the percent of correct choices for each of the eight spatial frequencies tested in method I. The intersection with the arbitrary discrimination level of 70% correct choices was used as an acuity estimate. Bars represent SEM. Asterisk denotes significant difference at *p≤ 0.05 compared to 0.17 cpd.

The spatial frequency at which animals' mean performance in the visual discrimination task decreased below 70% accuracy level (arbitrary discrimination level) was accepted as a mean estimate of the visual acuity in our C57BL6/J mice. As seen from the Figure 3.5, based on the group estimates, the visual acuity threshold was at 0.43 cpd.

One-way repeated measures ANOVA applied to these data, revealed the effect of spatial frequency on percent correct significant ($F(7, 42) = 3.89$, $p = 0.002$). Pairwise comparisons using Fisher's LSD (Least Significant Difference) post hoc test indicated that the mean percent correct levels at frequencies of 0.32 cpd and 0.43 cpd are significantly different. These results suggested that the mean percentage of correct choices of animals significantly decreased at spatial frequency of 0.43 cpd which was our estimated threshold. On the contrary, no significant difference was found between mean percent correct levels at frequencies of 0.43 cpd and 0.53 cpd, 0.43 cpd and 0.55 cpd, 0.32 cpd and 0.53 cpd, 0.32 cpd and 0.55 cpd. Spatial frequencies showing significantly different mean percentage of correct levels are listed in Appendix B. Paired Samples t-test also yielded a significant difference in mean percent correct levels at 0.32 cpd and 0.43 cpd; $t(6) = 2.53$, $p = 0.045$, while the differences between mean percent correct levels at 0.43 cpd and 0.53 cpd, 0.43 cpd and 0.55 cpd (the highest data point after the decrease at 0.43 cpd), 0.32 cpd and 0.53 cpd, 0.32 cpd and 0.55 cpd were insignificant.

Additionally, the Pearson product-moment correlation coefficient was computed to assess the relationship between spatial frequencies and numbers of correct choices. There was a negative correlation between the two variables; $r = -0.455$, $n = 56$, $p = 0.0004$. Decrease in the number of correct choices was correlated with increase in the spatial frequency. Figure 3.6 presents a scatterplot summarizing the results.
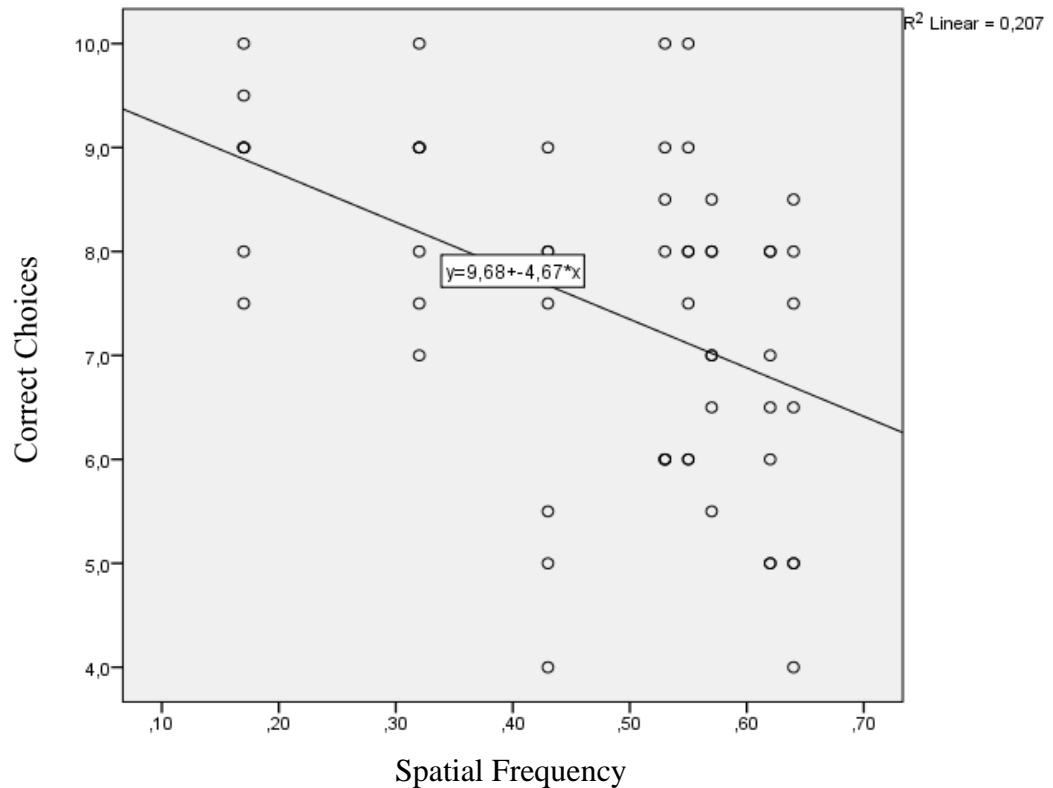
Figure 3.6: Scatterplot presenting negative correlation between spatial frequencies and correct choices.

A linear regression analysis was conducted to determine if the number of correct choices could be reliably predicted from spatial frequencies. The regression revealed that spatial frequency was a significant predictor of correct choices; $\beta = -0.455$, $t(54) = -3.76$, $p < .001$. Spatial frequency also explained a significant proportion of variance in the number of correct choices; $R^2 = 0.207$, $F(1, 54) = 14.10$, $p < .001$. Spatial frequency accounted for 20.7% of the variance in the number of correct choices. Regression equation was as follows:

Number of Correct Choices $= 9.682 - 4.670$ Spatial Frequency
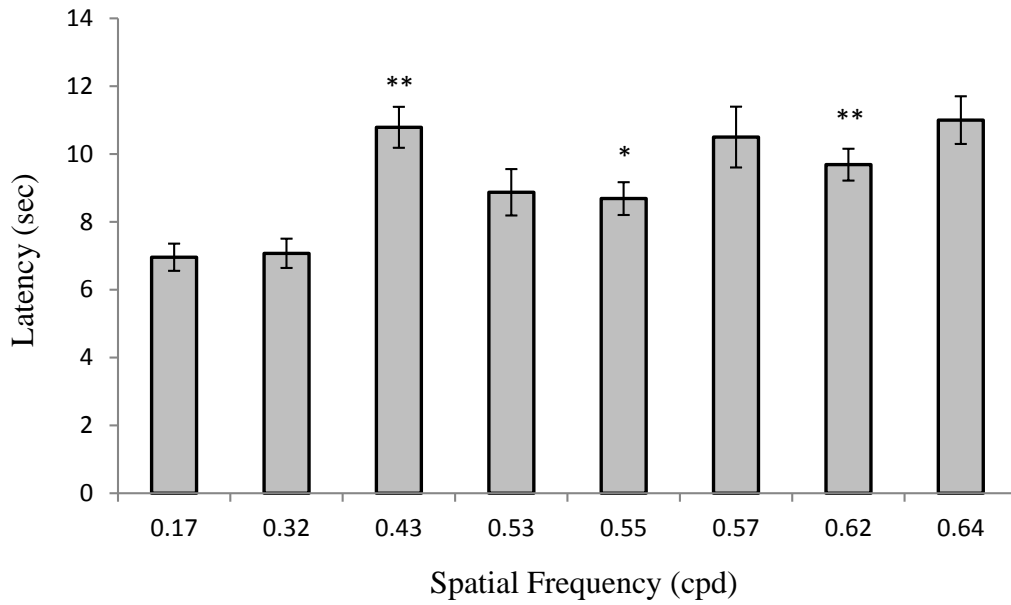
Figure 3.7: Mean escape latency (sec) calculated for each of the eight spatial frequencies tested in the visual acuity test in method I. Bars represent SEM. Asterisk denotes significant difference at *p≤ 0.05, **p≤ 0.01 compared to 0.17 cpd.

Figure 3.7 presents changes in the mean escape latency occurring along with increasing the grating frequency of the test stimuli which made the visual discrimination task more and more difficult. In most of animals, behavioral changes occurred as the spatial frequency of the stimulus was increased. At low spatial frequencies animals swam directly toward the grating after they had been released. As the spatial frequency increased and approached threshold, animals took more time to make their choices. The increase in escape latency near threshold was most often the result of swimming across the pool several times on the choice line while apparently inspecting the screens before making a choice. One-way repeated measures ANOVA revealed the effect of spatial frequency on escape latency significant ($F(7, 42) = 8.38$, $p = 2E-6$). Spatial frequencies showing significantly different mean escape latencies are listed in Appendix B.

The Pearson product-moment correlation coefficient was computed to assess the relationship between spatial frequency and escape latency. There was a positive correlation between the two variables; $r = 0.527$, $n = 56$, $p = 0.00003$. Increase in the escape latency was correlated with increase in the spatial frequency. A scatterplot summarizes the results (Figure 3.8).
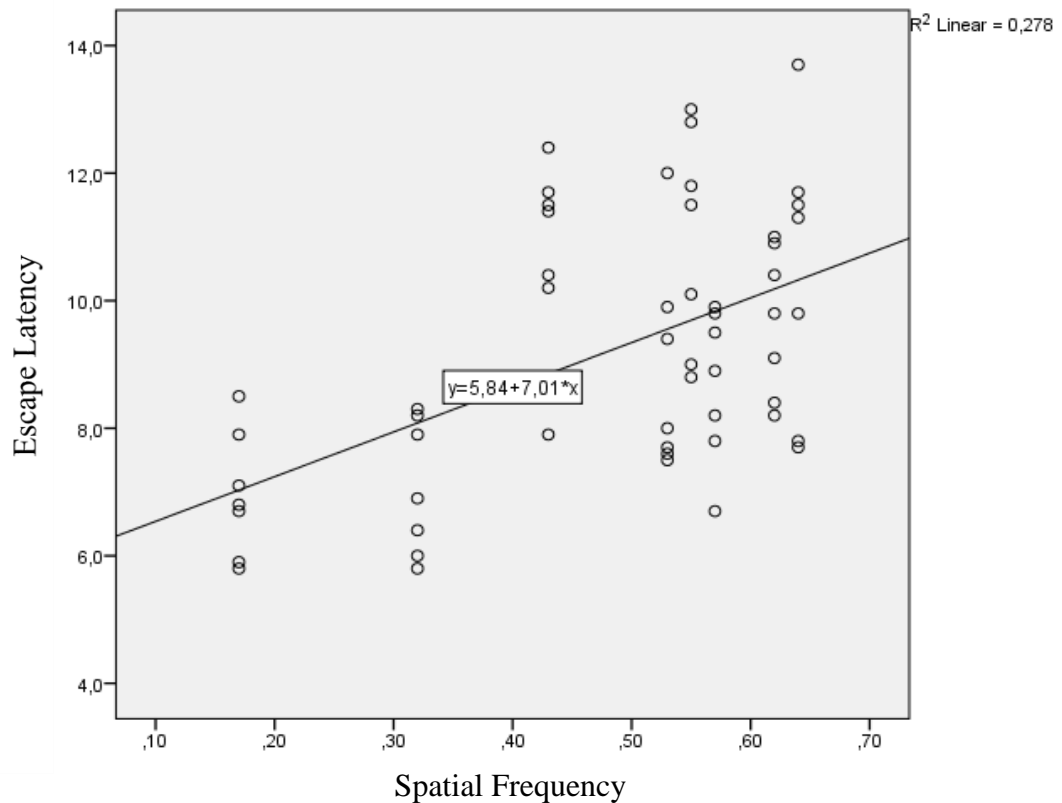
Figure 3.8: Scatterplot demonstrating positive correlation between spatial frequency and escape latency.

A linear regression analysis was also conducted to determine if escape latencies could be reliably predicted from spatial frequencies. The regression revealed that spatial frequency was a significant predictor of escape latency; $\beta = 0.527$, $t(56) = 4.56$, $p < .001$. Spatial frequency also explained a significant proportion of variance in escape latency; $R^2 = 0.278$, $F(1, 54) = 20.78$, $p < .001$. Spatial frequency accounted for 27.8% of the variance in escape latency. Regression equation was as follows:

Escape Latency = 5.839 + 7.009 Spatial Frequency

A Pearson product-moment correlation coefficient to assess a relationship between numbers of correct choices and escape latencies was also computed. There was a negative correlation between the two variables; $r = -0.431$, $n = 56$, $p = 0.001$. Decrease in the number of correct choices was correlated with increase in the escape latency. Partial correlation excluding the effect of spatial frequency yielded the correlation between number of correct choices and escape latency insignificant. A scatterplot summarizes the results (Figure 3.9).
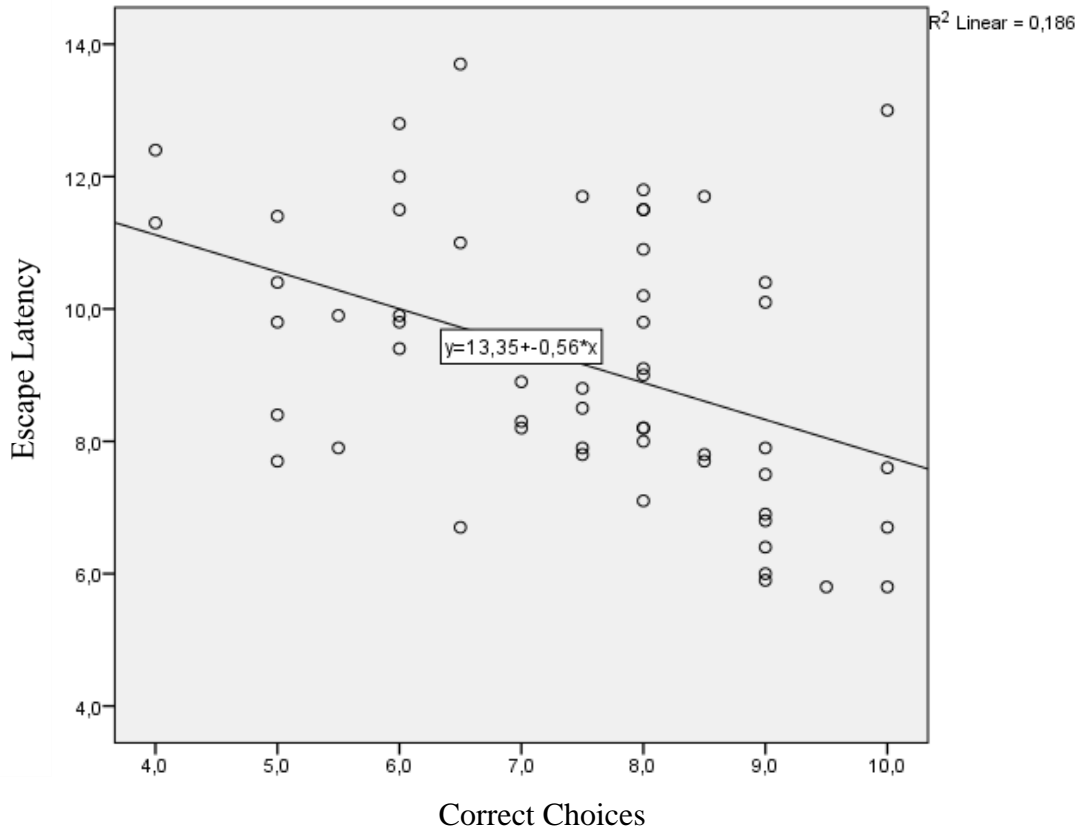
Figure 3.9: Scatterplot demonstrating negative correlation between correct choices and escape latencies.

3.2. Measuring Visual Acuity in Mice by Applying Repeated Visual Discrimination Training to Criterion (Effect of Training on Visual Functions)

3.2.1. Number of Trials to Reach Criterion

Alike in the method I, method II was testing animals' capability to discriminate between a homogeneous gray and a vertical grating of increasing spatial frequency. Unlike in method I, the tested spatial frequencies were not all shown in one daily session. Instead, an animal was trained with each spatial frequency of vertical grating, starting from the lowest one, until it reached a performance level of 75% correct choices during 3 consecutive daily sessions of 8 trials each (18 correct choices out of total 24 trials) in 8 days elapsed. The frequency of spatial grating was gradually increased in small steps (see Figure 3.10). In this test, inability to reach the arbitrary performance criterion of 75% correct choices in 8 training days (total 64 trials) was assumed as a behavioral visual acuity threshold.
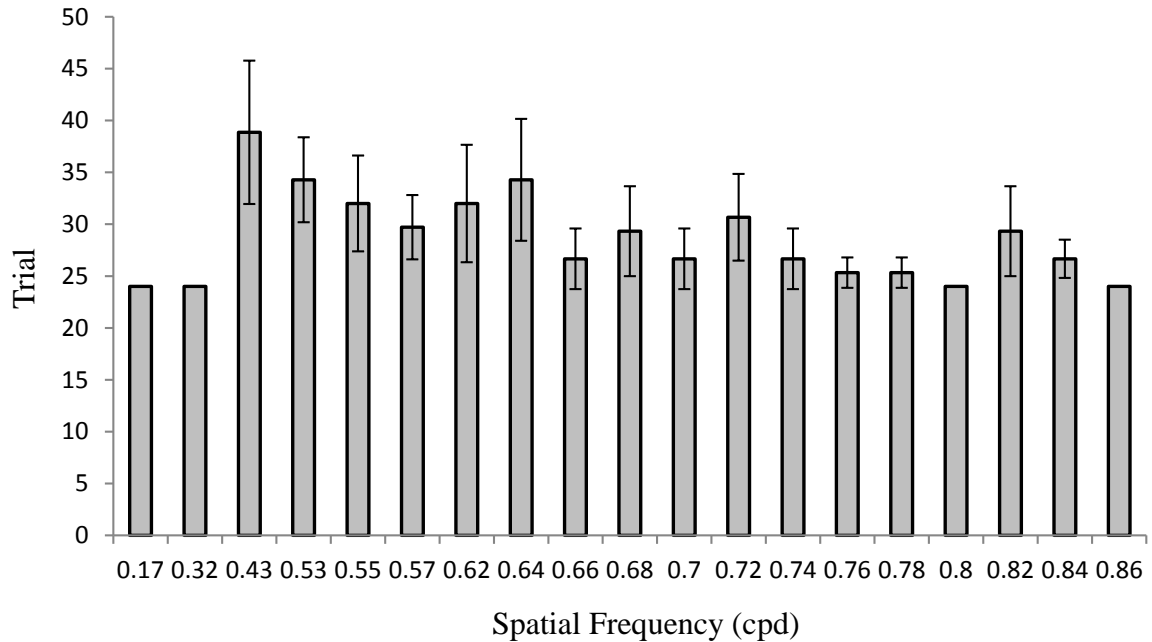
Figure 3.10: Mean number of trials to reach the performance criterion level of 75% correct choices for each spatial frequency tested in method II. Bars represent SEM.

Figure 3.10 represents group means of trial (choice) number to reach performance criterion for each spatial frequency tested, independently. In the course of experiments, we have lost some animals, therefore presented means were calculated from different numbers of subjects. Tests for the spatial frequencies between 0.17 cpd and 0.64 cpd were done on 7 animals; for the frequencies between 0.66 cpd and 0.84 cpd on 6 animals and for the frequency of 0.86 cpd on 5 animals.

As seen from Figure 3.10, at the grating frequency of 0.43 cpd, there was a sudden increase in the mean trial numbers to reach the arbitrary performance criterion of 75% correct choices accompanied by a substantial increase in the individual variation in the animals' performance. However, with training, despite of the continuing increase in the spatial frequencies tested, the animals were reaching performance criterion of 75% correct apparently at similar or even faster rates, although Friedman test and Wilcoxon signed-ranks tests for paired comparisons yielded no significant difference in the mean number of trials to reach the criterion in different spatial frequencies. The animals' capability to reach the performance criterion of 75% correct choices at all tested frequencies is clearly manifested in Figure 3.11 presenting the percentage of correct choices for each tested frequency independently. The percentages of correct choices for all tested frequencies are above the 75% performance level indicating a reliable visual discrimination. However, one-way repeated measures ANOVA applied to these data, revealed the main effect of spatial frequency on percent correct significant ($F(18, 90) =$

2.28, $p = 0.006$). The Fisher's LSD (Least Significant Difference) post hoc test yielded the mean percent correct levels significantly lower at the frequencies of 0.43, 0.53, and 0.64 cpd as compared to the frequency of 0.17 cpd. Spatial frequencies showing significantly different mean percentage of correct levels are listed in Appendix B.
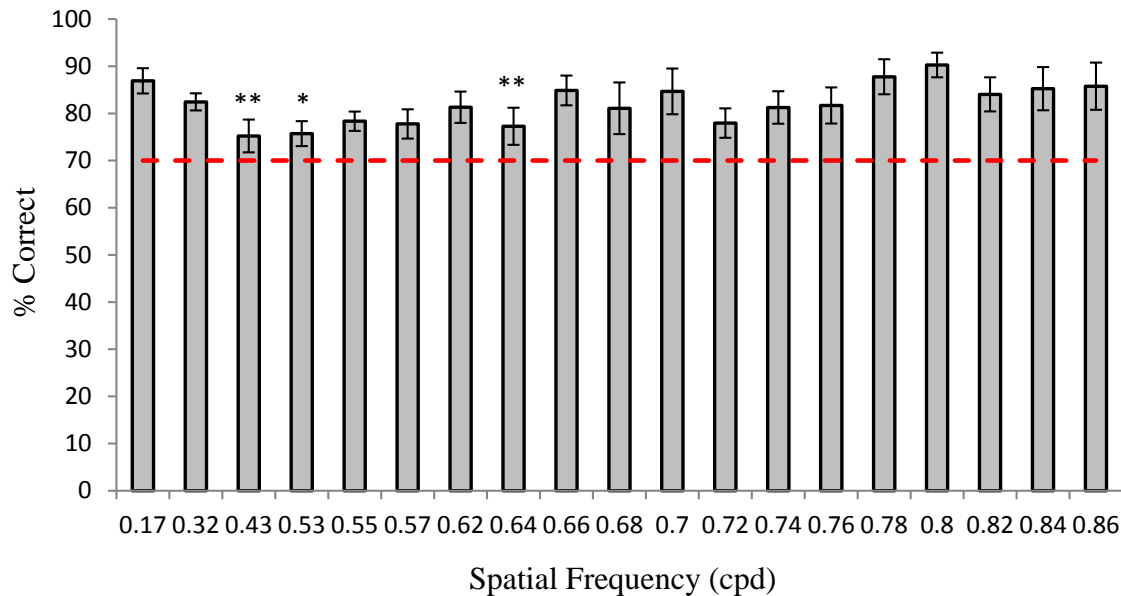
Figure 3.11: Mean percent of correct choices on each spatial frequency tested in method II. The dashed line indicates the arbitrary discrimination level of 70% correct choices. Bars represent SEM. Asterisk denotes significant difference at *p≤ 0.05, **p≤ 0.01 compared to 0.17 cpd.

For each of the spatial frequencies tested during repeated discrimination training, the mean escape latency has been calculated (Figure 3.12). The group mean latency was steadily rising along with the increase in the spatial frequency of the vertical grating, changing from 8 to 12 seconds. However, one-way repeated measures ANOVA revealed the effect of spatial frequency on escape latency insignificant. To assess the relationship between spatial frequency and escape latency the Pearson product-moment correlation coefficient was computed. There was a positive correlation between the two variables; $r = 0.286$, $n = 123$, $p = 0.001$.
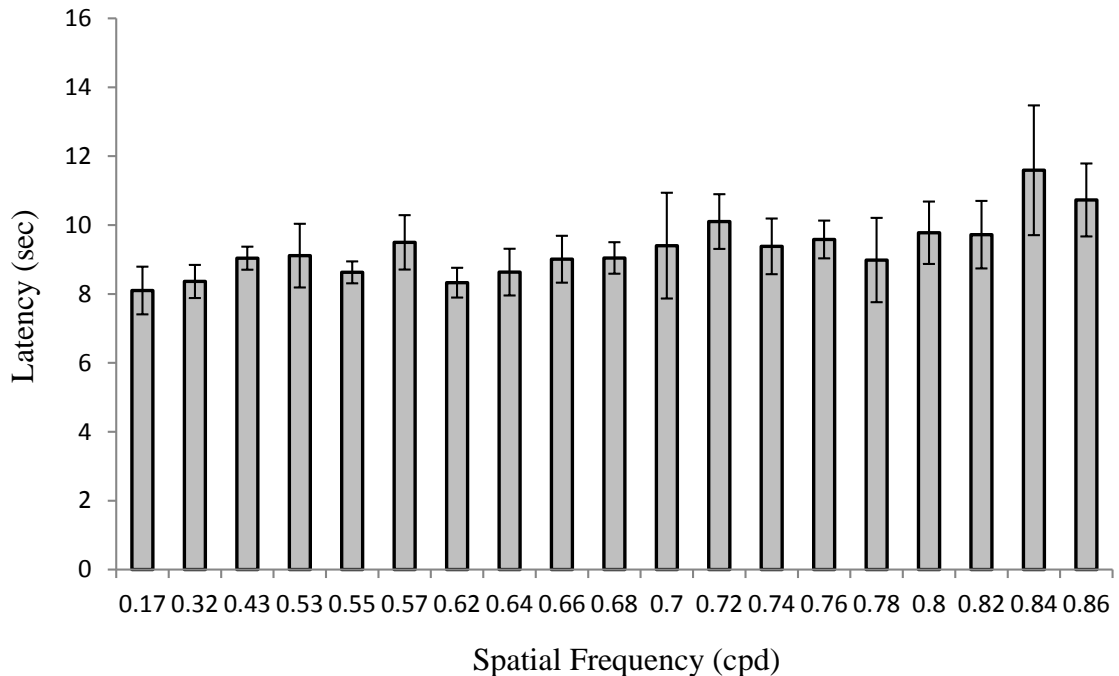
Figure 3.12: Mean escape latency (sec) on each spatial frequency tested in method II. Bars represent SEM.

3.2.2. Testing the Visual Discrimination by Training Animals to the Arbitrary Performance Criterion Using from the Beginning the Highest Grating Frequency That the Animals Were Able to Differentiate in the Previous Test

In order to control the effect of repeated visual discrimination training on visual acuity enhancement, a different group of mice (n=6) were trained to discriminate between homogenous gray and a spatial frequency grating of 0.17 cpd until they reach the arbitrary performance criterion of 75% correct choices (Fig. 3.13 and Fig. 3.14). After then, they were directly tested to discriminate between homogenous gray and a spatial frequency of 0.86 cpd which was the highest grating frequency used previously in the repeated visual discrimination task. Testing was carried out for 8 consecutive days.

Figure 3.13 presents percentage of correct choices per daily session during the preliminary training phase (rule learning). As seen from Fig. 3.12 there is an increase in the performance level from approximately 55% correct (random level) to over 75% correct (the criterion level). However, due to large individual variation one-way repeated measures ANOVA and nonparametric Wilcoxon signed-ranks test for paired comparisons yielded the day effect insignificant.
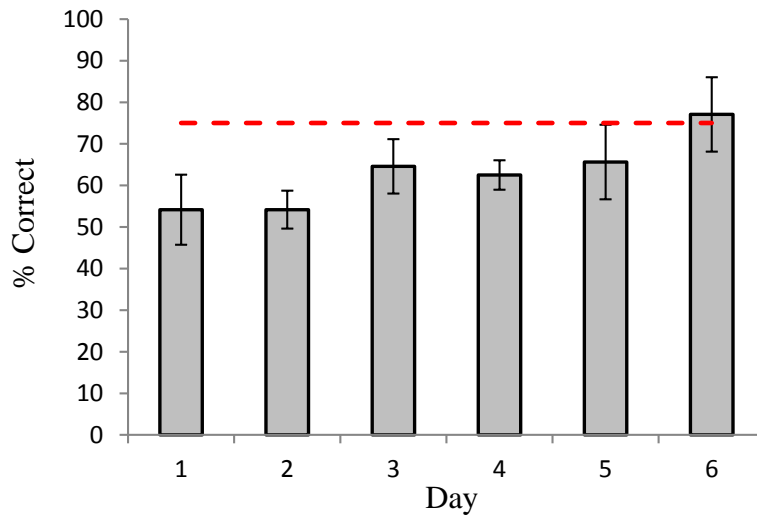
Figure 3.13: Mean percent of correct choices of a different group of mice on 6 days of preliminary shaping-training phase. The dashed line indicates the performance criterion level of 75% correct choices. Bars represent SEM.

Figure 3.14 presents changes in the mean escape latency throughout the preliminary training. One-way repeated measures ANOVA revealed the effect of day on mean latency significant ($F(5, 25) = 4.75$, $p = 0.003$).
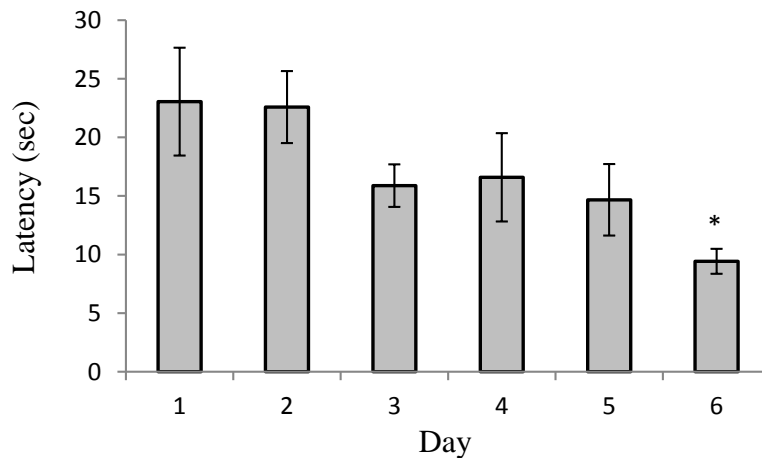
Figure 3.14: Mean escape latency (sec) of the different group of mice throughout the preliminary shaping-training phase. Bars represent SEM. Asterisk denotes significant difference at *p≤ 0.05 compared to day 3.

Figure 3.15 presents mean percent correct choices throughout the 8 days of discrimination testing between homogenous gray and a spatial frequency of 0.86 cpd. During this test, mean percentage of correct choices remained below the arbitrary discrimination level of 70% correct choices on all of the test days.
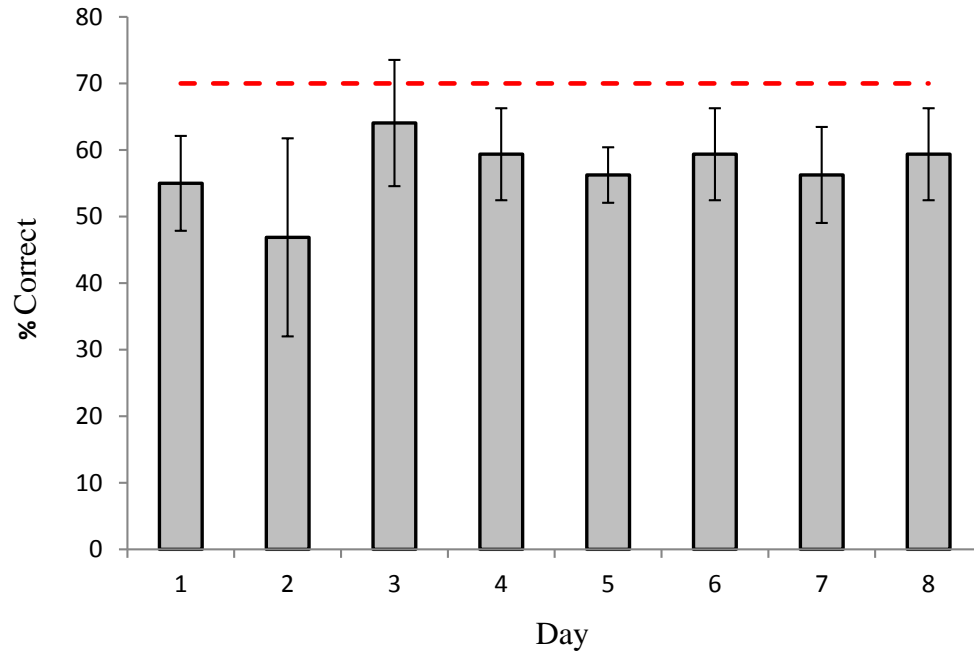
Figure 3.15: Mean percent of correct choices of the different group of mice on each daily session of 8 test days. The dashed line indicates the arbitrary discrimination level of 70% correct choices. Bars represent SEM.

One-way repeated measures ANOVA yielded the main effect of day on mean percentage of correct choices insignificant. Despite of this, a decrease in escape latency was observed across the discrimination training (Figure 3.16), however due to low number of subjects and large individual variation in escape latency, here too, the main effect of day was yielded insignificant.
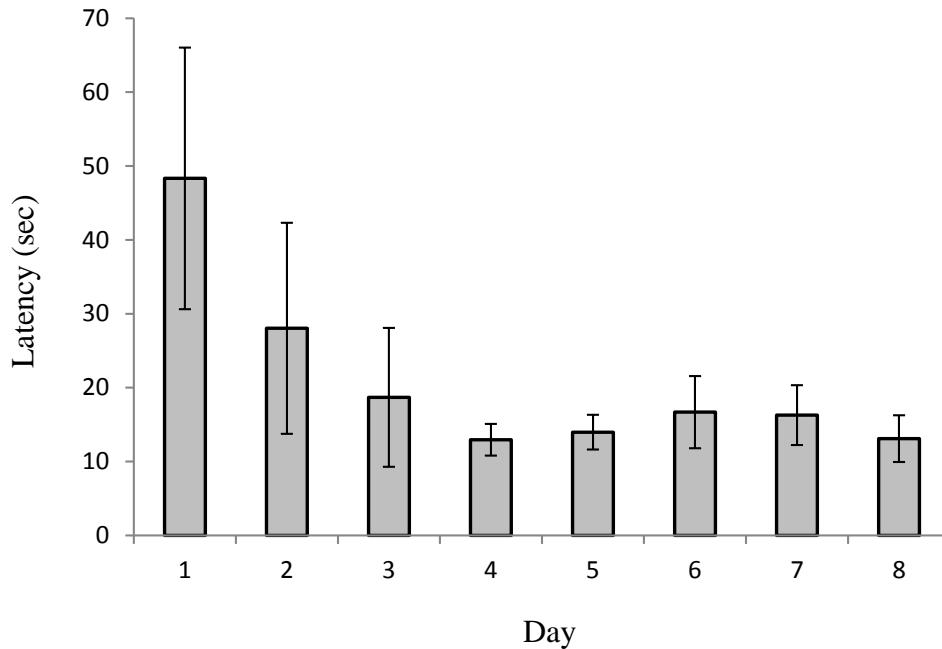
Figure 3.16: Mean escape latency (sec) of the different group of mice on each daily session of 8 test days. Bars represent SEM.

Mean percent correct levels for the spatial frequency of 0.86 cpd in procedures with repeated visual discrimination training (Procedure I) and without repeated visual discrimination training (Procedure II) were compared (Figure 3.17) and evaluated by the independent-samples t-test. Mean percent correct level in repeated visual discrimination training ($M = 6.91$, $SD = 1.54$) was significantly higher than the mean percent correct level without repeated visual discrimination training ($M = 4.56$, $SD = 1.12$); $t(48) = 6.18$, $p = 1.34E\text{-}7$.
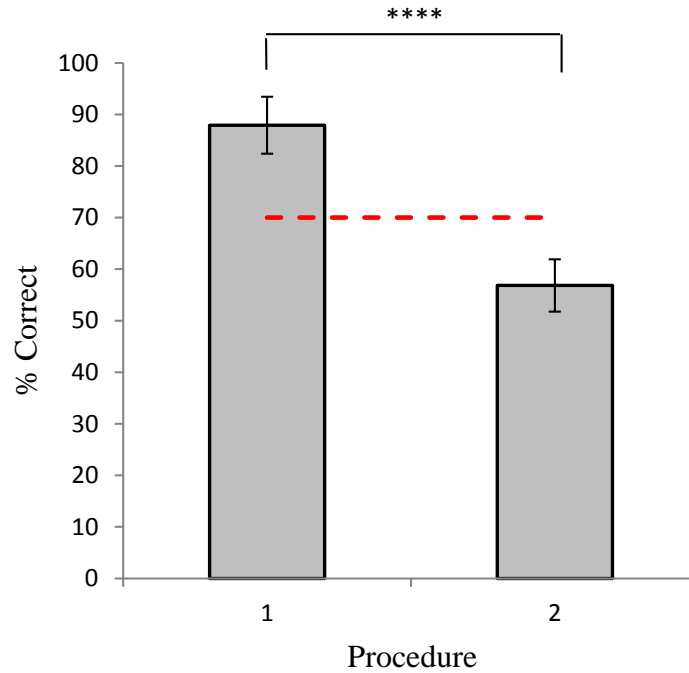
Figure 3.17: Mean percent correct levels for the spatial frequency of 0.86 cpd in procedures with repeated visual discrimination training (Procedure I) and without repeated visual discrimination training (Procedure II). The dashed line indicates the arbitrary discrimination level of 70% correct choices. Bars represent SEM. Asterisk denotes significant difference at ****p≤ 0.0001.

Figure 3.18 compares mean escape latencies for the spatial frequency of 0.86 cpd in procedures with and without repeated visual discrimination training. Mann-Whitney U test yielded mean escape latency in repeated visual discrimination training procedure significantly lower than the mean escape latency without repeated visual discrimination training procedure ($U = 120.5$, $Z = -3.18$, $p = .001$).
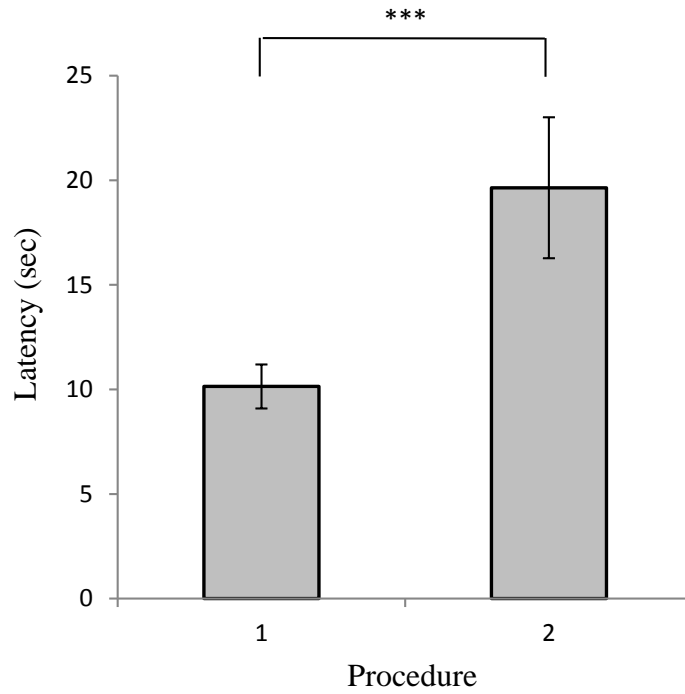
Figure 3.18: Mean escape latencies for the spatial frequency of 0.86 cpd in procedures with repeated visual discrimination training (Procedure I) and without repeated visual discrimination training (Procedure II). Bars represent SEM. Asterisk denotes significant difference at ***p$\leq$ 0.001.

CHAPTER 4

DISCUSSION

Visual acuity is a measure of the capability of determining fine details of the objects in the visual field and being so is one of the most important features of spatial vision. Therefore, it is important to have accurate estimation methods and be aware of all the factors that may affect visual acuity. In the present study, using natural tendency in mice and rats to escape from the water, two methods of measuring visual acuity in C57BL6/J mice were applied and compared. Both tasks were performed in a trapezoidal-shaped pool, with two computer-controlled monitors placed side-by-side at one end of the pool, and with an invisible platform located under the monitor which presented vertical gratings of different spatial frequencies (Prusky *et al*., 2000). First method was a combination of visual acuity task used previously by Prusky and colleagues (Prusky *et al*., 2000) and that described by Wong and Brown (2006). The second method comprised of repeated visual discrimination training to an arbitrary performance criterion. Both tasks were carried out on the same subjects, in the same experimental conditions of visual stimuli, luminance, contrast and choice distance.

In Prusky's method, first a preliminary shaping-training phase was performed during which animals learned to discriminate between a homogeneous gray and a vertical grating with a low spatial frequency of 0.17 cpd. After the shaping-training carried out to an arbitrary performance criterion level of 75% correct choices within the 3 consecutive daily sessions (18 correct choices out of total 24 trials), animals were subjected to 10 daily visual acuity tests each comprising of 8 trials with rising frequency of the spatial grating from 0.17 cpd throughout 0.64 cpd. Test sessions were alternating with retraining sessions with a low spatial frequency of 0.17 cpd as a positive conditioned stimulus. The purpose of giving retraining sessions with a low spatial frequency was to make sure that the animals remembered the discrimination rule of the task throughout the test. At the end of testing, percent of correct choices has been calculated for each frequency on the individual and group basis and the drop of animals' performance beneath 70% correct was accepted as visual acuity threshold. In contrast to this, in the second method, the animals' capability to discriminate high spatial frequencies was tested with step-wise increasing spatial frequencies in the repeated

discrimination training as long as the performance criterion of 75% correct had been reached each time.

During preliminary shaping-training with a vertical grating of 0.17 cpd, the percentage of correct responses progressively increased and performance above the criterion level of 75% correct choices was reached on day 9. Also, a successive decrease in the escape latency was noted throughout the training phase. Alike in the experiments by Wong and Brown (2006), also in this study, the day effect was significant both on the percentage of correct choices and on escape latency.

During the testing period, on all retraining sessions, animals maintained their performance at the relatively high level of 75% correct choices, and the effect of day on percent correct was insignificant, indicating that the decrease in the percent correct choices at higher spatial frequencies tested was a result of animals' inability to discriminate between vertical grating and the homogenous gray.

In the acuity test, a high individual variation was observed in the estimates of visual acuity thresholds which varied between 0.43 and 0.64 cpd in C57BL6/J mice. This range of individual threshold values is wider than 0.42-0.54 cpd range reported by Prusky *et al*. (2000) for C57BU6 mice and 0.4-0.59 cpd range reported by Gianfranceschi *et al*. (1999) for wild type mice. On the other hand, it is narrower compared to the individual threshold values in *bcl2* transgenic mice varying between 0.53 and 0.74 cpd as reported by Gianfrancheschi *et al.* (1999). In our study, the group mean calculated on the basis of individual threshold values was around 0.53 cpd. This threshold value is higher than 0.49 cpd estimate obtained by calculating the overall mean of individual thresholds in the study by Prusky *et al*. (2000) and 0.5 cpd estimate for C57B1/6J and reeler *(rlrl)* mutant mice obtained from an optokinetic investigation by Sinex *et al.* (1979) but it is falling into the range of 0.5-0.6 cpd estimate obtained by Gianfranceschi *et al.* (1999) in their studies on wild type and *bcl2* transgenic mice. However, to rely on the individual thresholds was difficult due to fluctuations in animals' performance after it first dropped below the visual acuity criterion of 70% correct choices. Based on the group data, the visual acuity threshold was estimated as 0.43 cpd. Because the frequency-of-seeing graph displayed some fluctuations across the spatial frequencies higher than the estimated threshold, mean percentage of correct values at specific spatial frequencies were compared. Decrease of performance between 0.32 cpd and 0.43 cpd was found significant, however increase between 0.43 cpd and 0.53 cpd or increase between 0.43 cpd and 0.55 cpd was found insignificant. Our visual acuity estimate of 0.43 cpd was lower than the 0.53 cpd estimate obtained from frequency-of-seeing curves for C57BU6 mice by Prusky *et al*. (2000) and the 0.6 cpd estimate for C57BL6/J mice obtained by recording visual evoked potentials (VEPs) from the primary visual cortex of wild-type mice by Prociatti *et al.* (1999) and the 0.65 cpd estimate obtained from a visual evoked potential study by Pizzorusso *et al*. (1997), but was higher than the 0.37 cpd estimate for C57BL/6J mice obtained by Wong and Brown (2006), the ~0.4 cpd estimate measured in C57BL/6 mice using a virtual optomotor system by Prusky *et al*. (2004) and the 0.3-

0.4 cpd estimate measured in wild-type mice using an automated optomotor paradigm by Schmucker *et al*. (2005).

Usually, reinforcement-based behavioral tasks reveal higher visual acuity thresholds than those obtained from virtual optomotor task. One reason of this difference can be different visual pathways contributing to behavioral responses and accordingly processing different features of the retinal output in optomotor and reinforcement-based tasks. In a virtual optomotor task, visual acuity is measured by the optokinetic eye movements and head tracking that are largely controlled by subcortical visual pathways. On the other hand, visual water task measures cortical vision (Prusky *et al*., 2004).

The discrepancies in the mice visual acuity threshold reported by different research groups can be partially related to the laboratory strain differences and partially arise from the differences in the testing method. For instance, in our experiments we used a standard set of eight spatial frequencies that were tested each day and increases in spatial frequency were larger for lower than for higher spatial frequencies tested, whereas Prusky *et al*. (2000) used a limits procedure, in which the spatial frequency of the positive stimulus was only increased or decreased by one cycle on a trial-by-trial basis depending on the mouse's response. Another possible reason of the discrepant results may be the inability to strictly control the viewing distance of freely moving animals. Since the spatial frequencies are calculated assuming that the gratings are inspected from the choice line at the end of the midline divider, the acuity values might be underestimated in case the animals make their decision before reaching the choice line. Still another reason for the differences in threshold estimates by different research groups might be differences in stimulus properties such as luminance and contrast. Abdeljalil and colleagues (2005) reported that in male C57BL/6J mice, visual acuity measured in an automated optomotor paradigm increased from 0.26 cpd in scotopic conditions to 0.52 cpd in photopic conditions. Schmucker *et al*. (2005) studying visual acuity in wild mice also observed an improvement in visual functions under bright luminance of 30 cd/m^2 and higher. Parallel to this, Prociatti *et al*. (1999) reported that visual evoked potential (VEP) amplitude is maximum at the highest level of luminance and decreases progressively as luminance is reduced. For the contrast, Prusky and Douglas (2004) reported that mice displayed an inverse ''U''-shaped contrast sensitivity curve with a maximum sensitivity near 0.2 cpd. In the present study, the mice visual acuity was measured under photopic conditions, however, contrast remained at 50% level which was lower than that was used in previous studies by Gianfranceschi *et al*. (1999) (75%) and Prusky *et al*. (2000) (97%) what could be the reason of the lower estimate of the group mean visual acuity value in this study compared to previous reports by Prusky and colleagues (2000). On the other hand, however, Wong and Brown (2006) used the same as our set of eight spatial frequencies for testing visual acuity in mice with 100% contrast but obtained a lower threshold value than our estimated threshold value. In addition, it must be taken into account that higher standard deviations in animals' data result in lower spatial frequency cutoff (Schmucker *et al*., 2005).

During the test phase of the first task, number of correct choices decreased as the spatial frequency of the grating increased. The effect of spatial frequency on percentage of correct choices was significant and a negative correlation was assessed between spatial frequency and percent correct. The linear regression analysis revealed that the spatial frequency was a significant predictor of correct choices and the spatial frequency accounted for 20.7% of the variance in the number of correct choices. The effect of spatial frequency was also significant on escape latency. As the frequency increased, the task became more difficult for the animals, and often, the increase in the escape latency was a result of animals swimming across the pool several times on the choice line and inspecting the screens before making their choices. The latency graph (Figure 3.7) was a mirror image of the frequency-of-seeing graph (Figure 3.5) confirming the breakdown of animals' performance at frequency of 0.43 cpd in the visual discrimination task and a significant negative correlation was assessed between escape latencies and numbers of correct choices. The same analysis performed for retraining days yielded the correlation between number of correct choices and escape latency insignificant, confirming that the negative correlation between number of correct choices and escape latency in testing sessions is an outcome of the spatial frequency.

In the alternative method of visual acuity testing, animals were trained with a particular grating frequency until reaching a demanding performance criterion of 75% correct choices (18 correct choices out of 24 trials within three consecutive training sessions). If an animal reached the criterion within eight days, it was tested again with an increased spatial frequency. In this task, the behavioral visual acuity estimate was supposed to be the first spatial frequency at which animals fail to reach the performance criterion of 75% correct in eight days of training. First eight spatial frequencies used in this task were the same as those applied in the first task but they were tested in an incremental order. On the following tests, frequency was increased by 0.02 cpd until reaching 0.86 cpd which was the last frequency tested. At frequency of 0.43 cpd, an increase in the mean trial number to reach the performance criterion of 75% correct and an increase in the variation of individual performances were observed. This break-down in the visual discrimination at the spatial frequency of 0.43 cpd was consistent with the results we obtained in the first task, however, animals managed to reach the 75% correct performance level at all frequencies tested up to 0.86 cpd and the differences in the numbers of trials to reach criterion were yielded insignificant. On the other hand, mean percent corrects were significantly lower at frequencies of 0.43, 0.53 and 0.64 cpd as compared to the frequency of 0.17 cpd but it was still above the level of 70% correct choices, the arbitrary visual acuity threshold .

The latter results show a positive effect of repeated visual discrimination training with step-wise increasing spatial frequencies of the vertical grating on visual acuity. To control the effect of repeated visual discrimination training on visual acuity enhancement, a naive group of mice was trained to discriminate between a homogeneous gray and a vertical grating with a low spatial frequency of 0.17 cpd until reaching the performance criterion level of 75% correct choices as in the training phase of the first

task. Then, for eight days, the same animals were tested to discriminate between a homogeneous gray and a vertical grating with the highest spatial frequency that the animals were able to differentiate during repeated visual discrimination training (0.86 cpd). During this test, on all eight daily sessions, mean percentage of correct choices remained below the arbitrary discrimination level of 70% and the day effect on percent correct was yielded insignificant. Although a decrease in the escape latency was observed throughout the test, the day effect was yielded insignificant. However, due to low number of subjects and high individual variation these results may be underestimated. Nevertheless, mean percent correct level at spatial frequency of 0.86 cpd was significantly higher in the alternative method of repeated visual discrimination training than in the control experiment without repeated visual discrimination training. Correspondingly, mean escape latency at 0.86 cpd was significantly lower in the alternative method of repeated visual discrimination training than in the control experiment without repeated visual discrimination training.

Taken together, these results demonstrate that mice, when trained in the visual water task, were capable to discriminate a high spatial frequency grating from an equiluminant homogeneous gray only after a repeated visual discrimination training which apparently procured an increase in their visual acuity. This result is consistent with the effects of introducing animals to the enriched environment (EE) providing increased sensory stimulation. It has been reported, for instance, that in female Swiss albino mice, rearing in EE for 3 months starting at weaning resulted in significantly higher visual acuity of 1.06 cpd compared to standard environment group showing a visual acuity of 0.55 cpd (Trévia *et al*., 2011). Also, it has been demonstrated that adult amblyopic rats after exposure to EE recovered normal visual acuity and ocular dominance (Sale *et al*., 2007). Neural mechanisms of an increase in visual functions in the adulthood due to the increased sensory stimulation resulting from an exposure to EE, or as in the present study, from a demanding stimulus discrimination training, are not fully clear.

Visual acuity is limited by the eye optics and maybe reduced by refractive errors, as well as the diffraction of the light with the latter depending on the size of light wavelength and diameter of the pupil. The resolution of two objects is possible if they are separated by the width of their point spread function. A large pupil will reduce diffraction but impairs the vision due to increase in spherical aberration. However, eye optics can doubtfully change as a result of increased sensory input. Another important factor limiting visual acuity is retinal photoreceptor spacing (Green, 1970). It has been postulated that a grating would be resolved if separated receptor arrays detect the two lines but also a gap in between which corresponds to 1-0-1 response of retinal photoreceptors. Naturally then, visual acuity is better during photopic vision than during scotopic vision since the density of cones is much higher than density of rods. However, an increase in the density of photoreceptors in adult retina never has been reported. Also, Gianfranceschi and colleagues (1999) have not found a significant difference in visual acuity of wild type and *bcl2* transgenic mice with the latter having twice more ganglion cells than the normal mice. Conclusion was that an increase in ganglion cells density is

not effective in improving visual resolution. However, bilateral ablation of striate cortex significantly reduced grating acuity and contrast sensitivity in C57BL/6 mice (Prusky & Douglas, 2004). On the other hand, it has been previously demonstrated that in adult rats, *in vivo* theta burst stimulation of the dorsal lateral geniculate nucleus induces long term potentiation (LTP) of evoked field potentials (EFPs) in the primary visual cortex. This potentiation of responses from striate cortex was shown to occur in thalamorecipient cortical layers (layer IV and deep layer III and supragranular layers II/III), to be NMDA receptor-dependent, accompanied by significant increase in the number of immediate early gene zif-268 expression in cortical layers II-IV, and enhanced responses to grating stimuli across a range of spatial frequencies (Heynen & Bear, 2001). It has been also demonstrated that in awake mice, visual evoked potentials recorded in layer 4 of binocular visual cortex undergo increases in amplitude not only with repeated electrical stimulation of thalamo-cortical pathway but also with repeated presentation of a sinusoidal grating stimulus over days (Cooke & Bear, 2010). Also exposure to enriched environment enhances synaptic strength at thalamocortical terminals by increasing expression of the vesicular glutamate transporter 2 (VGluT-2) in geniculocortical afferents to layer IV, up-regulation of the intracortical excitatory synaptic marker VGluT-1 and a decrease in the expression of the vesicular GABA transporter (vGAT), indicating a shift in the excitation/inhibition ratio (Mainardi *et al*., 2010). These results point towards a cortical mechanism of adult neuroplasticity responsible for improvement of visual acuity with increased visual training. However, in the enhancement of the amplitude of VEPs produced by LTP generalizes across multiple stimuli, spatial frequencies, and contrasts, similar enhancement of VEP by repeated presentation of a sinusoidal grating stimulus may be highly specific to the familiar stimulus.

CHAPTER 5

CONCLUSION

In summary, this study provides evidence that visual acuity may improve with increased visual training even during adulthood and that visual estimates depend on the assessment method and animal history. Our findings compared with the previous studies, confirm that different methods of visual acuity measurements involving behavioral methods, optomotor tasks and visual evoked potential (VEP) recordings reveal discrepant results and for accurate estimation of visual acuity environmental factors such as brightness, luminance and contrast of the stimuli, animals' strain and age, as well as their previous experience should be taken into consideration.

In the present study, the results obtained with two different methods, both using visual water task based on the natural tendency in mice to escape from water, indicate that the number correct responses and escape latency are reliable indices of the difficulty in the visual discrimination task and can be used for behavioral assessment of visual functions.

Repeated visual discrimination training results show that increased visual training procures an increase in the visual acuity during adulthood which supports the view that the neocortex (in this case the visual cortex) retains its capability for activity-dependent neuroplasticity also in the adulthood.

These experiments were initially planned as a pilot study, therefore the number of animals used was limited. Additionally, in the course of the experiments, we have lost three animals ending up with 7 subjects in a group. However, if we had opportunity to test a larger group of animals and thus had a larger data set, we could use flexible regression modeling as well as linear regression analysis of the data. Regression modeling is widely used to assess a relationship between some predictors and a response variable (Weber *et al*., 2012). Multivariate adaptive regression splines (MARS) is a non-parametric regression technique introduced by Jerome H. Friedman in 1991. It is an extension of linear models and automatically models non-linearities and interactions between variables by introducing piecewise linear regressions. The model is in the form of an expansion in product spline basis functions (Friedman, 1991). The number of basis functions and the parameters related with each one are automatically determined by the

data. The approach used in MARS model building is the same as that used by recursive partitioning. However, differing from recursive partitioning, MARS can handle both continuous and categorical data; it builds continuous models with continuous derivatives and has more power and flexibility to model relationships that are nearly additive or involve interactions in a few variables. By combining recursive partitioning and spline fitting, MARS aims to retain positive aspects of both but be less vulnerable to their unwanted properties (Friedman, 1991). Compared to recursive partitioning, MARS models have a good bias-variance trade-off. While being flexible enough to model non-linearities and variable interactions (fairly low bias), constrained form of MARS basis functions prevents too much flexibility (fairly low variance). MARS method consists of two subalgorithms for estimating the model function; forward stepwise algorithm and backward stepwise algorithm. In the forward stepwise algorithm MARS repeatedly adds basis function in pairs to the model. At each step it finds and adds the pair of basis functions that gives the maximum reduction in sum-of-squares residual error until the change in residual error is too small to continue or a user-specified maximum number of terms is reached. The forward algorithm builds an overfit model which has a good fit to the data used but will not generalize to new data. To prevent overfitting and give a better generalization ability to the model, the backward stepwise algorithm removes the least effective term at each step by decreasing the complexity of the model without degrading the fit to the data until producing the optimally estimated submodel (Weber *et al*., 2012). The backward algorithm uses generalized cross validation (GCV) to compare the performance of model subsets in order to choose the model which has the best generalization performance. A complementary and model-based alternative to the backward stepwise algorithm is used by an alternative modeling technique, named CMARS, which is introduced by Weber *et al*. (2012) as a contribution to MARS method. In CMARS method, the MARS algorithm is modified by constructing a penalized residual sum of squares (PRSS) as a Tikhonov regularization problem and solving this problem by using continuous optimization, particularly, conic quadratic programming (CQP). The 'C' in CMARS represents 'Conic' and also 'Convex' and 'Continous'. Instead of the backward stepwise algorithm of MARS, CMARS uses penalty terms in addition to the least squares estimation (LSE) to control the lack-of-fit from the viewpoint of the complexity of estimation. Both MARS and CMARS have success to build models with data sets involving moderate to high sample sizes and moderate to high scales. The distinction of CMARS is its utility to make parameter estimation by its substantial optimization technique. However CMARS may provide more complex models than MARS and is not as efficient as MARS in computational run times (Weber *et al*., 2012).

The limitation of this study to build a non-linear model was our small sample size. If the sample size is increased to 50 and over, both MARS and CMARS methods can be used to analyze the data and build a model. In recent years, MARS has been successfully applied to many research areas of biology. Chou *et al*. (2004) integrated artificial neural networks and MARS to propose a hybrid breast cancer diagnostic model. They firstly used MARS to model the breast cancer diagnostic problems and then significant

predictor variables obtained by MARS were used as the input nodes of the designed neural networks model. Analytic results showed that the integrated approach was more efficient in handling breast cancer diagnostic problems due to its classification accuracy and capability in identifying important predictor variables. Deconinck *et al*. (2005) used MARS and a derived method two-step MARS (TMARS) for modeling the gastrointestinal absorption of 140 drug-like molecules and evaluated their predictive abilities. They concluded that both types of models had good predictive abilities but MARS-model described the dataset better and had a better predictive ability. The lower performance of the TMARS method is explained by the fact that the TMARS model is based on a linear model and shows high similarity with the linear model. Leathwick *et al*. (2006) used generalized additive models (GAM) and MARS to analyze relationships between distributions of 15 freshwater fish species and their environment. Their results indicated little difference between the performance of GAM and MARS models, however, results from MARS models were much more easily incorporated into other analyses than those from GAM models. MARS was capable of both identifying the most parsimonious set of environmental predictors and describe the distribution of species within a multi-dimensional space defined by these predictors. The strong performance of MARS model, in analyzing the widely varying and generally non-linear relationships that exist between species and their environment, suggest that it could also have applications for the modeling of rare species which are difficult to model. Elith and Leathwick (2007) demonstrated the use of MARS for predicting species distributions from museum and herbarium records. They used data of 226 species from six regions of the world and their study showed that MARS has the advantage of combining information from a set of species to determine the dominant environmental drivers of variation in species composition and analysis results can easily be transferred to other computational environments such as Geographic Information System. Deconinck *et al*. (2008) explored the use of unconventional non-linear modeling techniques to model the blood-brain barrier (BBB) passage of drugs and drug-like molecules. The data set contained BBB passage values for 299 structural and pharmacological diverse drugs and models were built using boosted regression trees (BRT) and MARS, as well as their respective combinations with stepwise multiple linear regression (MLR) and partial least squares (PLS) regression in two-step approaches. They results showed that using combinations of MARS with either stepwise MLR or PLS provided best models. Combination of a linear with a non-linear modeling technique resulted in improved properties and for such combination using MARS as a non-linear technique should be preferred over those with BRT.

Higher number of subjects in the group and the application of MARS modeling technique to our data would allowed for more precise analysis of the within-subject variation in visual skills, more correct assessment of visual acuity thresholds, as well as establishing a more accurate prediction formula for animals' performance at different spatial frequencies.

For the future studies, it would be interesting to throughly examine the potential morphological and functional changes that may take place in the visual cortex after repeated discrimination training to get an additional insight to the mechanisms of adult neuroplasticity in the visual cortex. The repeated visual discrimination training may be also used to study the potential changes in the acuity of visual perception when spatial frequency is fixed at optimal level while other stimulus parameters such as brightness, luminance or contrast are changing. The further studies of adult neuroplasticity in the visual cortex combined with therapeutic interventions has potential to aid restoring or retaining visual ability in visual deficits or progressive vision loss, and also recovery after cortical injuries.

REFERENCES

Abdeljalil, J., Hamid, M., Abdel-Mouttalib, O., Stéphane, R., Raymond, R., Johan, A., Serge, P. (2005). The optomotor response: a robust first-line visual screening method for mice. *Vision Research*, *45*(11), 1439–46.

Aho, A.-C. (1996). The visual acuity of the frog (*Rana pipiens*). *Journal of Comparative Physiology A: Sensory, Neural, and Behavioral Physiology*, *180*(1), 19–24.

Aho, A.-C. (1997). Measuring frog visual acuity by a novel method. *Perception, 26* ECVP Abstract Supplement.

Artal, P., de Tejada, P. H., Tedo, C. M., & Green, D. G. (1998). Retinal image quality in the rodent eye. *Visual Neuroscience*, *15*(04), 597–605.

Ash, P. (1951). The sensory capacities of infrahuman mammals: vision, audition, gustation. *Psychological Bulletin*, *48*(4), 289-326.

Bailey, I. L., & Lovie, J. E. (1976). New design principles for visual acuity letter charts. *American Journal of Optometry and Physiological Optics*, *53*(11), 740–5.

Baker, A. G., & Emerson, V. F. (1983). Grating acuity of the Mongolian gerbil (*Meriones unguiculatus*). *Behavioural Brain Research*, *8*(2), 195–209.

Birukow, G. (1937). Untersuchungen über den optischen Drehnystagmus und über die Sehschärfe des Grasfrosches (*Rana temporaria*). *Zeitschrift Für Vergleichende Physiologie*, *25*(1), 92–142.

Block, M. T. (1969). A note on the refraction and image formation of the rat's eye. *Vision Research*, *9*(6), 705–711.

Brown, J. E. (1965). Dendritic fields of retinal ganglion cells of the rat. *Journal of Neurophysiology*, *28*(6), 1091–1100.

Campbell, F. W. (1957). The depth of field of the human eye. *Optica Acta: International Journal of Optics*, *4*(4), 157–164.

Cavonius, C. R., & Robbins, D. O. (1973). Relationships between luminance and visual acuity in the rhesus monkey. *The Journal of Physiology*, *232*(2), 239–246.

Chou, S. M., Lee, T. S., Shao, Y. E., & Chen, I. F. (2004). Mining the breast cancer pattern using artificial neural networks and multivariate adaptive regression splines. *Expert Systems with Applications*, *27*(1), 133-142.

Cooke, S. F., & Bear, M. F. (2010). Visual experience induces long-term potentiation in the primary visual cortex. *The Journal of Neuroscience*, *30*(48), 16304–16313.

Corsini, R. J. (2002). Yerkes-Watson discrimination apparatus. In *The dictionary of psychology* (pp. 1081). New York, NY: Brunner-Routledge.

Dabrowska, B. (1975). Investigations on visual acuity of some corvine species. *Folia Biologica*, *23*(3), 311–332.

Daw, W. N. (1995). *Visual development*. New York, NY: Plenum Press.

Deconinck, E., Xu, Q. S., Put, R., Coomans, D., Massart, D. L., & Heyden, Y. V. (2005). Prediction of gastro-intestinal absorption using multivariate adaptive regression splines. *Journal of Pharmaceutical and Biomedical Analysis*, *39*(5), 45, 1021–1030.

Deconinck, E., Zhang M. H., Petitet, F., Dubus, E., Ijjaalid, I., Coomans, D., Heyden, Y. V. (2008). Boosted regression trees, multivariate adaptive regression splines and their

two-step combinations with multiple linear regression or partial least squares to predict blood–brain barrier passage: a case study. *Analytica Chimica Acta*, *609*(1), 13–23.

Deegan II, J. F., & Jacobs, G. H. (1993). On the identity of the cone types of the rat retina. *Experimental Eye Research*, *56*(3), 375-377.

Detwiler, S. R. (1949). The eye of the Chinchilla (*C. lanigera*). *Journal of Morphology*, *84*(1), 123–144.

De Valois, R. L., De Valois, K. K. (1990). *Spatial vision*. Oxford, NY: Oxford University Press.

Ekesten, B., Gouras, P., & Yamamoto, S. (2000). Cone inputs to murine retinal ganglion cells. *Vision Research*, *40*(19), 2573–2577.

Elith, J., & Leathwick, J. (2007). Predicting species distributions from museum and herbarium records using multiresponse models fitted with multivariate adaptive regression splines. *Diversity and Distributions*, *13*(3), 265–275.

Engen, T. (1988). Psychophysics, In J. A. Hobson (Eds.), *States of brain and mind* (pp. 89-91). Boston, MA: Birkhäuser Boston.

Fite, K. V. (1973). Anatomical and behavioral correlates of visual acuity in the great horned owl. *Vision Research*, *13*(2), 219–230.

Fite, K. V., & Rosenfield-Wessels, S. (1975). A comparative study of deep avian foveas. *Brain, Behavior and Evolution*, *12*(1-2), 97–115.

Friedman, J. H. (1991). Multivariate adaptive regression splines. *The Annals of Statistics*, *19*(1), 1-67.

Fu, Y., & Yau, K.-W. (2007). Phototransduction in mouse rods and cones. *European Journal of Physiology*, *454*(5)(805-819).

Gaffney, M. F., & Hodos, W. (2003). The visual acuity and refractive state of the American kestrel (*Falco sparverius*). *Vision Research*, *43*(19), 2053–2059.

Gagnon, Y. L., Sutton, T. T., & Johnsen, S. (2013). Visual acuity in pelagic fishes and mollusks. *Vision Research*, *92*, 1–9.

Garhart, C., & Lakshminarayanan, V. (2012). Anatomy of the eye, In J. Chen, W. Cranton, & M. Fihn (Eds.), *Handbook of visual display technology* (pp. 73-83). Berlin, Heidelberg: Springer Berlin Heidelberg.

Ghim, M. M., & Hodos, W. (2006). Spatial contrast sensitivity of birds. *Journal of Comparative Physiology A, 192*(5), 523–534.

Gianfranceschi, L., Fiorentini, A., & Maffei, L. (1999). Behavioural visual acuity of wild type and *bcl2* transgenic mouse. *Vision Research*, *39*(3), 569–574.

Gibbs, P. (1996). *Can a human see a single photon?* Retrieved March 10, 2014, from University of California, Riverside, Department of Mathematics Web site: http://math.ucr.edu/home/baez/physics/Quantum/see_a_photon.html

Goldstein, E. B. (2010). *Sensation and perception*. Belmont, CA: Wadsworth, Cengage Learning.

Gorgels, T. G. M. F., & Norren, D. V. (1992). Spectral transmittance of the rat lens. *Vision Research*, *32*(8), 1509–1512.

Green, D. G. (1970). Regional variations in the visual acuity for interference fringes on the retina. *The Journal of Physiology*, *207*(2), 351–356.

Green, D. G., Powers, M. K., & Banks, M. S. (1980). Depth of focus, eye size and visual acuity. *Vision Research*, *20*(10), 827–835.

Hahmann, U., & Güntürkün, O. (1993). The visual acuity for the lateral visual field of the pigeon (*Columba livia*). *Vision Research*, *33*(12), 1659–1664.

Harland, D. P., Li, D., & Jackson, R. R. (2012). How jumping spiders see the world, In O. F. Lazareva, T. Shimizu, & E. A. Wasserman (Eds.), *How animals see the world: Comparative behavior, biology, and evolution of vision* (pp. 133-163). New York: Oxford University Press.

Hecht, S. (1927). A quantitative basis for the relation between visual acuity and illumination. *Proceedings of the National Academy of Sciences of the United States of America*, *13*(8), 569–574.

Hecht, S. (1928). The relation between visual acuity and illumination. *The Journal of General Physiology*, *11*(3), 255-281.

Hecht, E. (2002). *Optics*. San Francisco, CA: Pearson Addison Wesley.

Heynen, A. J., & Bear, M. F. (2001). Long-term potentiation of thalamocortical transmission in the adult visual cortex in vivo. *The Journal of Neuroscience*, *21*(24), 9801–9813.

Hirsch, J. (1982). Falcon visual sensitivity to grating contrast. *Nature*, *300*(5887), 57–58.

Hodos, W., Leibowitz, R. W., & Bonbright, J. C. (1976). Near-field visual acuity of pigeons: effects of head location and stimulus luminance. *Journal of the Experimental Analysis of Behavior*, *25*(2), 129–141.

Hodos, W., Miller, R. F., & Fite, K. V. (1991a). Age-dependent changes in visual acuity and retinal morphology in pigeons. *Vision Research*, *31*(4), 669–677.

Hodos, W., Miller, R. F., Fite, K. V., Porciatti, V., Holden, A. L., Lee, J.-Y., Djamgoz, M. B. A. (1991b). Life-span changes in the visual acuity and retina in birds, In P. Bagnoli, & W. Hodos (Eds.), *NATO Advanced Research Workshop on the Changing Visual System: From Early to Late Stages of Life--Maturation and Aging in the Central Nervous System, NATO ASI Series A Vol. 222. The changing visual system: Maturation and aging in the central nervous system* (pp. 137-148). Newyork: Plenum Press.

Hodos, W. (1993). The visual capabilities of birds, In H. P. Zeigler & H.-J. Bischof (Eds.), *Vision, brain, and behavior in birds* (pp. 63-76). Cambridge, MA: MIT Press.

Hodos, W., Ghim, M. M., Potocki, A., Fields, J. N., & Storm, T. (2002). Contrast sensitivity in pigeons: a comparison of behavioral and pattern ERG methods. *Documenta Ophthalmologica*, *104*(1), 107–118.

Hodos, W. (2012). What birds see and what they don't, In O. F. Lazareva, T. Shimizu, & E. A. Wasserman (Eds.), *How animals see the world: Comparative behavior, biology, and evolution of vision* (pp. 5-24). New York: Oxford University Press.

Hughes, A. (1977). The refractive state of the rat eye. *Vision Research*, *17*(8), 927–939.

Jacobs, G. H., Neitz, J., & Deegan, J. F. (1991). Retinal receptors in rodents maximally sensitive to ultraviolet light. *Nature, 353*(6345), 655-656.

Jacobs, G. H., Fenwick, J. A., & Williams, G. A. (2001). Cone-based vision of rats for ultraviolet and visible lights. *The Journal of Experimental Biology*, *204*(14), 2439–2446.

Johnson, G. L. (1900). Contributions to the comparative anatomy of the mammalian eye, chiefly based on ophthalmoscopic examination. *Proceedings of the Royal Society of London, 66*(1899-1900)*,* 474-478.

Kalloniatis, M., & Luu, Cu. (2007). Visual acuity by Michael Kalloniatis and Charles Luu, In H. Kolb, R. Nelson, E. Fernandez, & B. Jones (Eds.), *Webvision: The organization of the retina and visual System*. Retrieved March 15, 2014 from The University of Utah Web site: http://webvision.med.utah.edu/

Kolb, H. (2011). Simple anatomy of the retina by Helga Kolb, In H. Kolb, R. Nelson, E. Fernandez, & B. Jones (Eds.), *Webvision: The organization of the retina and visual system*. Retrieved March 15, 2014 from The University of Utah Web site: http://webvision.med.utah.edu/

Kolb, H. (2012). Gross anatomy of the retina by Helga Kolb, In H. Kolb, R. Nelson, E. Fernandez, & B. Jones (Eds.), *Webvision: The organization of the retina and visual*

system. Retrieved March 15, 2014 from The University of Utah Web site: http://webvision.med.utah.edu/

Kurkjian, M. L., & Hodos, W. (1992). Age-dependent intensity-difference thresholds in pigeons. *Vision Research*, *32*(7), 1249–1252.

Lashley, K. S. (1930). The mechanism of vision: I. A method for rapid analysis of pattern-vision in the rat. *The Pedagogical Seminary and Journal of Genetic Psychology*, *37*(4), 453–460.

Lashley, K. S. (1932). The mechanism of vision: V. The structure and image-forming power of the rat's eye. *Journal of Comparative Psychology, 13*(2), 173-200.

Leathwick, J. R., Elith, J., & Hastie, T. (2006). Comparative performance of generalized additive models and multivariate adaptive regression splines for statistical modelling of species distributions. *Ecological Modelling*, *199*(2), 188–196.

Luce R. D., & Krumhansl C. L. (1988). Measurement, scaling and psychophysics, In R. C. Atkinson, R. J. Herrnstein, G. Lindzey, & R. D. Luce (Eds.), *Stevens' handbook of experimental psychology* (pp. 1-74). New York: Wiley.

Mainardi, M., Landi, S., Gianfranceschi, L., Baldini, S., De Pasquale, R., Berardi, N., Caleo, M. (2010). Environmental enrichment potentiates thalamocortical transmission and plasticity in the adult rat visual cortex. *Journal of Neuroscience Research*, *88*(14), 3048–3059.

Martin, G. R., & Gordon, I. E. (1974). Visual acuity in the tawny owl (*Strix aluco*). *Vision Research*, *14*(12), 1393–1397.

Martin, G. R. (1982). An owl's eye: schematic optics and visual performance in *Strix aluco* L. *Journal of Comparative Physiology A*, *145*(3), 341–349.

Matsuzawa, T. (1990). Form perception and visual acuity in a chimpanzee. *Folia Primatologica*, *55*(1), 24–32.

Miller, T. J., Crowder, L. B., & Rice, J. A. (1993). Ontogenetic changes in behavioural and histological measures of visual acuity in three species of fish. *Environmental Biology of Fishes*, *37*(1), 1–8.

Morris, R. G., Garrud, P., Rawlins, J. N., & O'Keefe, J. (1982) Place navigation impaired in rats with hippocampal lesions. *Nature*, 297, 681-683.

Neitz, J., & Jacobs, G. H. (1986). Reexamination of spectral mechanisms in the rat (*Rattus norvegicus*). *Journal of Comparative Psychology, 100*(1), 21-29.

Pizzorusso, T., Porciatti, V., Strettoi, E., & Maffei, L. (1997). The visual physiology of the mouse determined with VEPs. A comparison between wild type and Bcl-2 overexpressing mice. *Society for Neursocience Abstracts*, *23*, 82.

Porciatti, V., Fontanesi, G., & Bagnoli, P. (1989). The electroretinogram of the little owl (*Athene noctua*). *Vision Research*, *29*(12), 1693–1698.

Porciatti, V., Hodos, W., Signorini, G., & Bramanti, F. (1991). Electroretinographic changes in aged pigeons. *Vision Research*, *31*(4), 661–668.

Porciatti, V., Pizzorusso, T., & Maffei, L. (1999). The visual physiology of the wild type mouse determined with pattern VEPs. *Vision Research*, *39*(18), 3071–3081.

Powers, M. K., & Green, D. G. (1978). Single retinal ganglion cell responses in the dark-reared rat: grating acuity, contrast sensitivity, and defocusing. *Vision Research*, *18*(11), 1533–1539.

Prusky, G. T., West, P. W. R., & Douglas, R. M. (2000). Behavioral assessment of visual acuity in mice and rats. *Vision Research*, *40*(16), 2201–2209.

Prusky, G. T., & Douglas, R. M. (2003). Developmental plasticity of mouse visual acuity. *European Journal of Neuroscience*, *17*(1), 167–173.

Prusky, G. T., & Douglas, R. M. (2004). Characterization of mouse cortical spatial vision. *Vision Research*, *44*(28), 3411–3418.

Prusky, G. T., Alam, N. M., Beekman, S., & Douglas, R. M. (2004). Rapid quantification of adult and developing mouse spatial vision using a virtual optomotor system. *Investigative Ophthalmology & Visual Science*, *45*(12), 4611–4616.

Rabinowitz, Y. S. (1998). Keratoconus. *Survey of Ophthalmology*, *42*(4), 297–319.

Radlwimmer, F. B., & Yokoyama, S. (1998). Genetic analyses of the green visual pigments of rabbit (*Oryctolagus cuniculus*) and rat (*Rattus norvegicus*). *Gene*, *218*(1-2), 103–109.

Reymond, L. (1985). Spatial visual acuity of the eagle *Aquila audax*: a behavioural, optical and anatomical investigation. *Vision Research*, *25*(10), 1477–1491.

Reymond, L. (1987). Spatial visual acuity of the falcon, *Falco berigora*: a behavioural, optical and anatomical investigation. *Vision Research*, *27*(10), 1859–1874.

Robinson, L., Bridge, H., & Riedel, G. (2001). Visual discrimination learning in the water maze: a novel test for visual acuity. *Behavioural Brain Research*, *119*(1), 77–84.

Rochon-Duvigneaud, A. (1947). Les yeux et la vision des vertébrés. *Journal of the American Medical Association*, *133*(6), 433.

Rounsley, K. J., & McFadden, S. A. (2005). Limits of visual acuity in the frontal field of the rock pigeon (*Columba livia*). *Perception*, *34*(8), 983–993.

Sale, A., Vetencourt, J. F. M., Medini, P., Cenni, M. C., Baroncelli, L., De Pasquale, R., Maffei, L. (2007). Environmental enrichment in adulthood promotes amblyopia recovery through a reduction of intracortical inhibition. *Nature Neuroscience*, *10*(6), 679–681.

Schmucker, C., Seeliger, M., Humphries, P., Biel, M., & Schaeffel, F. (2005). Grating acuity at different luminances in wild-type mice and in mice lacking rod or cone function. *Investigative Ophthalmology & Visual Science*, *46*(1), 398–407.

Seymoure, P., & Juraska, J. M. (1997). Vernier and grating acuity in adult hooded rats: the influence of sex. *Behavioral Neuroscience, 111*(4) 792-800.

Shlaer, R. (1972). An eagle's eye: quality of the retinal image. *Science*, *176*(4037), 920–922.

Sinex, D. G., Burdette, L. J., & Pearlman, A. L. (1979). A psychophysical investigation of spatial vision in the normal and reeler mutant mouse. *Vision Research*, *19*(8), 853–857.

Spence, K. W. (1934). Visual acuity and its relation to brightness in chimpanzee and man. *Journal of Comparative Psychology, 18*(3), 333-361.

Szél, Á., Lukáts, Á., Fekete, T., Szepessy, Z., & Röhlich, P. (2000). Photoreceptor distribution in the retinas of subprimate mammals. *Journal of the Optical Society of America A*, *17*(3), 568-579.

Thompson, R., & Bryant, J. H. (1955). Memory as affected by the activity of the relevant receptor. *Psychological Reports*, *1*, 393-400.

Trévia, N., Almeida, I. N. F., Oliveira, P. S., Warwick, L. V., Marques, V., dos Santos, D. C., et al. (2011). Enriched environment contributes to recovery of visual acuity and increases perineuronal nets in monocular-deprived animals. *Psychology & Neuroscience*, *4*(1), 49–56.

Veilleux, C. C., & Kirk, E. C. (2014). Visual acuity in mammals: effects of eye size and ecology. *Brain, Behavior and Evolution*, *83*(1), 43–53.

Waller M. B., Waller, P. F., & Brewster, L. A. (1960). A water maze for use in studies of drive and learning. *Psychological Reports*, *7*, 99-102.

Walls, G. L. (1942). *The vertebrate eye and its adaptive radiation*. Oxford, England: Cranbrook Institute of Science.

Weber, G. W., Batmaz, İ., Köksal, G., Taylan, P., & Yerlikaya-Özkurt, F. (2012). CMARS: a new contribution to nonparametric regression with multivariate adaptive regression splines supported by continuous optimization. *Inverse Problems in Science and Engineering*, *20*(3), 371-400.

Weinstein, B., & Grether, W. F. (1940). A comparison of visual acuity in the rhesus monkey and man. *Journal of Comparative Psychology, 30*(2), 187-195.

Wiesenfeld, Z., & Branchek, T. (1976). Refractive state and visual acuity in the hooded rat. *Vision Research*, *16*(8), 823–827.

Wilcox, W. W. (1932). The basis of the dependence of visual acuity on illumination. *Proceedings of the National Academy of Sciences of the United States of America*, *18*(1), 47–56.

Wong, A. A., & Brown, R. E. (2006). Visual detection, pattern discrimination and visual acuity in 14 strains of mice. *Genes, Brain, and Behavior*, *5*(5), 389–403.

Wong, A. A., & Brown, R. E. (2007). Age-related changes in visual acuity, learning and memory in C57BL/6J and DBA/2J mice. *Neurobiology of Aging*, *28*(10), 1577–1593.

Woolf, D. (1956). A comparative cytological study of the ciliary muscle. *The Anatomical Record*, *124*(2), 145–163.

Yerkes, R. M., & Watson, J. B. (1911). Methods of studying vision in animals. *Animal Behavior Monographs*, *1*(2).

Yokoyama, S., Radlwimmer, F. B., & Kawamura, S. (1998). Regeneration of ultraviolet pigments of vertebrates. *FEBS Letters*, *423*(2), 155–158.

APPENDIX A: GRAPHS OF VISUAL ACUITY MEASUREMENTS IN EACH
MOUSE USING METHOD I
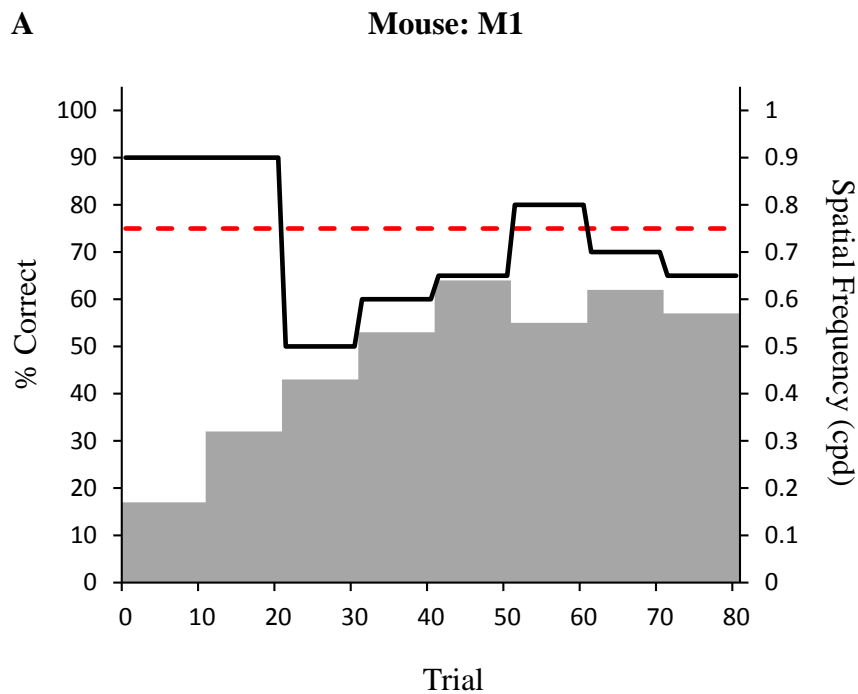
A   **Mouse: M1**

Figure A: Measurements of visual acuity in each mouse separately. A) Mouse: M1, B) Mouse: M2, C) Mouse: M3, D) Mouse: M4, E) Mouse M5, F) Mouse M6, G) Mouse: M7. Gray bars indicate gradually increased spatial frequencies during testing. Solid lines indicate percentage of correct choices. Dashed line indicates the arbitrary discrimination level of 75% correct choices.
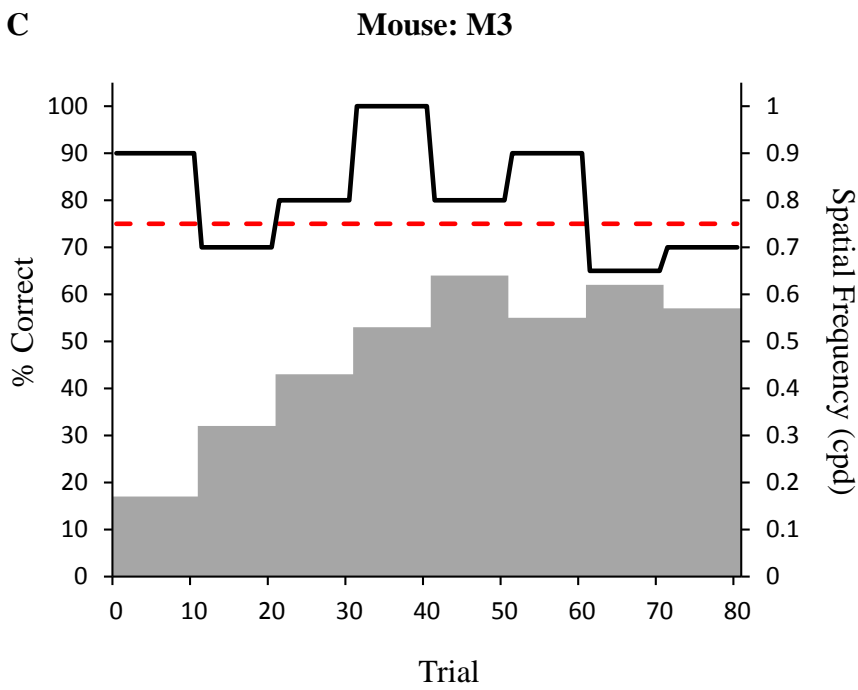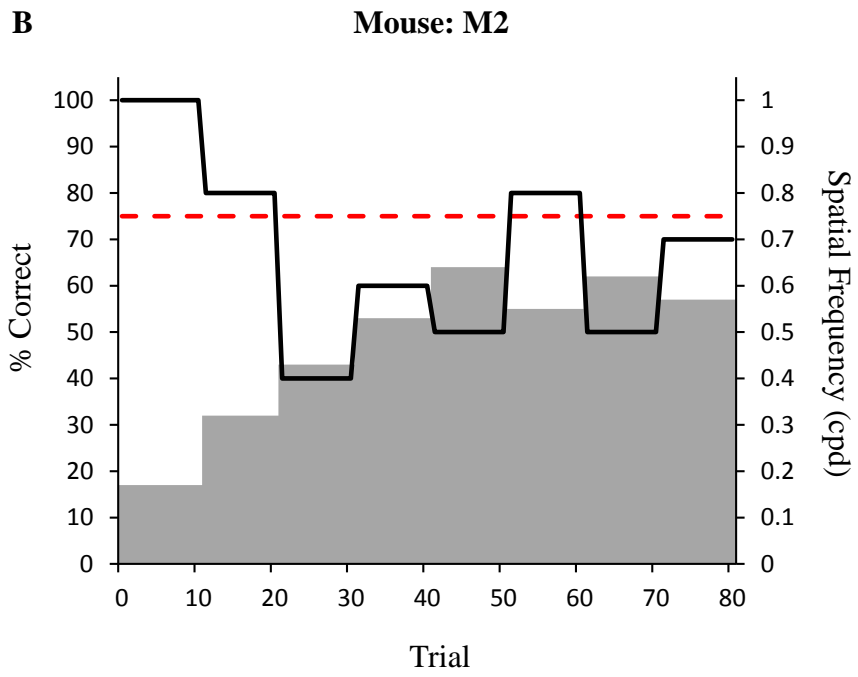
B   **Mouse: M2**

C   **Mouse: M3**

Figure A (Continued): Measurements of visual acuity in each mouse separately.

D   **Mouse: M4**

E   **Mouse: M5**
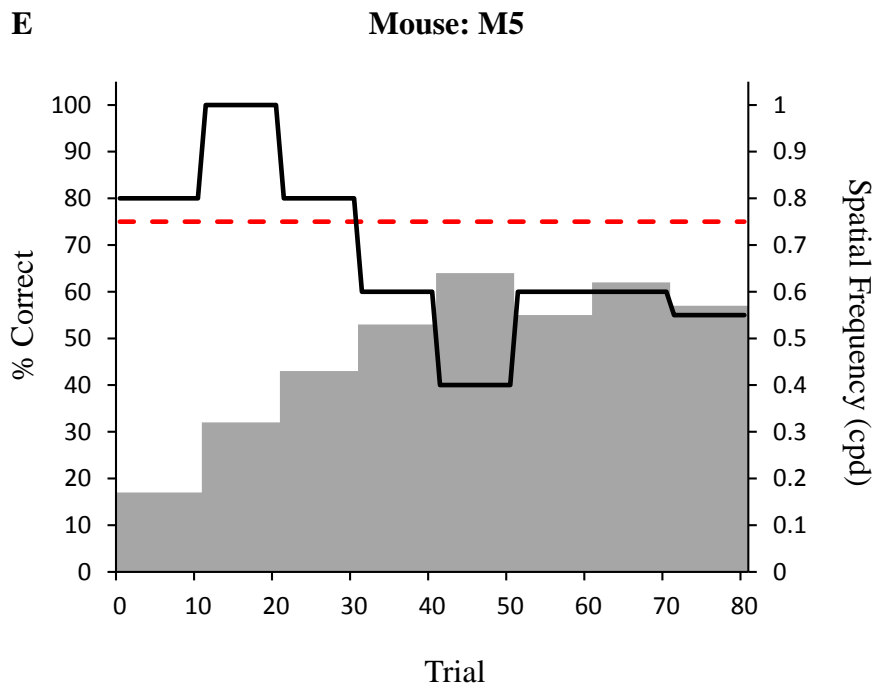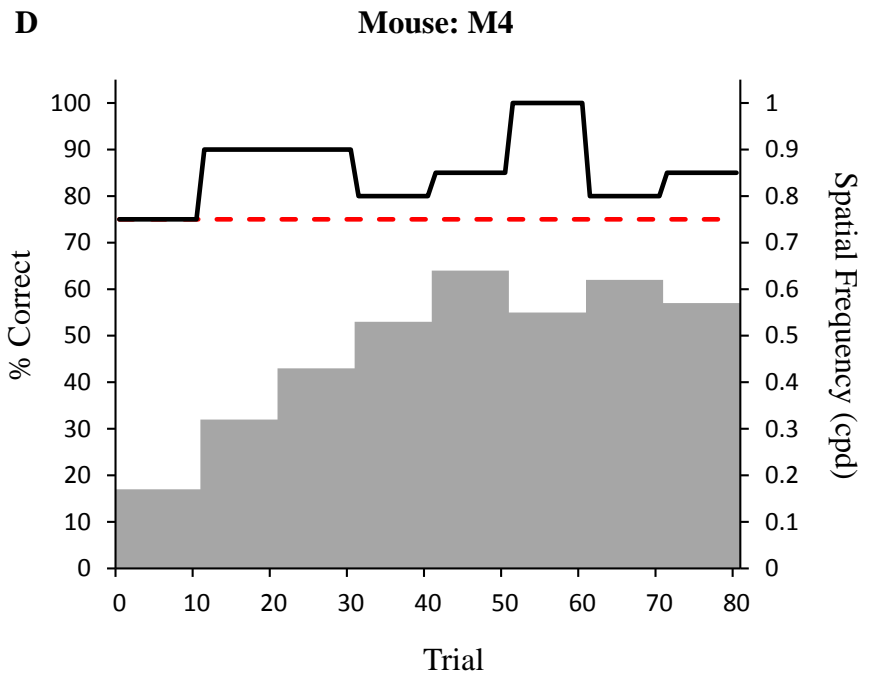
Figure A (Continued): Measurements of visual acuity in each mouse separately.

F   **Mouse: M6**

G   **Mouse: M7**
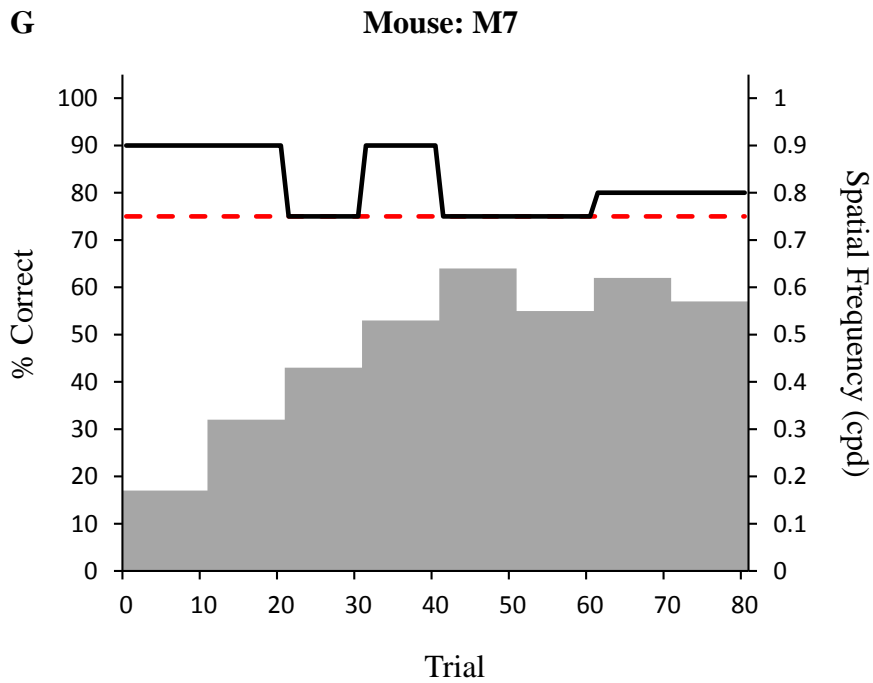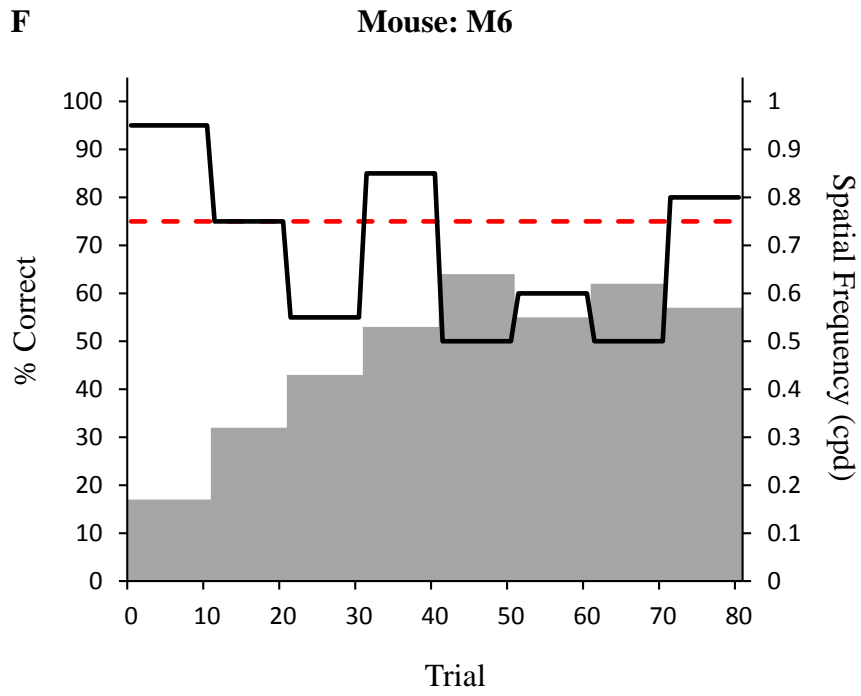
Figure A (Continued): Measurements of visual acuity in each mouse separately.

APPENDIX B: PAIRWISE COMPARISIONS

1. **Pairwise Comparisons of the Mean Percentage of Correct Choices in Testing Phase of Method I**

Pairwise comparisons using Fisher's LSD (Least Significant Difference) post hoc test indicated that the mean percentage of correct choices were significantly different at spatial frequencies of;

0.17 cpd ($M = 8.86$, $SD = 0.85$) and 0.57 cpd ($M = 7.21$, $SD = 1.04$),
0.17 cpd ($M = 8.86$, $SD = 0.85$) and 0.62 cpd ($M = 6.50$, $SD = 1.26$),
0.17 cpd ($M = 8.86$, $SD = 0.85$) and 0.64 cpd ($M = 6.36$, $SD = 1.73$),
0.32 cpd ($M = 8.50$, $SD = 1.04$) and 0.43 cpd ($M = 6.71$, $SD = 1.87$),
0.32 cpd ($M = 8.50$, $SD = 1.04$) and 0.62 cpd ($M = 6.50$, $SD = 1.26$),
0.32 cpd ($M = 8.50$, $SD = 1.04$) and 0.64 cpd ($M = 6.36$, $SD = 1.73$),
0.55 cpd ($M = 7.79$, $SD = 1.47$) and 0.62 cpd ($M = 6.50$, $SD = 1.26$),
0.55 cpd ($M = 7.79$, $SD = 1.47$) and 0.64 cpd ($M = 6.36$, $SD = 1.73$).

2. **Pairwise Comparisons of the Mean Escape Latencies in Testing Phase of Method I**

Pairwise comparisons using post hoc Bonferroni correction indicated that the mean escape latencies were significantly different at spatial frequencies of;

0.17 cpd ($M = 6.96$, $SD = 0.99$) and 0.43 cpd ($M = 10.79$, $SD = 1.48$),
0.17 cpd ($M = 6.96$, $SD = 0.99$) and 0.55 cpd ($M = 11.00$, $SD = 1.72$),
0.17 cpd ($M = 6.96$, $SD = 0.99$) and 0.62 cpd ($M = 9.69$, $SD = 1.15$),
0.32 cpd ($M = 7.07$, $SD = 1.06$) and 0.55 cpd ($M = 11.00$, $SD = 1.72$),
0.32 cpd ($M = 7.07$, $SD = 1.06$) and 0.62 cpd ($M = 9.69$, $SD = 1.15$).

3. **Pairwise Comparisons of the Mean Percentage of Correct Choices in Testing Phase of Method II**

Pairwise comparisons using Fisher's LSD (Least Significant Difference) post hoc test indicated that the mean percentage of correct levels were significantly different at spatial frequencies of;

0.17 cpd ($M = 6.97$, $SD = 0.57$) and 0.43 cpd ($M = 5.83$, $SD = 0.50$),
0.17 cpd ($M = 6.97$, $SD = 0.57$) and 0.53 cpd ($M = 5.96$, $SD = 0.49$),
0.17 cpd ($M = 6.97$, $SD = 0.57$) and 0.64 cpd ($M = 5.96$, $SD = 0.56$),

0.32 cpd ($M = 6.58$, $SD = 0.39$) and 0.43 cpd ($M = 5.83$, $SD = 0.50$),
0.32 cpd ($M = 6.58$, $SD = 0.39$) and 0.80 cpd ($M = 7.22$, $SD = 0.47$),
0.43 cpd ($M = 5.83$, $SD = 0.50$) and 0.62 cpd ($M = 6.63$, $SD = 0.61$),
0.43 cpd ($M = 5.83$, $SD = 0.50$) and 0.66 cpd ($M = 6.84$, $SD = 0.66$),
0.43 cpd ($M = 5.83$, $SD = 0.50$) and 0.76 cpd ($M = 6.54$, $SD = 0.69$),
0.43 cpd ($M = 5.83$, $SD = 0.50$) and 0.78 cpd ($M = 7.02$, $SD = 0.66$),
0.43 cpd ($M = 5.83$, $SD = 0.50$) and 0.80 cpd ($M = 7.22$, $SD = 0.47$),
0.43 cpd ($M = 5.83$, $SD = 0.50$) and 0.86 cpd ($M = 7.03$, $SD = 0.79$),
0.53 cpd ($M = 5.96$, $SD = 0.49$) and 0.78 cpd ($M = 7.02$, $SD = 0.66$),
0.53 cpd ($M = 5.96$, $SD = 0.49$) and 0.80 cpd ($M = 7.22$, $SD = 0.47$),
0.53 cpd ($M = 5.96$, $SD = 0.49$) and 0.82 cpd ($M = 6.72$, $SD = 0.65$),
0.53 cpd ($M = 5.96$, $SD = 0.49$) and 0.86 cpd ($M = 7.03$, $SD = 0.79$),
0.55 cpd ($M = 6.37$, $SD = 0.39$) and 0.80 cpd ($M = 7.22$, $SD = 0.47$),
0.64 cpd ($M = 5.96$, $SD = 0.56$) and 0.66 cpd ($M = 6.84$, $SD = 0.66$),
0.64 cpd ($M = 5.96$, $SD = 0.56$) and 0.76 cpd ($M = 6.54$, $SD = 0.69$),
0.64 cpd ($M = 5.96$, $SD = 0.56$) and 0.78 cpd ($M = 7.02$, $SD = 0.66$),
0.64 cpd ($M = 5.96$, $SD = 0.56$) and 0.80 cpd ($M = 7.22$, $SD = 0.47$),
0.66 cpd ($M = 6.84$, $SD = 0.66$) and 0.72 cpd ($M = 6.24$, $SD = 0.56$),
0.72 cpd ($M = 6.24$, $SD = 0.56$) and 0.78 cpd ($M = 7.02$, $SD = 0.66$),
0.72 cpd ($M = 6.24$, $SD = 0.56$) and 0.80 cpd ($M = 7.22$, $SD = 0.47$).